UNIVERSITÀ DEGLI STUDI DI PALERMO

PhD Course in Biomedicine, Neuroscience and Advanced diagnostics
Dipartimento di Biomedicina, Neuroscienze e Diagnostica avanzata
BIO/09

Retinal neurodegeneration and an innovative nanostructured approach in an iron overload in vivo model

IL DOTTORE
IRENE DEIDDA

IL COORDINATORE
PROF. FABIO BUCCHIERI

IL TUTOR
PROF. PIERANGELO SARDO

CICLO XXXII CICLO – TRIENNIO 2016-2019
ANNO CONSEGUIMENTO TITOLO 2020

ABSTRACT

The ocular diseases are currently the principal causes of age-related disabilities involving an irreversible visual impairment. Iron is essential for normal retinal function but, being the most powerful generator of free radicals, its excess may contribute to the development of retinal disorders. To date, the mechanisms underlying iron excess in the retina are not perfectly known. The first objective of this study was to deepen the knowledge about the role of iron in the retina, analyzing the *in vivo* effects of retinal iron accumulation. We conducted intravitreal injection of ferrous sulfate in Wistar rats and analyzed the progressive degeneration of retina and RPE/choroid structures at different stages from iron insult. Using biochemical and immunostaining analyses, we investigated the cellular mechanisms underlying iron-dependent retinal degeneration, including morphological alterations, iron overload, oxidative stress, neuroinflammation and amyloid accumulation, thus providing an ideal animal model of retinal degeneration.

The iron overload *in vivo* model of retinal degeneration was used to test the effectiveness of an innovative nanostructured therapeutic approach. Targeted therapies and efficient drug delivery systems in the treatment of ocular disorders are central objective of the biomedical research. In this regard, the growing field of nanotechnology in ophthalmic drug delivery offers efficient nanocarrier systems with several advantages, including the enhanced targeting and time-controlled drug release, improved stability and bioavailability of large or poorly water-soluble molecules. Therefore, the next objective of this study was the *in vivo* analysis of topical treatment as eye drop based on the choline-calix[4]arene nanocarrier, an innovative platform for the ocular delivery of silibinin, a flavonoid with possible neuroprotective activity. The results obtained suggested that the topical eye treatment with silibinin conjugated to choline-calix[4]arene nanocarrier has a greater neuroprotective effect in the ocular structures compared to free silibinin or nanocarrier alone, by reducing oxidative stress, inflammation and neovascularization processes in the iron-induced retinal degeneration animal model. Our results provide evidence of the potential of calixarene macrocycle as a promising platform for topical ocular drug delivery systems.

INTRODUCTION

Eye: Neuroretina and Retinal Pigment Epithelium (RPE)

The structure of the eye can be classified into two segments: anterior and posterior (Figure 1). The anterior segment of the eye occupies approximately one-third while the remaining portion is accommodated by the posterior segment. Tissues such as cornea, conjunctiva, aqueous humor, iris, ciliary body and lens make up the anterior portion. The posterior segment of the eye includes sclera, choroid, retinal pigment epithelium (RPE), neural retina, optic nerve and vitreous humor. Diseases affecting anterior segment of the eye include, but are not limited to glaucoma, allergic conjunctivitis, anterior uveitis and cataract. Age-related macular degeneration (AMD) and diabetic retinopathy (DR) are the most prevalent diseases affecting posterior segment of the eye.

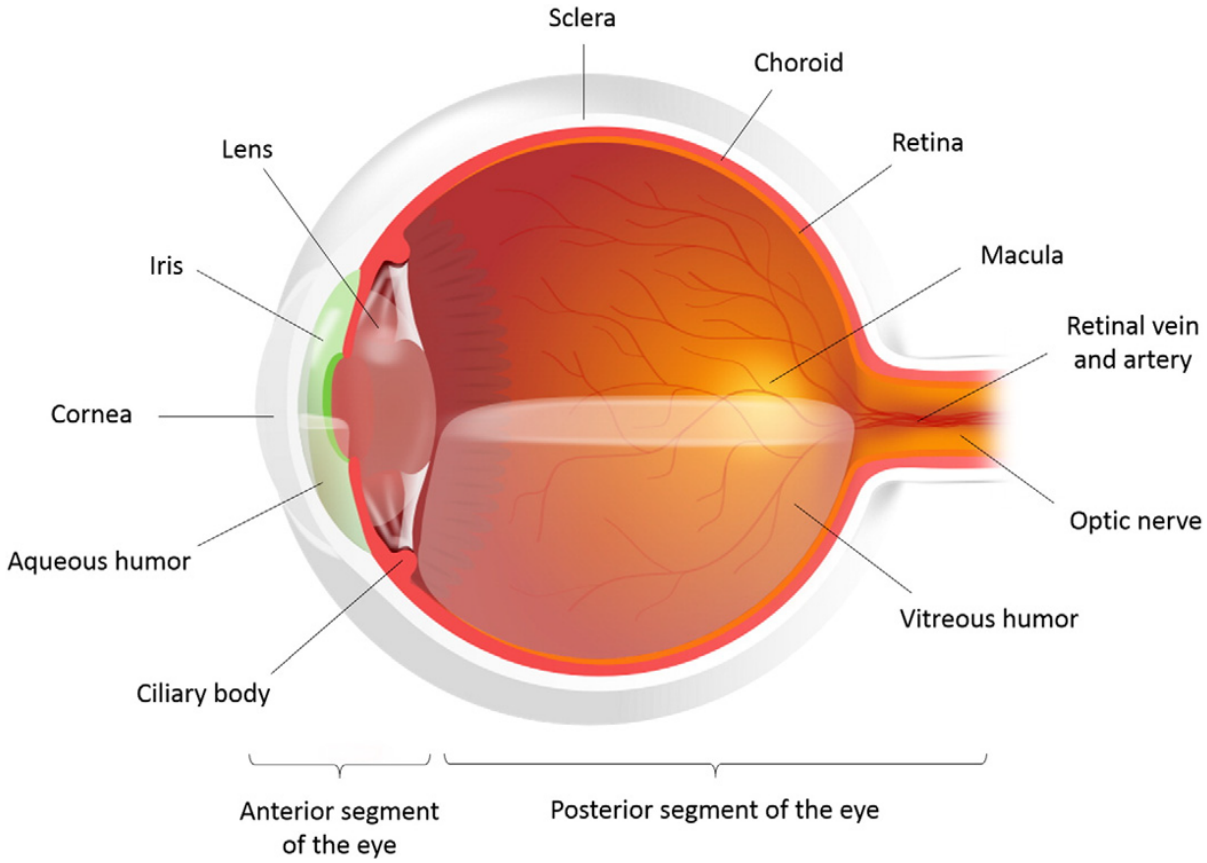

Figure 1. Anatomy of the mammalian adult eye (Delplace et al., 2015).

The retina, posterior light-sensitive tissue of the eye, is an extension of the central nervous system (CNS) originating from the embryonic diencephalon (London et al., 2013).

Architecturally and functionally the neuroretina is similar to the brain: indeed they share many features such as embryological origin, strict control of blood barriers and specialized immune system, which is activated to respond to diverse types of insult.

Multiple cell layers highly ordered compose the retinal architecture. Five types of specialized neurons as well as glial cells are distributed in three nuclear layers separated by two plexiform layers composed by synaptic contacts (Figure 2).

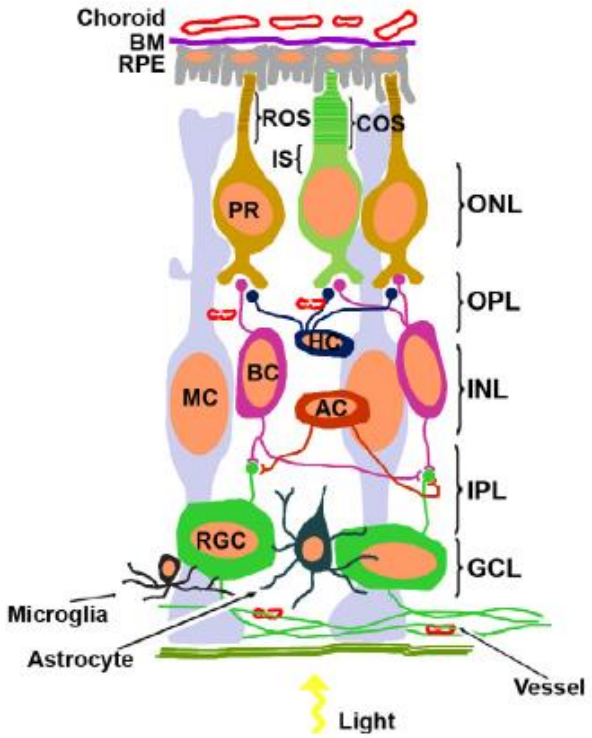

Figure 2. Cellular architecture of the mammalian retina. Schematic cross section showing retinal layers constituted by photoreceptors (rods and cones), neurons (horizontal, amacrine, bipolar and retinal ganglion cells), glial cells (Müller cells, astrocytes and microglia) and vessels. The yellow arrow indicates the way light enters the retina. Abbreviations here and in the following figures: BM, Bruch's membrane; RPE, retinal pigment epithelium; ROS and COS, rod and cone outer segments; IS, inner segments; PR, photoreceptors; ONL, outer nuclear layer; OPL, outer plexiform layer; HC, horizontal cells; BC, bipolar cells; MC, Müller cells; AC, amacrine cells; INL, inner nuclear layer; IPL, inner plexiform layer; GCL, ganglion cell layer; RGC, retinal ganglion cells. (Cascio et al., 2015)

The most external retinal layer, the outer nuclear layer (ONL) and the outer and inner segments (OS and IS) are constituted by photoreceptors (cones and rods), which convert the light energy into an electrochemical signal. In particular, the process of vision includes the light absorption by the visual pigments, the apoprotein opsin and the chromophore 11-cis retinal, located in the photoreceptors and, after a series of biochemical changes, the cell hyperpolarization and the

start of electrical current flow through the retina, thus reaching the retinal ganglion cells (RGCs). The RGCs are located in the innermost nuclear layer of the retina, the ganglion cell layer (GCL), and their axons project out from the retina forming the optic nerve crossing in the optic chiasm. Once RGCs are activated by light rays coming from the right or left visual hemi field, their axons carry the message to reach the visual cortex of the occipital lobe in opposite side of the brain. Bipolar cells (BCs) contact both photoreceptors and RGCs, transferring the neuronal signal from one layer to the other of the retina. The other retinal cells integrate and refine the visual output from the retina, including the horizontal cells (HCs) that are involved in contrast enhancement, and the amacrine cells (ACs) that contribute to a precomputation of visual stimuli via feedback between ganglion and bipolar cells. These neuronal cells (bipolar, horizontal and amacrine cells), together with the Müller glia cells (MCs), form the inner nuclear layer (INL), which is located between the ONL and the GCL. A particular subgroup of ACs, the displaced amacrine cells, is also found in the GCL. In the outer plexiform layer the horizontal cells are found, whereas the amacrine cells are present in the inner plexiform layer.

A crucial role in retinal homeostasis has been attributed to retinal glial cells, which provide structural support, regulate retinal metabolism and neuronal activity, phagocytosis and release of transmitters, inflammatory modulators and trophic factors. Müller cells, astrocytes, and microglia are the three types of glia cells contained in the mammalian retina (Vecino et al., 2016, Karlstetter et al., 2015). Müller cells are the major glial cells in the retina (about 90% of the retinal glia), whose cell bodies reside in the INL, whereas their processes reach all retina layers contacting neurons and other glial cells. These cells release trophic factors, recycle glutamate neurotransmitter and regulate extracellular ion homeostasis, thus supporting neuroretina function and metabolism. Astrocytes are confined in the innermost retinal layer and perform similar functions to Müller cells. Retinal astrocyte processes cover the blood vessels in the INL contributing, together with Müller cells, to maintain the blood retinal barrier integrity. Microglia, resident tissue macrophages, represent the first line of defense and surveillance of the retina following injuries or diseases. Crucial role is attributed to them not only in the phagocytosis of toxic products and antigen presentation, but also in the neurogenesis, synaptic pruning, neuroprotection and recovery from injury and progression of disease (Madeira et al., 2015). Among other activities, microglia can interact with other glial cells and neurons by secreting growth factors.

The blood retinal barrier (BRB) is a physiological barrier essential to preserve the eye as a privileged site and to maintain the suitable environment for visual function. BRB regulates the flow of nutrients, ions, proteins, waste products and water flux incoming and outgoing from the

retina similarly to the blood-brain-barrier (BBB). It consists of two components: the inner and outer endothelial blood-retina-barrier (iBRB and oBRB) (Figure 3).

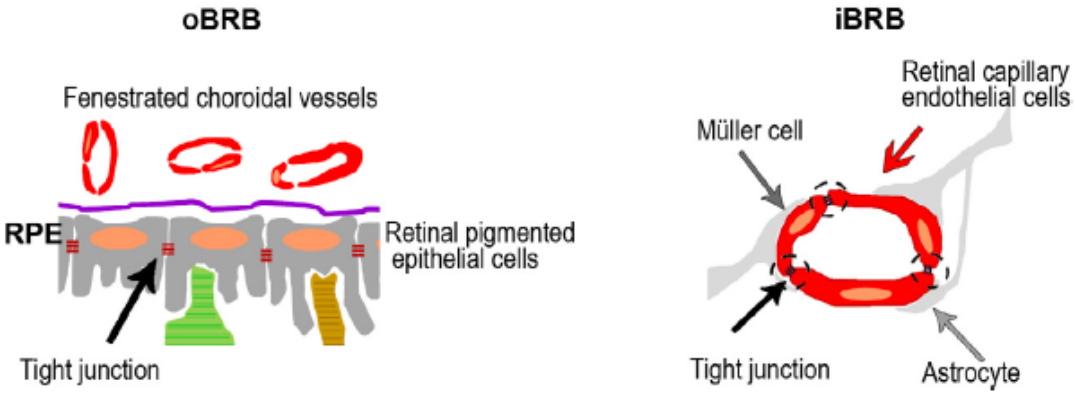

Figure 3. Blood retina barriers (BRBs). Retinal pigmented epithelial cells (outer BRB, oBRB) and retinal capillary endothelial cells (inner BRB, iBRB) are formed by tight junctions between their respective adjacent cells. In oBRB, fenestrated choroidal vessels, major blood supplier for the retina, are kept out. In iBRB, astrocytes and Müller cells surrounding blood capillaries contribute to the formation of barrier properties (Cascio et al., 2015).

The iBRB is composed of tight junctions between retinal capillary endothelial cells; pericytes and the processes of Müller cells and astrocytes cover the vascular components being in close contact with endothelial cells. The oBRB is established by the tight junctions between the RPE cells. The Retinal Pigment Epithelium is the outermost monolayer of cells that lies beneath the neuroretina, separating it from the fenestrated choriocapillaris. Amongst its many functions, the RPE regulates the uptake of blood nutrients by photoreceptors as well as the export of metabolic waste products. To prevent the toxic effects of accumulated photo-oxidative products, photoreceptors undergo a daily renewal process in which they are shed and subsequently phagocytosed by microvilli on the apical RPE surface. This is a crucial role for the maintenance of visual function that is attributed to the RPE. The underlying choriocapillaris, a dense capillary network, regulates the removal of the retinal waste also through the support given by Bruch's membrane (BM), the basal membrane located between the choroid and RPE structures.

Retinal neurodegenerative diseases

The ocular diseases are currently the principal causes of age-related disabilities, relating an irreversible visual impairment with a negative impact on the individual quality of life and considerable socio-economic costs (Pascolini and Mariotti, 2012). Being a structurally and functionally complex tissue, the retina is extremely vulnerable to alterations caused from any sort of injury, including gene defects, dyslipidemia, hypertension, hyperinsulinemia, hyperglycemia and aging.

Retinal neurodegenerative diseases, like age related macular degeneration (AMD), glaucoma, diabetic retinopathy and retinitis pigmentosa, are multifactorial disorders, each of which have a different etiology and pathogenesis (Cuenca et al., 2014). However, at the cellular and molecular level, the response to retinal injury is similar in all of them, resulting in similar morphological and functional changes of retinal cells, including cell death and retinal remodelling. Interestingly, inflammatory response, oxidative stress and activation of apoptotic pathways are common features in all these ocular diseases.

The glaucoma comprises a group of neurodegenerative disorders characterized by progressive retinal ganglion cell (RGC) degeneration and optic neuropathy. It constitutes the second leading cause of irreversible blindness worldwide and several clinical studies demonstrated that the intraocular pressure (IOP) is one of the most important risk factors for glaucoma onset and progression, whereas age and familiarity are closely related to the disease (Actis et al., 2016). Age is also the most significant risk factor of Age-related macular degeneration (AMD), a multifactorial and progressive degenerative disorder that is the leading cause of severe and irreversible loss of vision in the elderly in developed countries (Tomany et al., 2004). In this disease, impairment of RPE cells and photoreceptors as well as vascular angiogenesis are the main cause of central visual acuity loss. Diabetic retinopathy (DR) is a complication of diabetes caused by changes in blood glucose levels, resulting in alterations in retinal blood vessels that alter the retinal structure. Retinitis pigmentosa (RP) is the most frequent hereditary dystrophy of the retina causing progressive loss of photoreceptor cells. The underlying mechanism of the most forms of RP involves primarily loss of the rods, followed by the cone damage. Because rods are concentrated in the peripheral retina, people suffering this disease show a progressive diminution of the peripheral visual field, ending in a complete blindness (Yuxi et al., 2015).

To protect retinal tissue from damage and/or to preserve retinal function, both neuronal and glial cells respond to any type of injury and disease initiating mechanisms of protection and tissue regeneration, including the stimulation of the antioxidant machinery, the activation of the mechanisms of programmed cell death, and the promotion of the inflammatory response (Figure 4).

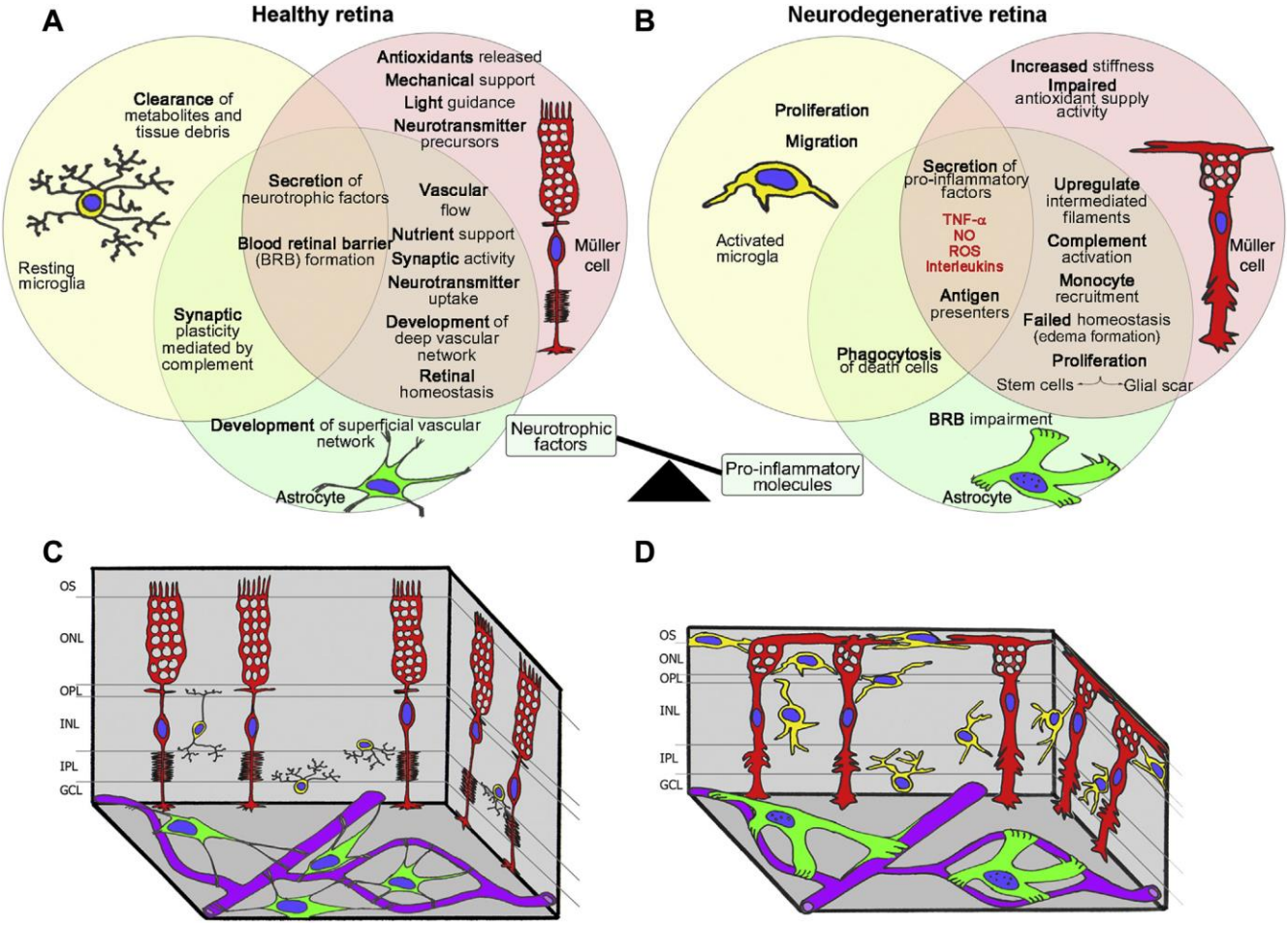

Figure 4. The role of glial cells in the retina. Schematic representation of the main morphological and functional features of glial cells in normal (A, C) and injured retinas (B, D). In the normal retina, glial cells play a key role in maintaining homeostasis and preserving the survival of neurons (A). Retinal injury triggers the activation of glial cells, characterized by secretion of pro-inflammatory factors and phagocytosis (B), and by the decrease or absence of their normal functions as in healthy retina (Cuenca et al., 2014).

Retinal alterations in neurodegenerative diseases

Visual symptoms have been described in human neurodegenerative disorders, such as Alzheimer's disease (AD), Parkinson's diseases (PD), multiple sclerosis and amyotrophic lateral sclerosis (ALS), showing the involvement of the retina and/or optic nerve (Yap et al., 2019). Furthermore, several studies have also showed that glaucoma, diabetic retinopathy and AMD may manifest in patients with Alzheimer or Parkinson, or other neurodegenerative disorders (Bodis-Wollner, 1990, Bayer et al., 2002, Ohno-Matsui, 2011, Kaarniranta et al., 2011, Williams et al., 2014, Biscetti et al., 2017, Moon et al., 2018, Matlach et al., 2018).

The retina is an attractive source of biomarkers since it shares many risk factors and many causative diseases' features with the brain, such as generation of oxidative stress, inflammation, neovascularization, altered metabolic supply, glutamate excitotoxicity and protein misfolding cytotoxicity. Therefore, the ophthalmic manifestations could have remarkable importance in the diagnosis and monitoring of some neurodegenerative diseases and the neuroretina could provide further insights into pathogenetic mechanisms of disease.

There are several advantages/benefits in the use of retinal imaging as approach for the neurological disorders diagnosis in comparison to brain imaging, including the direct (in vivo) analysis and high resolution with or without the use of contrast agents (Yap et al., 2019). The extraordinary evolution in the *in vivo* retinal analysis techniques (including the optical coherence tomography [OCT]) has provided early and non-invasive methods not only for diagnosis of neurodegenerative diseases, but also to monitoring over time specific retinal cells without risk of neurosurgery and ionizing radiation (Pircher and Zawadzki, 2017, MacCormick et al., 2015).

Alzheimer's disease is the most prevalent aging dementia worldwide characterized by neuronal and synaptic loss of brain cognitive regions. The main pathological AD hallmarks are the extracellular deposits of amyloid β (Aβ) as senile plaques and intracellular hyperphosphorylated Tau in neurofibrillary tangles (NFTs). The diagnosis of AD is very often late, thus causing detrimental effects on efficacy of pharmacological treatments as well as wider ranging social and economic effects. There is a growing appreciation that retinal degeneration occurs in AD patients (London et al., 2013, Dehabadi et al., 2014, Guo et al., 2010) and visual abnormalities in AD are often detectable at early stages of the disease. Patients with AD exhibit altered contrast sensitivity and colour recognition, susceptibility to visual masks, impaired pupil

response and motion perception (Iseri et al., 2006). Besides these alterations in the central visual pathway, retinal abnormalities appear also to occur in the AD and contribute to visual failure (Hinton et al., 1986, Sadun and Bassi, 1990, Blanks et al., 1989, Koronyo-Hamaoui et al., 2011, Chiu et al., 2012, Dehabadi et al., 2014, Tzekov and Mullan, 2014). Retinas of AD patients exhibit the typical Aβ and p-Tau hallmarks accompanied by a defective microvasculature, thinning of retinal layers and RGC loss (Liu et al., 2009, Williams et al., 2015). Aβ deposition, Tau pathology along with reactive gliosis and neuroinflammation, have been reported in the retina of transgenic animal models of AD (Ning et al., 2008, Liu et al., 2009, Cheung et al., 2014, Perez et al., 2009, Dutescu et al., 2009, Alexandrov et al., 2011, Gasparini et al., 2011, Edwards et al., 2014, Tsai et al., 2014, Grimaldi et al., 2018, Chiasseu et al., 2017). Furthermore, intraocular injections of Aβ have been previously shown to primary cause sub-RPE deposits, known as drusen constituted by cellular debris and lipids, high metal ions, inflammatory mediators and finally resulting in death of photoreceptors and whole retina (Liu et al., 2013). Aβ accumulation has been reported also in the retinal pigment epithelium (RPE) and vascular choroid of AD patients, affecting the same regions of AMD patients.

Parkinson's disease (PD) is a neurodegenerative condition characterized by intraneuronal aggregation of α-synuclein in the substantia nigra and progressive degeneration of dopaminergic neurons (DA). The visual alteration is one of the non-motor symptoms found in PD that can be identified in early stages, even before pathological manifestations of brain such as rigidity, tremor and bradykinesia (Devi et al., 2020). PD patients show colour discrimination, visual acuity, contrast sensitivity, blurred image, motion perception and blindness (Archibald et al., 2009, Bodis-Wollner, 2009, Bodis-Wollner, 1990). Depletion of dopamine content and α-synuclein accumulation have been observed specifically in the INL, IPL and GCL of the retina in PD patients (Aydin et al., 2018). It has been demonstrated that dopamine has a central role in the retinal development, visual signalling and refractive development, thus its abnormal change and reduction in the amacrine cells lead to alteration in RGC cells and consequent dysfunctional visual processing in PD patients (Djamgoz et al., 1997). Several studies have suggested that retinal imaging methods could be a potential early biomarker for PD (Devi et al., 2020).

Multiple sclerosis (MS) is an autoimmune disorder characterized by chronic inflammation and demyelination of the CNS. The pathological hallmark of MS is the formation of demyelinating lesions in the brain and spinal cord, which can be associated with neuro-axonal loss, progressive neurological disability and functional decline. Optic nerve fiber loss and degeneration of RGC cells are common events observed in the retina of MS patients (Levin et al., 2013, Graham and

Klistorner, 2017). In particular, a study has estimated that a common initial symptom of MS is the optic neuritis, considered the principal cause of permanent visual disabilities (Kale, 2016). Additional visual abnormalities in MS are retrobulbar pain on eye movement, proceeding to visual loss and dyschromatopsia. Also in this neurodegenerative disease, the OCT has proven to be a useful test for diagnosis and monitoring of inflammatory optic neuritis (Soelberg et al., 2018). Amyotrophic lateral sclerosis (ALS) is a neurodegenerative disease characterized by loss of the upper and lower motor neurons leading to a progressive muscle weakness and atrophy (Bruijn et al., 2004, Kiernan et al., 2011). Only recently, structural and functional changes in the visual system have been identified in ALS patients caused by degeneration of grey matter in the occipital cortex (Agosta et al., 2015). As extramotor features, oculomotor dysfunctions, visual acuity and contrast sensitivity are some of visual alterations observed in ALS disease (Sharma et al., 2011, Moss et al., 2012).

Iron, the heavy metal for life

Iron, the most powerful generator of free radical, is an essential element for life being a cofactor for numerous fundamental biological processes. Iron is needed to transport hemoglobin-bound oxygen and to produce the adenosine triphosphate (ATP) serving as a cofactor for enzymes of the citric acid cycle and electron transport chain (Poss and Tonegawa, 1997, Lill et al., 2012). Iron is also involved in the nitric oxide metabolism and in the DNA synthesis being required for the ribonucleoside reductase activity (Wigglesworth and Baum, 1988).

In mammalian organisms, numerous proteins are involved in the systemic iron homeostasis. Food is the source of iron, which is absorbed by the duodenum until it reaches the systemic bloodstream. Duodenal iron uptake is strictly regulated through different mechanisms. Two proteins can regulate this process: the divalent metal transporter 1 (DMT1) that regulates the iron uptake located at apical surface of polarized intestinal epithelial cells, and ferroportin 1 (FPN1) that regulates the export of iron at the basolateral membranes. Duodenal ferroportin can bind to hepcidin, a peptide hormone secreted by iron-loaded hepatocytes, triggering its own intracellular degradation and thus reducing the duodenal iron uptake. In addition, transcriptional expression of DMT1 is regulated by hypoxia inducible factor 2α (HIF2α), which coordinately regulates the transcriptional response to hypoxia and iron deficiency in the duodenal mucosa.

The membrane-bound ferroxidase, the hephaestin, oxidizes ferrous iron (Fe^{2+}) to ferric iron (Fe^{3+}), thus promoting iron binding with transferrin protein. The uptake of iron from the systemic circulation to most tissues is mediated by transferrin that usually binds two atoms of ferric iron per molecule forming holo-trasferrin. Subsequently, the transferrin binds to the transferrin receptor 1 (TFR1) expressed on the cellular surface leading to formation of the transferrin receptor-holo-transferrin complex that undergoes clathrin-mediated endocytosis (Figure 5).

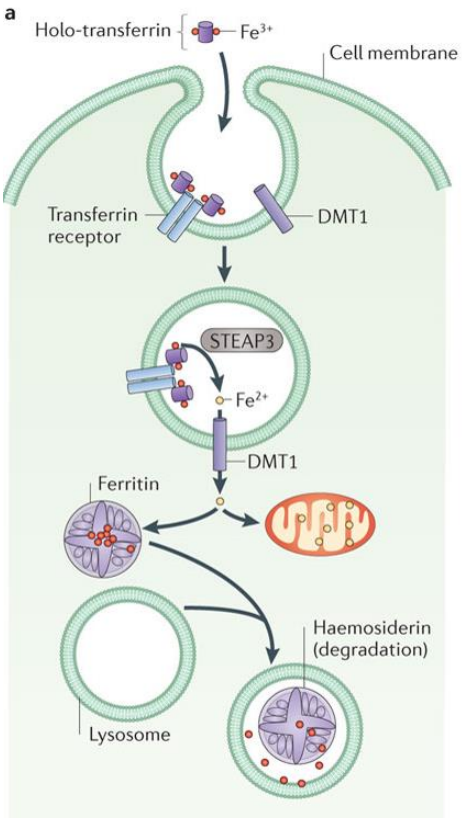

Figure 5. Cellular iron metabolism in mammalian cells. Ferric iron in the bloodstream circulation binds to transferrin to form holo-transferrin. Holo-transferrin binds to transferrin receptors on the cell surface and the transferrin receptor–holo-transferrin complex undergoes endocytosis mediated by clathrin-coated pit formation. The metalloreductase STEAP3 allows iron to be transported into the cytosol by DMT1. Iron can enter mitochondria or it can be stored in cytosolic proteins such as ferritin. Degradation of ferritin in lysosomes leads to the formation of disorganized iron-rich deposits known as haemosiderin (Rouault, 2013).

Following endosome acidification, the ferric iron is reduced to ferrous by endosomal metalloreductase STEAP3 and it is transported into the cytosol by DMT1 protein. In the cytosol, iron may bind to chaperones that donate iron to specific target proteins or may be directed to mitochondria where, through specific mitochondrial iron transporters (mitoferrin 1 or mitoferrin 2), it reaches the matrix and may be used for the synthesis of iron–sulphur clusters and haeme. Iron can also be stored by cytosolic ferritin, the iron storage protein, which can sequester up to 4,500 iron atoms transforming it in a non-reactive form, thus preventing free

iron from reaching high concentrations in the cytosolic and nuclear compartments. Iron stored with ferritin can be released following degradation of lysosomes bringing to the formation of disorganized iron-rich deposits known as haemosiderin. Intracellular storage iron may be exported in its ferrous state by the transport protein, ferroportin. For export and bind with transferrin, the iron must be oxidized and ceruloplasmin and hephaestin enzymes accomplish this. Ceruloplasmin is a copper binding protein, which contains over 95% of copper found in plasma. Central role in the iron export has been attributed to these ferroxidases and it has been observed that the alteration in one of these enzymes lead to cellular iron accumulation and subsequent tissue degeneration.

Iron and neurodegeneration

Iron is essential for central brain function inasmuch as it regulates many CNS processes. In particular, iron is a critical cofactor for enzymes involved in synthesis and metabolism of neurotransmitters including dopamine, norepinephrine, and serotonin. Iron is also requested in myelogenesis and myelin maintenance by oligodendrocytes, glial cells of CNS (Youdim, 1990, LeVine and Macklin, 1990, Morris et al., 1992). Iron deficiency has injurious effects on the brain development and neurocognitive functions (Crichton, 2016, Zhukovskaya et al., 2019). The iron homeostasis in the CNS is tightly regulated through the same proteins described for non-polarized cells with some exceptions. The BBB and the blood–CSF barrier limit free access of nutrients to cells of CNS, including iron. On the luminal side of the BBB, the iron uptake is mediated by transferrin receptor expressed by endothelial cells that binds the holo-transferrin circulating in the brain capillaries. The mechanisms of iron internalization are the same as those described for non-polarized cells, including endocytosis or transcytosis models (Figure 6). Conflicting data have been presented about the role of iron transporter ferroportin in the CNS, which seem to regulate the iron efflux in the brain microvascular endothelial cells and the entrance in the interstitial fluid (Wu et al., 2004, McCarthy and Kosman, 2013, Moos et al., 2007). Alternatively, iron goes through the choroid plexus to the ventricle bound to transferrin, and diffuses in between ependymal cell (Rouault et al., 2009). In interstitial fluid and cerebrospinal fluid, the iron seems to be acquired by neurons and glial cells through the

transferrin receptors and holo-transferrin. All glial cells express the iron-related proteins so regulating brain iron homeostasis. Oligodendrocytes together with the cells of the choroid plexus synthesize high quantity of the transferrin protein that it is secrete in the brain interstitial fluid (Zakin et al., 2002).

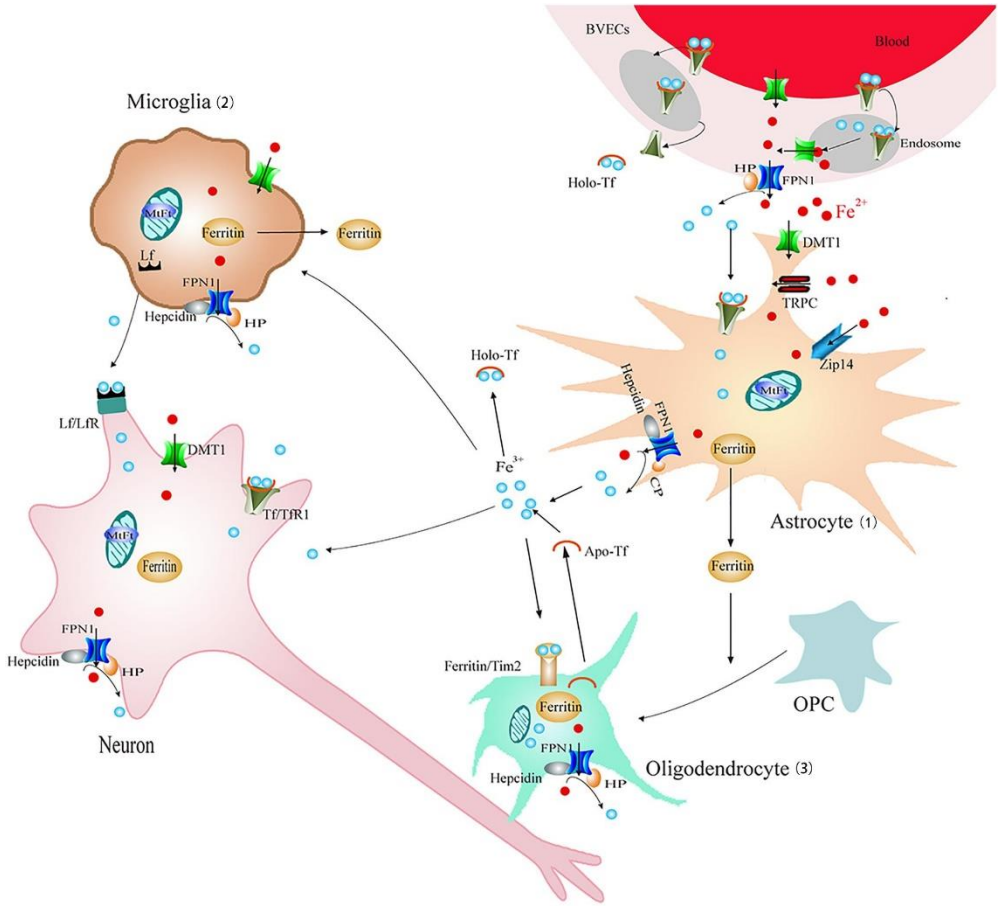

Figure 6. Brain iron metabolism. Iron could cross BBB through endocytosis of holo-Tf, followed by iron detachment from Tf inside endosomes and FPN1-mediated iron efflux or transcytosis of holo-Tf through the BVECs. Astrocytes (1), microglia (2), and oligodendrocytes (3) express all different iron-related proteins responsible for iron uptake, storage, use and export (Xu et al., 2018).

The astrocytes are involved in the formation of BBB by covering about 95% of the brain capillary surface with their end-feets. Therefore, astrocytes play a central role in the iron transport across BBB (Dringen et al., 2007). In addition, these cells express the ferroxidase ceruloplasmin, which may facilitate the export activity of ferroportin on adjacent cells (Kono, 2012). Also numerous studies have reported that microglia plays a key role in the brain iron homeostasis, requiring iron as co-factor to perform its different and important functions [1,27,28]. Furthermore, it has been observed that glia can store iron more efficiently compared to neurons and, among them, microglia is considered the most efficient in the non-transferrin-

bound iron accumulation (Bishop et al., 2011). In addition, several studies have found that the excess of iron could cause the activation of microglial and astroglial cells promoting the release of inflammatory and neurotrophic factors and changing iron metabolism of the neurons (Zhang et al., 2014b).

Iron levels increase with age in certain human tissues and many studies have suggested that the brain iron overload can lead to the development of neurodegenerative diseases (Crichton and Ward, 2013). Although iron is essential for the survival of cells, its excess is toxic leading to release of reactive oxygen species (ROS) via the Fenton reaction and consequently to oxidative damage. In this reaction, free ferrous iron (Fe^{2+}) reacting with hydrogen peroxide (H_2O_2) is oxidized to ferric iron (Fe^{3+}) producing hydroxyl ion (OH-) and hydroxyl radical (OH·), the most reactive and dangerous of the reactive oxygen species. Free radical species can damage lipids, proteins and nucleic acids causing lipid peroxidation, protein aggregation and DNA damage (Halliwell and Gutteridge, 1984). Alterations in iron homeostasis have been implicated in the pathogenesis of several CNS neurodegenerative diseases, such as ALS, Friedreich's ataxia, PD and AD (Andersen et al., 2014, Rouault, 2013, Dev and Babitt, 2017, Liu et al., 2018). Furthermore, several studies have demonstrated that, in several neurodegenerative diseases, the iron overload is accompanied by the presence of iron-positive microglial cells at the focal point of the lesions, which are activated and stimulated to release of pro-inflammatory cytokines and free radicals (Thomsen et al., 2015, Nnah and Wessling-Resnick, 2018).

The underlying mechanisms of AD are still puzzling; it is still a matter of debate the "amyloid cascade hypothesis" according to which amyloid is an initialling pathogenic factor of AD, and it is doubted whether amyloid may alone completely explain the neuronal loss (Struble et al., 2010). Several lines of evidence support the hypothesis that metals, such as copper, iron, zinc and magnesium, are important contributing factors in AD pathology (Cristovao and Santos, 2016, Wang and Wang, 2017). It has been suggested that metal ions play a role in Aβ fibril formation and, therefore, alterations in their homeostasis influence Aβ deposition in senile plaques as well as NFTs formation. Numerous studies have evaluated the strict association between brain iron dyshomeostasis and AD (Peters et al., 2015, Ayton et al., 2013). It has been shown that Aβ plaques co-localize with focal iron deposition in postmortem AD tissues as well as in several AD mouse models (Smith et al., 1996, Connor et al., 1992, Collingwood et al., 2008, Peters et al., 2015, Meadowcroft et al., 2009, Tayara et al., 2006, Chamberlain et al., 2011). Moreover, altered regulation of proteins involved in iron metabolism have been observed around Aβ plaques in AD cortical tissue. In addition, Aβ can bind Fe^{3+} and incorporation of Aβ fibrils into plaques appears to be accelerated in an iron-enriched environment (Bush, 2002). Aβ

plaques containing iron become more prone to catalytic redox activity and therefore associated with endoplasmic reticulum stress, apoptosis, oxidative stress and cellular damage (Rottkamp et al., 2001). Additionally, in regions where Aβ plaques accumulate and no iron is present, no oxidative stress or apoptosis have been detected, suggesting the importance of iron accumulation in and around plaques in promoting the cellular damage (Ghribi et al., 2006). In addition, iron may modulate APP processing, by putative iron-responsive elements (IREs) in APP mRNA thus enhancing the expression of endogenous APP (Cahill et al., 2009).

Alterations in brain iron homeostasis have been also detected in Parkinson's disease (Xu et al., 2018). Several reports have demonstrated that iron levels were significantly higher in the substantia nigra (SN) of PD patients compared to normal subjects and subsequently implicated in numerous neurological disorders with symptoms of Parkinson disease. These levels have been associated with the severity of motor symptoms (Wang et al., 2007, Jiang et al., 2017, Song et al., 2010, Martin et al., 2008, Guan et al., 2017). A growing body of evidence suggests that glial population may play a critical role in the pathophysiology of PD. In particular, several studies have demonstrated that activation of microglia in the SN, probably due to the presence of Lewy bodies and accumulation of α-synuclein, is responsible for initiating an inflammatory process that may contribute to the degeneration of dopaminergic neurons (Ransohoff, 2016). In correlation with this, elevated levels of pro-inflammatory cytokines, such as interleukin-1β (IL-1β) and tumor necrosis factor-α (TNF-α), have been found in the cerebrospinal fluid, SN and striatum in post-mortem of PD patients (Mogi et al., 1994). Moreover, it was found that iron have a pivotal role in the aggregation of phosphorylated aSyn and depletion of dopaminergic neurons also in the retinal cells of PD patients (Funke et al., 2013).

Iron homeostasis in the retina

Iron has a critical role also in the retina regulating the retinal metabolism and the visual cycle phototransduction cascade (Dunaief, 2006, Blasiak et al., 2011, Song and Dunaief, 2013). Several retinal proteins require iron as cofactor, among them, the RPE65, an isomerohydrolase expressed by RPE cells and implicated in the regeneration of 11-cis retinol in the visual cycle (Moiseyev et al., 2005). Iron is also a cofactor for the enzyme guanylate cyclase, which synthesizes cGMP, the second messenger in the phototransduction pathway (Yau and Baylor, 1989). Furthermore, fatty acid desaturase, an iron-containing enzyme necessary for the synthesis of membrane lipids, is heavily required by photoreceptors to constantly release and synthesize their outer segment containing disc membranes (Shichi, 1969).

While iron is required for retinal function, its excess can be dangerous. Due to intense tension and metabolism of oxygen as a result of constant exposure sunlight and the presence of high concentrations of oxidized polynsatured fatty acids in the photoreceptors, the retina is one of the most susceptible tissues to oxidative stress to which iron can contribute. For this reason, the regulation of iron retinal homeostasis is extremely crucial to reduce the excessive levels of free radicals, responsible of lipid peroxidation, RNA/DNA oxidation, protein misfolding, glial activation and retinal cell death (Chen et al., 2012, Li et al., 2013). It has also been observed that excessive iron impairs the regular phagocytosis of shed OS made by RPE that plays a critical role in sustaining/maintaining of excitability and subsequent survival of photoreceptors (Yefimova et al., 2002).

As an integral part of the CNS, the retina is isolated from the systemic circulation by BRBs, the iBRB and oBRB, that prevent intercellular diffusion and preserve its integrity. Regarding the regulation of iron homeostasis in the retina, immunohistochemical studies have revealed that RPE structure is the main site of transferrin synthesis, which is also expressed in the IS and OS of photoreceptors and in the inner retina (Figure 7). Transferrin receptor 1 (TfR1) has been detected in several retinal layers, including the GCL, INL, OPL, IS of photoreceptors and in the basolateral and apical surfaces of RPE cells. It has been suggested that this receptor may be responsible of iron bidirectional flow through its endocytosis in the RPE cells. In accordance with this, it is believed that transferrin-bound iron in the choroidal circulation could be captured by high affinity transferrin receptors at the basolateral surfaces of RPE cells. Then, this complex is internalized into a low pH endosome, where iron can dissociate from transferrin. Iron enters a cytoplasmic pool of ferritin-bound iron, where it can bind to ferritin or be further processed.

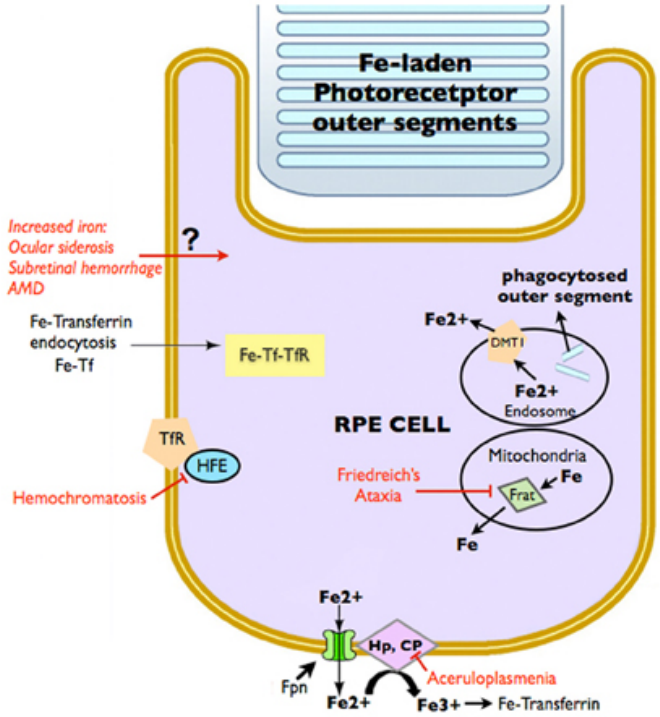

Figure 7. RPE iron metabolism. Proteins involved in iron transport and several diseases that disrupt retinal iron transport are illustrated. Abbreviations here: Cp,ceruloplasmin; DMT1, Divalent metaltranporter-1; Fe,iron; Fe^{2+}, ferrousiron; Fe^{3+}, ferriciron; Fpn, ferroportin; Frat, Frataxin; HFE,histocompatibility leukocyte antigen class I- like protein involved in iron homeostasis; Hp, Hephaestin; Tf, transferrin; TfR, Transferrin receptor (Song and Dunaief, 2013).

Iron is transported to the apical surfaces of RPE cells, where it is released to the neuroretina via a Tf-TfR-dependent mechanism. Among proteins involved in the retinal iron import, there is DMT1 protein that is expressed in the IS of photoreceptors, rod bipolar cells (bodies and axons) and horizontal cells (He et al., 2007). The portions of the retina with the highest iron levels coincide with the regions of ferritin expression, the principal protein involved in intracellular iron storage. Ferritin is expressed in RPE phagosomes, choroid, INL, GCL, and in the disc membranes of photoreceptors (IS) (He et al., 2007, Yefimova et al., 2002). The strong immunolabeling of ferritin in the INL suggests that ferritin may have a crucial role in the iron transport or storage in the presynaptic terminals of the rod bipolar cells (Hahn et al., 2004b). In the retina, ferroportin is also present at high levels in the endfeet of Müller cells and in the RPE (He et al., 2007), in addition to other less conspicuous locations, including IS of photoreceptors, IPL, OPL and GCL (Hahn et al., 2004a). In the RPE, the localization is primarily basolateral, suggesting that the ferroportin may facilitate iron export from RPE into choroidal capillaries (He et al., 2007). In addition, ceruloplasmin and hephaestin are also co-expressed with ferroportin in RPE and Müller cells collaborating with this protein in the oxidation and export

of iron (Hahn et al., 2004b). Hepcidin is an iron-regulatory hormone that has the ferroportin as target. Recent studies have demonstrated that hepcidin is detectable throughout the retina showing its abundant level of expression in the Müller cells, photoreceptors, and RPE cells (Gnana-Prakasam et al., 2008). It has been supposed that the hepcidin originated from the retina may play a key role in the regulation of ferroportin in the inner retina independent of the liver-derived hepcidin, but still little is known about its function (Gnana-Prakasam et al., 2008, Gnana-Prakasam et al., 2010).

Iron and retinal degenerative diseases

Several lines of evidence suggest that alterations in retinal iron metabolism may cause a variety of retinal diseases, such as ocular siderosis, subretinal haemorrhage, aceruloplasminemia, hemochromatosis, Friedreich's ataxia and age-related macular degeneration (AMD) (Song and Dunaief, 2013, Dunaief, 2006, Wong et al., 2007, Blasiak et al., 2011).

AMD represents the principal cause of irreversible visual impairment among people over the age of 40 in western countries (Congdon et al., 2004). AMD is a multifactorial and progressive degenerative disorder that affects the maculae, a well-defined region of the retina responsible for the central and "high-resolution" vision. Early stage is associated with the formation of pathologic deposits referred to as drusen, between the Bruch's membrane and the RPE that cause functional changes of the RPE. Biochemically, drusen contains lipids, inflammatory mediators, metals and glycoproteins (Crabb et al., 2002). As the disease progresses, patients may develop geographic atrophy in non-exudative AMD (or dry AMD) and choroidal neovascularization in exudative AMD (or wet AMD); both AMD forms are characterized by loss of photoreceptors and severe visual impairment. Currently, there is no treatment available for the dry form of AMD. The only effective and promising therapeutic strategy is directed to AMD wet form by blocking the VEGF expression. Patients receive the anti-VEGF antibody treatment via an intravitreal injection at regular intervals with a high risk of adverse effects (Stewart, 2014, Farnoodian et al., 2017). VEGF plays a critical role in the pathogenesis of neovascular AMD and increased expression levels of VEGF-A were found in the RPE and in the ONL of AMD patients (Kliffen et al., 1997). VEGF participates in many physiological and

pathological events, including vasculature formation, cell proliferation, inflammation and angiogenesis and is also implicated in the development of several ophthalmic diseases(Abu El-Asrar et al., 2013, Cornel et al., 2015).

One of the major risk factor associated with AMD is the age, but oxidative stress is also prominently involved in the AMD pathogenesis. Several scientific reports have suggested that iron may be the principal source of oxidative stress in AMD disease (Song and Dunaief, 2013). Higher levels of iron have been found in retinas of AMD patients compared to retinas of healthy age-matched subjects (Hahn et al., 2003). Specifically, iron deposits was found by Perl's staining in the RPE and Brunch's membrane of AMD patients at different stages of disease; only in AMD patients with advanced geographic atrophy was detected iron accumulation in the photoreceptors (Dentchev et al., 2005, Hahn et al., 2006). Although iron overload has been observed in ocular structures of AMD patients, it is unclear if iron is directly involved and contributes to AMD pathogenesis or it is a secondary effect. In support of the direct role of iron in AMD disease, several experimental evidences have been shown in AMD patients as well as in animal models of AMD and they are listed below. Retinal levels of iron increase with age in humans (Hahn et al., 2003, Hahn et al., 2006) and rodents (Chen et al., 2008, Chen et al., 2009). Furthermore, intraocular implantation of iron particles or direct injections of iron cause retinal degeneration (Rogers et al., 2007, Burger and Klintworth, 1974, Wang et al., 1998). In particular, iron sulfate intravitreal injections in adult C57BL/6 mice resulted in increased superoxide radicals in the IS of photoreceptors, lipid peroxidation of the photoreceptors and retinal degeneration characterized by selective loss of cones (Rogers et al., 2007). Furthermore, retinal explants subjected to iron sulphate insult are considered a good model for the study of oxidative stress-induced retinal degeneration (Rodriguez Diez et al., 2012, Rodriguez Diez et al., 2013). Retinal iron overload is observed in mice carrying mutations in genes involved in iron metabolism (Cp/Heph; Ceruloplasmin and Hephaestin), which showed AMD-like retinal abnormalities, including sub-RPE deposits, RPE disorganization (hypopigmentation and hypertrophy) and RPE lysosomal and phagosomal inclusions (Hahn et al., 2004b, Hadziahmetovic et al., 2008). The transgenic mice lacking both Cp and Heph (Cp −/− Heph −/Y) also developed activation of oxidative stress, subretinal macrophage infiltration, progressive RPE degeneration, subsequent focal loss of photoreceptors and subretinal neovascularization, typical feature of advanced stage of AMD (Hadziahmetovic et al., 2008, Hahn et al., 2004b). In addition, rats carrying mutations in the receptor tyrosine kinase Mertk, involved in the interactions between RPE and photoreceptors, showed RPE inability to phagocytise shed outer segments and the development of a layer of undigested outer segment

in the subretinal space (Yefimova et al., 2002). These animal models were characterized by decreased levels of transferrin in the photoreceptor layer, iron overload in the debris layer and resulting photoreceptor loss (Yefimova et al., 2002). Other lines of evidence suggest a central role of iron in the AMD pathogenesis. Elevated levels of transferrin expression have been found in retinas of AMD patients (Chowers et al., 2006), especially revealed in photoreceptors, Müller cells, and drusen deposits. In addition, hereditary disease aceruloplasminemia causes retinal iron overload with retinal degeneration and early onset subretinal lesions, similar to drusen in AMD patients (Dunaief et al., 2005). This degeneration primarily involves RPE cells characterized by hypo- and hyper-pigmentation, autofluorescence and sub-RPE and subretinal deposits (Wolkow et al., 2011).

Although the mechanism of iron overload in AMD disease is unknown, many evidences supposed that its retinal toxicity is caused by the activation of oxidative stress, inflammation, hypoxia and impairment of RPE phagocytosis (Ugarte et al., 2013).

Oxidative stress and inflammation in the retinal degenerative diseases

Oxidative stress is considered the main contributor to the development and progression of multiple neurodegenerative diseases, such as ALS, PD and AD and Huntington disease (Niedzielska et al., 2016).

Oxidative stress and neurodegeneration are also involved in retinal degenerative disorders (Chen et al., 2012, Blasiak et al., 2014, Cuenca et al., 2014, Masuda et al., 2017).

Aging, gene abnormalities and exposure to exogenous oxidative stressors cause an increased risk of oxidative damage in the eye (Zhou et al., 2011, Hanus et al., 2015, Cai et al., 2000, Cai and McGinnis, 2012). Among the exogenous sources of ROS, the cigarette smoking has been considered capable to increase the lipid peroxidation, induce alterations to mitochondrial integrity and cause the death of RPE cells. It has been observed that nicotine may cause the release of nitric oxide (NO) and consequent increase in the expression of proangiogenic factors in the RPE (Pons and Marin-Castaño, 2011, Deisinger, 1996). Moreover, smoking appears to be one of the most important risk factors in the development of AMD (Khan et al., 2006,

Tomany et al., 2004). In addition, the continuous light exposure can contribute to ocular oxidative stress causing RPE disruption and the reduction of the retinal autofluorescence, an indication of lipofuscin photooxidation (Morgan et al., 2009, Hunter et al., 2012, Putting et al., 1992). In particular, light damage is widely used as a model of oxidative damage-induced retinal degeneration, characterized by photoreceptor loss and closely associated with AMD (Grimm and Remé, 2013, Marc et al., 2008, Chalam et al., 2011).

Oxidative damage has been also implicated in the pathogenesis and progression of AMD (Beatty et al., 2000, Winkler et al., 1999). There are several evidences to support this hypothesis: (i) the presence of many oxidized proteins in the drusen deposits from eyes of AMD patients, including the advanced glycation end-products (AGEs) and carboxyethyl pyrrole adducts (produced by the oxidative modification of fatty acids in photoreceptors) (Crabb et al., 2002, Farboud et al., 1999); (ii) the administration of antioxidant vitamins and/or Zn significantly may delay the progression of advanced AMD or vision loss due to AMD (2001); (iii) protective effects observed following the free radical scavengers treatment as therapeutic strategy for treatment of diverse animal models of AMD (Masuda et al., 2016, Masuda et al., 2017). Although the excessive amount of ROS has been shown to be in close correlation with AMD, the antioxidant defense pathways are also believed to play a key role in this disease. In this regard, it has been observed that the decrease in the activation of the nuclear factor erythroid 2- related factor 2 (Nrf2) pathway may cause an increase of vulnerability to oxidative damage in aging RPE cells (Sachdeva et al., 2014).

Oxidative stress is closely linked to inflammation as well (Biswas, 2016, Tsubota, 2007). It has been reported that intracellular and extracellular ROS production in human RPE cells is induced by the expression of inflammatory cytokines, such as tumor necrosis factor-α (TNF-α), interleukin-1β (IL-1β), or interferon-γ (IFN-γ) (Yang et al., 2007). Indeed, these proinflammatory cytokines are upregulated in the eyes of patients with glaucoma, DR and AMD (Kauppinen et al., 2016, Vohra et al., 2013, Rubsam et al., 2018).

The processes of inflammation and angiogenesis are intimately linked and several studies have demonstrated that, in particular, the cytokine TNFα plays a major role in several retinal vascular diseases, such as DR and AMD, acting through various pathogenic pathways, such as endothelial and retinal cell injury, apoptosis, angiogenesis and vascular leakage (Al-Gayyar and Elsherbiny, 2013). Moreover, RPE interacts with endothelial cells (ECs) directly and can enhance the proangiogenic potential of the ECs, such as proliferation and migration. For example, it have been observed that TNF-α has proangiogenic effects in RPE cells by

upregulating VEGF expression, the principal activator of angiogenesis, via the ROS-dependent β-catenin activation (Wang et al., 2016a). ROS also cause the dimerization and autophosphorylation of the principal VEGF receptor, the VEGF receptor 2 and, conversely, VEGF further stimulates ROS production through the activation of NOX in endothelial cells (Maraldi et al., 2010).

Furthermore, it has been demonstrated that neuroinflammation is intimately tied to iron metabolism, being accompanied by the downregulation of iron-interacting proteins and accumulation of intracellular iron, in turn strongly associated with oxidative stress and neuronal degeneration, as described above (Thomsen et al., 2015, Wessling-Resnick, 2010). In addition, the inflammatory cytokines, TNF-α and IL-1β, secreted by microglial cells can lead to an increase in neuronal iron uptake (Wang et al., 2013). Several reports have shown that pro-inflammatory mediators strongly influence the microglia iron transport and metabolism (Thomsen et al., 2015, Urrutia et al., 2013).

In the retina, microglia constitutes an important component of the immune system, playing a key role in the initiation and maintenance of the neuroinflammation. Therefore, chronic activation of microglia seems to be implicated in diverse retinal diseases, due to their excessive release of inflammatory mediators and subsequent neuronal cell death (Vecino et al., 2016, Madeira et al., 2015, Langmann, 2007), thus representing a potential therapeutic target that could be modulated in the treatment of retinal degenerative diseases (Karlstetter et al., 2015).

Oxidative damage, inflammation and, in some conditions, angiogenesis and increased vascular permeability have been associated with the pathogenesis of most ocular diseases including AMD disease (Majumdar and Srirangam, 2010). Therefore, ideal therapeutic strategies for eye disorders should have the ability to act on the several pathological pathways just described.

Therapeutic approaches for posterior retinal degenerative diseases (flavonoids)

To date, the identification of targeted therapies for retinal diseases is one of the greatest challenges in the biomedical research. There are numerous natural compounds containing active components with advantageous properties that may be useful in the prevention and treatment of many ocular disorders (Cuenca et al., 2014, Huynh et al., 2013, Chu and Pang, 2014).

The bioflavonoids are a group of plant polyphenols considered as potential therapeutic agents in the prevention and treatment of ocular disorders (e.g. diabetic retinopathy, macular degeneration and cataract) (Majumdar and Srirangam, 2010). The poor solubility as well as the intestinal and hepatic metabolism limit the oral bioavailability of flavonoids, also at the ocular level.

Silibinin (Slb) is the main constituent of the Silymarin, a flavonoid mixture extracted from the milk thistle seeds (*Silybum marianum Gaertneri*). Numerous biological activities have been attributed to Slb, including cardio- and hepato-protective, antitumor, antioxidant, anti-inflammatory and neuroprotective effects (Gazak et al., 2007, Karimi et al., 2011, Surai, 2015, Esmaeil et al., 2017).

The cytoprotection activities of Slb due to its antioxidant and radical scavenging activities have been documented in the field of various pathologies, including cancer, nephro- and hepato-toxicity, lung and prostate diseases (Karimi et al., 2011). Furthermore, several studies have reported that oral or systemic administration of Slb exerted neuroprotective effects in *in vivo* experimental models of cerebral ischemia injury,(Hou et al., 2010, Wang et al., 2012, Liu et al., 2014, Wang et al., 2016b), diabetes (Marrazzo et al., 2011, Tota et al., 2011), neurotoxicity induced by different insults including aluminium (Jangra et al., 2015), 1-methyl-4-phenylpyridinium ion (MPP+) (Jung et al., 2014, Geed et al., 2014, Lee et al., 2015), ethanol (Das and Mukherjee, 2012), iron-overload (Chen et al., 2015) and amyloid β (Lu et al., 2009, Duan et al., 2015, Song et al., 2017).

The Slb protective effects have also been attributed to its ability to reduce inflammation. Indeed, this flavoinoid has been described to exhibit potent anti-inflammatory effects and different immunomodulatory activities (immunostimulatory and immunosuppression) in a dose and time-dependent manner. It has been demonstrated that Slb may suppress the expression of

diverse inflammatory mediators, including TNF-α, IL-1β, IL-6, cyclooxygenase-2, COX-2, prostaglandin E2 and PGE2, by affecting of NF-κB signaling (Esmaeil et al., 2017). Besides, direct inhibition on glial activation and proliferation has been attributed to neuroprotective effects of Slb in mesencephalic and spinal mixed neuronal-glial cultures subjected to different injuries (Tsai et al., 2010, Wang et al., 2002). In addition, it has also been reported that Slb is capable to ameliorate learning and memory impairment and reduce proinflammatory cytokines and amyloidogenesis in some nervous structures of lipopolysaccharide (LPS)-induced animal model (Song et al., 2016, Joshi et al., 2014).

In the ophthalmic field, it has been observed that Slb attenuates ocular inflammation in RPE cells and macrophages cell cultures by inhibitory effects on ICAM-1 expression deregulating the activated NF-kB and STAT1 pathways. In addition, it has been shown that the treatment with intraperitoneal injection of Slb is able to reduce cell infiltration and the increased expression of multiple proinflammatory mediators in *in vivo* model of uveitis (Chen et al., 2014, Chen et al., 2017). The anti-angiogenic effects of Slb have also been shown in terms of direct inhibition of VEGF secretion and VEGFR2 expression in several cell cultures and tumour models (Deep et al., 2012, Nambiar et al., 2013, Yoo et al., 2004, Deep et al., 2017, Ramasamy et al., 2011). These observations are in broad agreement with previous work by Lin et al., who reported antiangiogenic potential of Slb in the eyes. In particular, it has been observed that Slb reduced the VEGF expression on ARPE-19 cells subjected to hypoxia. In addition, Slb oral treatment rescued retinal neovascularisation in AMD animal model subjected to VEGF-injection and exposed to hypoxia, thus suggesting the Slb as possible therapeutic agent for AMD disease (Lin et al., 2013). Moreover, it have been demonstrated the protective effects of Slb in Streptozotocin-induced diabetic model, in which it has been capable to reduce vascular damage, retinal leukostasis and the retinal expression of ICAM-1 (Zhang et al., 2014a).

Silibinin, belonging to the group of Biopharmaceutics Classification System (BCS) class II drugs, has high permeability and poor solubility in the water (0.4mg/ml in H_2O) and, similarly to other flavonoids, is characterised by low bioavailability and fast metabolism (Zhu et al., 2013, Wu et al., 2007). When administered orally, Slb is metabolized rapidly via phase II enzymes (Kren et al., 2013, Lorenz et al., 1984) and therefore its fast elimination, in addition to low absorption, reduces 10-100-fold the concentration of its active form in the target tissues compared with the given dose (Surai, 2015). Therefore, several nanostructurated formulations have been proposed to enhance the bioavailability of Slb, such as lipid microspheres, self-micro emulsifying, phospolipid complex and nanostructured lipid carriers (Wang et al., 2014, Sahibzada et al., 2017).

Until now, oral and intraperitoneal routes are the only ways of Slb administration investigated for the treatment of ocular diseases (Lin et al., 2013, Zhang et al., 2014a, Chen et al., 2017). In particular, beneficial effects of Slb have been demonstrated in diabetic retinopathy complications (Marrazzo et al., 2011, Tota et al., 2011, Zhang et al., 2014a), in experimental models of AMD (Lin et al., 2013), uveitis (Chen et al., 2017), retinal and cerebral ischemia (Hou et al., 2010, Wang et al., 2012, Liu et al., 2014, Wang et al., 2016b). No data exist about ocular treatment using topical administration of Slb.

Biological barriers of the eye and ocular drug delivery systems

Ophthalmic drug delivery is one of the greatest challenges facing the scientific community and pharmaceutical companies hampered by particular anatomy and physiology of the eye. The drug delivery to the targeted ocular tissues is limited by ocular barriers, including static barriers (cornea, sclera, retina and BRBs) and dynamic barriers (choroidal and conjunctival blood flow, lymphatic clearance and tear dilution). For the treatment of anterior or posterior segment diseases, the routes of drug administration are different, including topical and systemic administration and periocular and intravitreal injections (Figure 7).

Topical administration is the most common route used for the treatment of anterior segment diseases. Conversely, topical formulations, such as eye drops, are inefficient for drug delivery into the posterior segment of the eye (neuroretina, RPE and choroid) (Figure 1), due to the pre-corneal factors and anatomical barriers (Mannermaa et al., 2006).

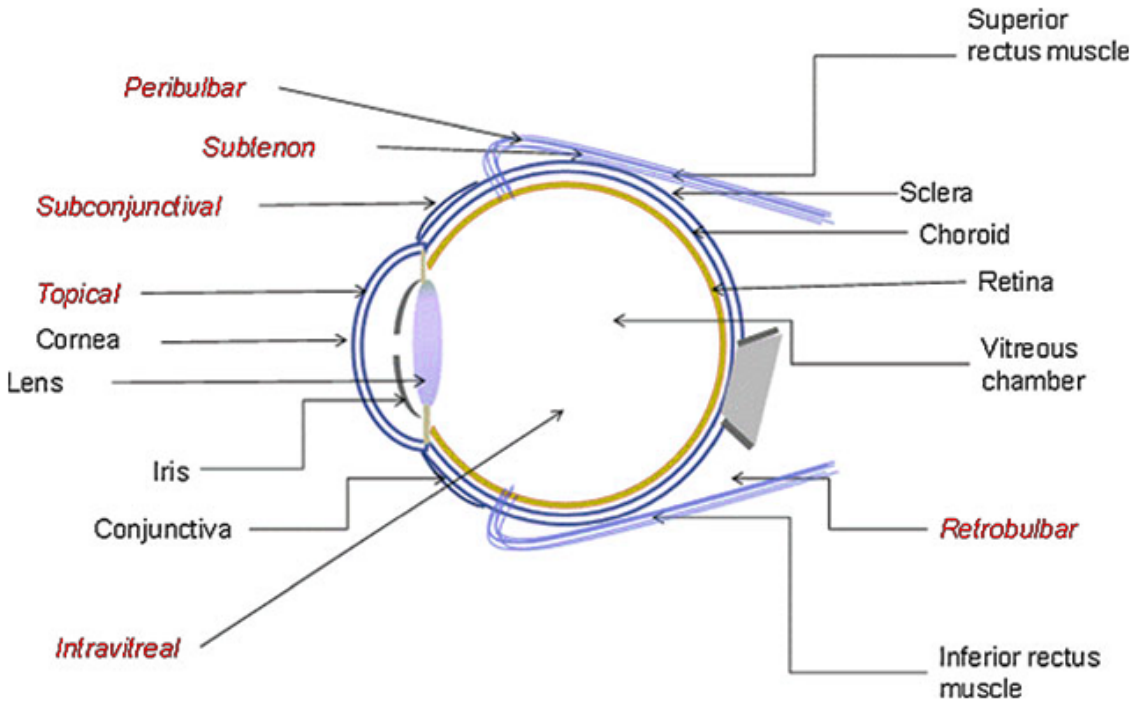

Figure 7. Routes of drug administration to eye (Gaudana et al., 2010).

Pre-corneal factors include drainage, blinking, tear film and tear turn over (Gaudana et al., 2010). The tear film is the first tissue of the eye to interact with the external environment and the first resistance of drug permeation determined by its high turnover rate (Figure 8). The hydrophilic layer of the pre-corneal tear film contains various factors, such as nutrients, electrolytes, proteins lipids and mucin. The ocular surface epithelia express glycosylated mucins, which provide lubrication, maintain the hydration of the ocular surface, and show antiadhesive and protective properties by removing debris and pathogens (Watanabe, 2002, Gipson and Argueso, 2003). After passing the tear film barrier, to reach deeper ocular tissues, drugs administered topically are faced with another important barrier, the cornea that consists of several layers with different polarity and potential rate-limiting for drug permeation: epithelium, Bowman's layer, stroma, Descemet's membrane and endothelium (Figure 8) (Li et al., 2018) .

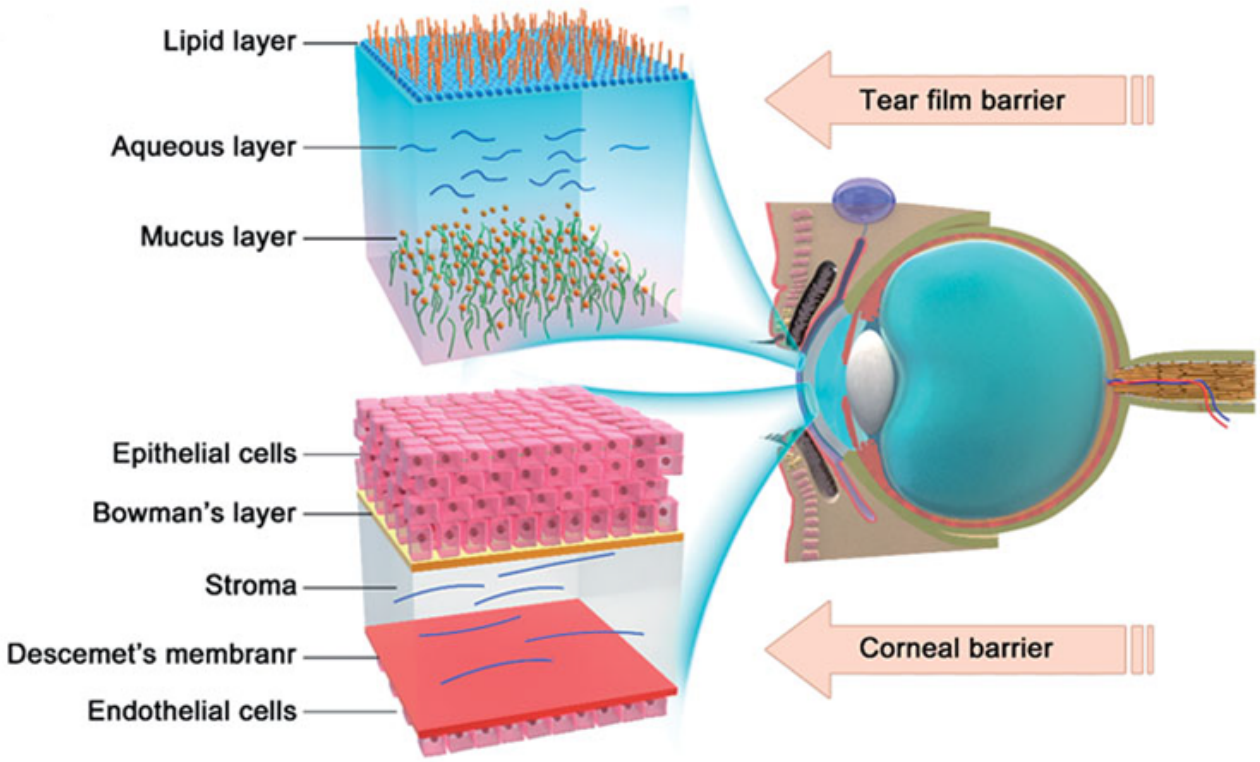

Figure 8. Two major barriers to topical ocular drug delivery. Tear film barrier: a high tear turnover rate and gel-like mucus layer. Corneal barrier: tight junctions in the corneal epithelial cells and alternating polarity five-layer structure (Li et al., 2018)

An efficient resistance for permeation of topically administered hydrophilic drugs is provided by lipophilic corneal epithelium, which hampers paracellular diffusion of macromolecules from the tear film into inner layers of the cornea with the presence of ribbon-like intercellular tight junctions (zonula occludens). The corneal stroma comprises 90% of the corneal thickness and it is composed by highly hydrated collagen fibrils and proteoglycans immersed in an organized matrix with interspersed cells (keratocytes). This biostructure permits only the diffusion of hydrophilic molecules up to 500 kDa of size, restricting the entry of most lipophilic drugs (Wadhwa et al., 2009). Lastly, the corneal endothelium is a monolayer of hexagonal-shaped cells between the stroma and aqueous humor. This layer has a central role in maintaining the aqueous humor and corneal transparency through its selective carrier-mediated transport and secretory functions (Barar et al., 2008). Furthermore, the leaky tight junctions of the corneal endothelium facilitate the passage of macromolecules (dimensions up to about 20 nm) between the aqueous humor and stroma (Sunkara and Kompella, 2003). Thus, corneal layers, particularly the epithelium and stroma, are considered as major barriers for ocular delivery of topically administrated drugs. In general, the corneal route represents the main pathway of absorption for

most ophthalmic therapeutic strategies, although the process is limited by the presence of the corneal epithelium (Macha et al., 2003, Ghate and Edelhauser, 2006).

The second pathway involves diffusion across non-corneal route (the conjunctival/scleral pathway) into the intraocular tissues. The conjunctiva is a thin and transparent mucous membrane covering the anterior surface of the sclera. The conjunctiva has a rich vasculature (blood capillaries and lymphatics), which plays an important role in drug delivery triggering to significant drug loss into the systemic circulation and thus reducing ocular bioavailability from target sites. Conjunctival epithelial tight junctions can further retard passive transport of hydrophilic drugs (Saha et al., 1996). The sclera is continuous with the cornea and extends posteriorly from the limbus. It is structurally and functionally similar to the corneal stroma consisting of collagen fibers and proteoglycans embedded in an extracellular matrix. A reduced number of vessels are present with the function of regulation of scleral permeability, which is comparable to that of the corneal stroma. The permeability across the sclera is low for positively charged molecules, probably due to their binding to the negatively charged proteoglycan matrix (Kim et al., 2007) and it is inversely proportional to the molecular radius (Geroski and Edelhauser, 2001).

For the treatment of posterior ocular diseases, the ocular bioavailability of topically applied ophthalmic drugs is, therefore, extremely low, typical less than 5% of the total drug administrated (Gaudana et al., 2010, Urtti, 2006).

To overcome these anatomical barriers and enhance ocular drug bioavailability, the main prerequisite is a prolonged preocular residence of the drug delivery system and enhanced corneal permeability (Perri et al., 2015). Thus, the development of novel topical administration formulations that enhances the ocular penetration of eye drops remains one of the most challenging tasks in ophthalmic drug delivery (Mannermaa et al., 2006).

Among other routes of drug administration, the oral one is, together to topical delivery, a non-invasive and patient preferred route for treatment of chronic retinal diseases, as for example in the glaucoma therapy. Usually, a high dosage is required to observe a significant therapeutic response in the eyes after oral administration, due to limited accessibility to the eye target. However, a high dosage of oral drugs can cause systemic toxicity. Following systemic administration, the blood–aqueous barrier and blood–retinal barrier are the major barriers for anterior segment and posterior segment ocular drug delivery, respectively. Two discrete cell layers form the blood–aqueous barrier: the endothelium of the iris/ciliary blood vessels and the non-pigmented ciliary epithelium. Both of these cell layers express tight junctional complexes

that prevent non-specific passage of solutes into the intraocular environment, permitting to maintain the transparency and chemical composition of the ocular fluids (Barar et al., 2008). Blood–retinal barriers strictly restrict the drug permeation from blood into the posterior segment including the retina. The structure of these ocular barriers has been previously discussed. The tight junctions of the RPE (oBRB) efficiently limit intercellular permeation of drugs. Drugs administered systemically or orally can easily enter into fenestrated choriocapillaris.

A compromise between risks and benefits has been obtained using the periocular administration (peribulb, posterior juxtasclerar, retrobulbar subtenon and subconjiuctival), that is considered more effective and safer than topical or systemic administration, although less efficient than intravitreal route for drug delivery to the posterior ocular tissues. The drug administered by periocular injections can reach the posterior segment by three different pathways: transscleral pathway, systemic circulation through the choriocapillaris and the anterior pathway through the tear film, cornea, aqueous humor, and the vitreous humor (Ghate and Edelhauser, 2006). Subconjunctival injection obviates the conjunctival epithelial barrier, which is rate-limiting for permeation of water-soluble drugs. Thus, the transscleral route bypasses cornea–conjunctiva barrier. Although transscleral delivery is comparatively easy and patient compliant, various dynamic and static barriers limit drug permeation to the posterior eye segment. Dynamic barriers include lymphatic circulation and the blood flow in the conjunctiva from which the drugs are readily eliminated (Kim et al., 2007, Lee et al., 2010).

Therefore, in order to increase the drug concentrations in the retina and vitreous, intravitreal injection (into the vitreous humor) is the conventional and currently preferred route of drug administration to treat posterior ocular diseases (Kim et al., 2007). However, the drug distribution in the vitreous is non-uniform and depends on the pathophysiological conditions and molecular weight of the administered drug (Gaudana et al., 2010, Mitra et al., 2006). The therapeutic efficacy is also regulated by half-life of drug in the vitreous that, following intravitreal injection, can be eliminated by either the anterior route or posterior route. Finally, usually the rapid metabolic clearance of the molecules requires repeated and invasive injections with consequent increased risk of complications, such as retinal detachment, iritis, uveitis, cataract, endophthalmitis, intraocular haemorrhage and poor patient tolerance (Peyman et al., 2009, Chong and Adewoyin, 2007).

Nanotechnology for treatment of retinal diseases

Nanomedicine is the science that uses the nanotechnology for diagnosis, prevention and treatment of human diseases with the ultimate goal of preserving and improving the human health. The nanotechnology is based on the use of various polymers or materials with a dimension of/from one nanometer to hundreds of nanometers. In the last decade, nanomedicine has provided newer diagnostic tools and promising therapies for a variety of scientific fields including ophthalmology (Diebold and Calonge, 2010, Bisht et al., 2018, Patel et al., 2013).

The growing field of nanotechnology has been particularly focused on designing and validating efficient nanocarrier-based delivery systems to overcome the ocular barriers and improve bioavailability in the posterior segment of the eye, thus decreasing the frequency of treatment. The advantages of using nanostructured formulations are related to the pharmacologic mechanisms of ocular nanosystems, including: (i) the improvement of solubility, stability, permeability and bioavailability of molecules; (ii) the enhanced targeting to ocular structures reducing the precorneal drug loss; (iii) the time-controlled drug release from its carrier performing a sustained delivery of a predetermined dosage; (iv) the extending of retention time of the drug in the cornea/conjunctiva at therapeutic concentrations; (v) the use of convenient routes of administration for drugs able to reach posterior ocular structures reducing undesirable side effects (Diebold and Calonge, 2010, Barar et al., 2008, Pignatello and Puglisi, 2011).

Among nanostructured drug delivery systems, there are different kind of nanostructured formulations that differ in composition (Figure 9). (i) Polymeric nanoparticles (NPs) are colloidal carriers (10-100 nm), generally composed of natural or synthetic polymers, metals, lipids or phospholipids (e.g. dextran, albumin, sodium alginate, chitosan, gelatin, alginate, collagen, hyaluronic acid, polylactideepolyglycolide PLGA and polylactide PLA). In these nanostructures, the drug can be uniformly distributed throughout the particle matrix (nanospheres) or encapsulated inside a polymer shell (nanocapsules). These nanocarriers contain a matrix material with several properties: the ability to encapsulate and protect hydrophilic or lipophilic drugs, physical stability, controlled release, biocompatibility depending upon the type of lipid used, ease of production and sterilization. The current generations of lipid systems consist of a mixture of solid and liquid lipids and exhibit a higher drug-loading capacity, longer-term stability in comparison to first generation of nanoparticles and some of them also intrinsic therapeutic abilities (e.g. antioxidant, anti-inflammatory and anti-angiogenetic activities) (Beloqui et al., 2016).

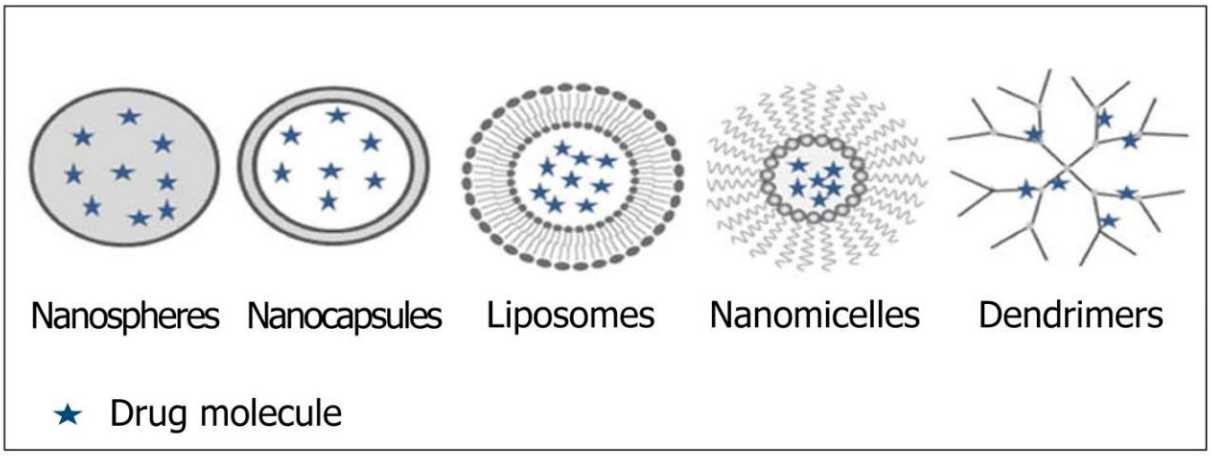

Figure 9. Nanocarriers for ocular drug delivery (Patel et al., 2013).

(ii) Liposomes are formed by an outer bilayer of amphiphilic molecules, such as phospholipids, with an aqueous core. These systems are generally ideal delivery system for ocular applications, due to the optimal biocompatibility and the ability to encapsulate both hydrophilic or lipophilic drugs. They can be easily modified on the surface to improve the tissue-targeting and the drug release. (iii) Nanomicelles consist of an amphiphilic block of copolymers with a hydrophobic core and a hydrophilic shell (Nishiyama and Kataoka, 2006). They are the most commonly used carrier systems to entrap drugs formulating it in clear aqueous solutions. The great interest in the development of nanomicellar formulations could be ascribed to ease of preparation, small size, surface charge of micelles, their high encapsulation capability and minimal degradation of drug (Vadlapudi and Mitra, 2013, Cholkar et al., 2012). (iv) Dendrimers are well-defined, multivalent molecules having branched structure of nanometer size (1–100 nm). They consist of three components: a central core, an interior dendritic structure (the branches), and terminal functional groups at the outer surface. These branched polymeric systems are available in different molecular weights with amine, hydroxyl or carboxyl terminal functional groups. These functional structures may be conjugate to specific moieties increasing targeting posterior segments (Fischer and Vogtle, 1999). The highly branched structure allows incorporation of wide range of drugs, hydrophobic as well as hydrophilic. In ocular drug delivery, few promising results were reported with these polymeric systems (Patel et al., 2013, Bisht et al., 2018, Spataro et al., 2010). (v) Emulsions consist of two types: oil-in-water (o/w) or water-in-oil (w/o) mixtures (Vandamme, 2002). For ophthalmic drug delivery, o/w emulsion is common and widely preferred comparing to w/o system. Both formulations offer some advantages, including

improved solubility and bioavailability of drugs. Others nanosystems include nanosuspensions, nanoparticle-loaded contact lenses, nanotubes and fullerenes composed of carbon-based nanomaterials, and quantum dots made of semiconductor materials with fluorescent properties and covered with other materials.

Among the different nanostructured formulations, the calixarene-based nanotechnology has shown a great potential as drug delivery systems in the ophthalmological field (Blanco, 2016, Granata et al., 2017, Consoli et al., 2018). These cationic nanocarriers are safe, well tolerated and characterized by positive charges that allow them to create electrostatic interactions with the ocular surface, enhancing the mucoadhesion and the residence time, thus promoting ocular targeting (Lallemand et al., 2012). Calix[n]arenes are a class of macrocyclic compounds produced through the condensation of p-substituted phenols and formaldehyde and they include several oligomers that differ in the number of the phenolic units with a range from 4 to 20 (Figure 10). Some of these have the ability to self-assemble in an aqueous medium into stable micelles and host in their well-defined hydrophobic cavity a variety of guests, including bioactive molecules (Neri, 2016).

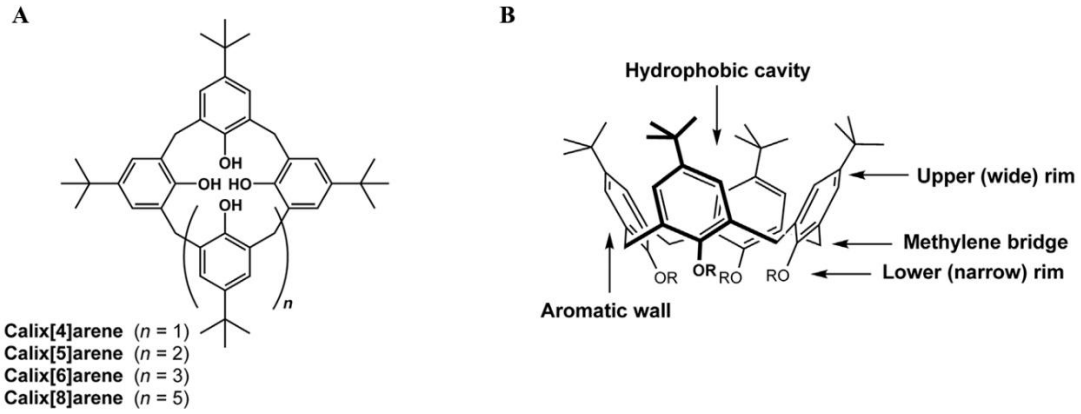

Figure 10. The calix[n]arene class. (A) The structure of calix[4,5,6,8]arene oligomers. (B) The calixarene backbone composed by a "lower or narrow rim," an "upper or wide rim," and a central hydrophobic cavity (Consoli et al., 2018).

The functionalization of calixarenes at their rims (upper and lower) with hydrophilic and hydrophobic groups permits the synthesis of a variety of derivatives with different properties and ideal controlled drug delivery systems (Yousaf et al., 2015, James et al., 2013, Nimse and Kim, 2013).

Furthermore, several promising biological activities have been attributed to these cationic nanocarriers such as antiviral, antibacterial, antifungal, and anticancer properties (Mokhtari and Pourabdollah, 2013, Hussain et al., 2017). The calix[4]arene, the smallest macrocycle among several calix[n]arenes composed by four phenolic moieties, has aroused particular interest for its easy synthesis, even at low cost, its predisposition toward postmacrocyclic modifications, exclusive conformation and intrinsic antioxidant properties (James et al., 2013, Naseer et al., 2017).

PRELIMINARY RESULTS

In collaboration with the Institute of Biomolecular Chemistry (ICB)-CNR and SIFI S.p.a., it has been synthesized and functionalized a new nanocarrier, the calix[4]arene, whose synthesis has been performed by adapting the procedure reported in (Rodik et al., 2015) and described in detail in (Granata et al., 2017). To improve ocular bioavailability and facilitate the transport to posterior ocular tissues, the amphiphilic calix[4]arene derivatives have been designed with aliphatic chains at the calix[4]arene lower rim and polar choline groups at the upper rim. The choline has been chosen as cell-specific targeting ligand to mediate the drug delivery to the posterior segment of the eye. Several mechanisms of choline transport are known in the eye: the Organic-Cationic-Transporters, OCT1 and OCT2, located at the BRB that bind choline with low affinity (Tomi et al., 2007); the high affinity choline transporter (CHT-1) that it is expressed in several retina layers including the photoreceptors (Matsumoto et al., 2012); and finally, the choline-transporter-like proteins (CTL) that are expressed in the retinal capillary endothelial cells (Tomi et al., 2007).

The potential of various choline-calix[4]arene conjugates as nanocarriers for gene delivery is well known (Rodik et al., 2015), but only recently it has been demonstrated the applicability of this platform as a versatile drug delivery system in ophthalmologic field (Di Bari et al., 2016b, Blanco, 2016, Granata et al., 2017, Di Bari et al., 2016a). In particular, it has been demonstrated the ability of nanoaggregate choline-calix[4]arene to improve the ocular drug delivery of the Slb or other active ingredients for the treatment of retinal degenerative diseases (Blanco, 2016).

We have investigated the cytocompatibility of the carrier choline-calix[4]arene coniugated with Slb (CalixSlb) on human retinal pigment epithelial (ARPE-19) cells (Blanco, 2016), a dependable immortal RPE cell line widely accepted/considered as an alternative to primary/native RPE cells exhibiting its own structural and functional features (Karakocak et al., 2016, Samuel et al., 2017, da Silva et al., 2016), used as *in vitro* cell culture models. As shown in the Figure 11, no evident change in ARPE cell viability has been detected after 23 hours incubation with all formulations (CalixSlb, Calix, Slb) with different concentrations (0.01-1μM) through monitoring of the LDH release used as a signal of cellular membrane disruption and cell death (Blanco, 2016).

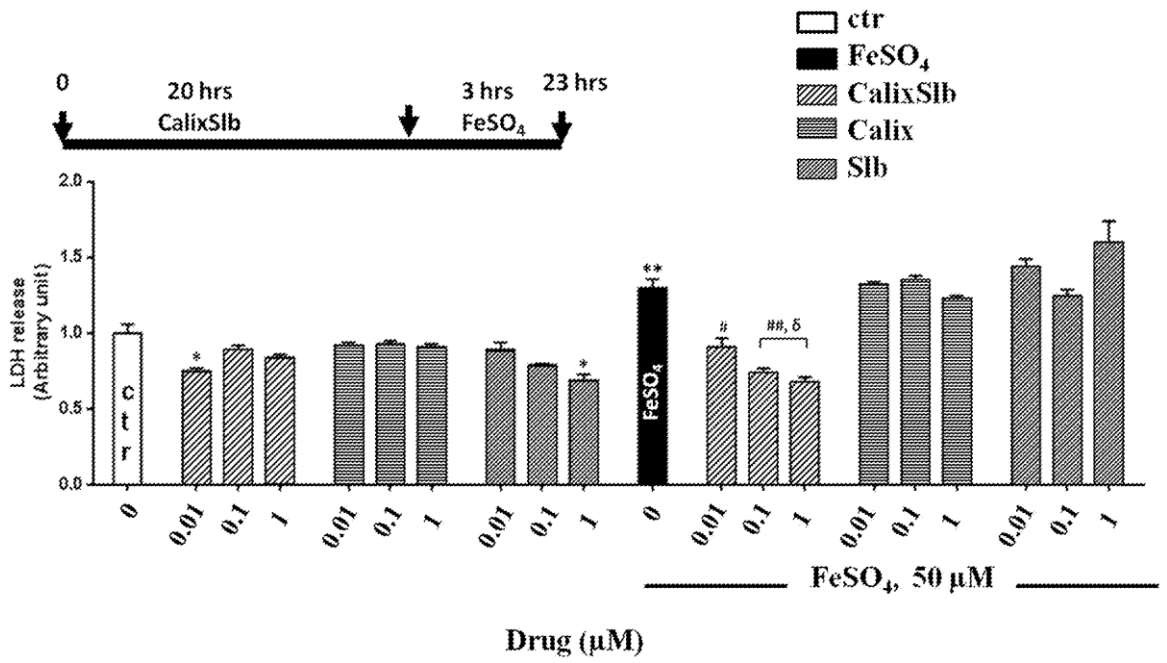

Figure 11. Evaluation of CxSlb treatment on cell viability and protective effect on $FeSO_4$-insulted cells. ARPE-19 cells were treated with CalixSlb, Calix and Slb for 23h at different concentrations (0.01-1µM). To test the protective effects of CalixSlb, ARPE-19 cells were pre-treated with different concentration of CalixSlb and free Slb for 20h and then incubated with 50µM $FeSO_4$ for 3h. At the end of the incubation time, cell viability was determined by LDH release. The data represent mean ±SD of three independent experiments in quadruplicate (n=12). $^{*}P < 0.1$, $^{**}P < 0.01$ vs. control cells (ctr); $^{\#}P < 0.1$, $^{\#\#}P < 0.01$, $^{\#\#\#}P< 0.001$, $^{\#\#\#\#}P<0.001$ vs. $FeSO_4$-stressed cells (One-way ANOVA followed by Bonferroni multiple comparison test) (Blanco, 2016).

When the ARPE cells were exposed to $FeSO_4$ insult (50µM), pre-treatment with CalixSlb showed protective effects reducing the LDH release. No change in the LDH levels was observed in the samples pre-treated with free Calix or only Slb (Blanco, 2016). Therefore, these results suggested no toxicity of all formulations used and that the CxSlb showed protective effects against oxidative stress induced by iron insult.

In addition, it has been demonstrated that the topical treatment with the same nanocarrier, the choline-calix[4]arene was able to improve the ocular delivery of another poorly water-soluble flavonoid compound, the curcumin, and to enhance its anti-inflammatory and protective effects in a rat model of LPS-induced anterior uveitis (Granata et al., 2017).

.

OBJECTIVES

The first objective of this study is to deepen the knowledge about the role of iron in the retina, analyzing the *in vivo* effects of iron accumulation in both the neuroretina and RPE structures. It is well known that iron has an essential role in the retina but, being the most powerful generator of free radical, its excess may contribute to development of retinal disorders. To date, the mechanisms underlying iron excess in the retina are not perfectly known. This study aims to have an ideal *in vivo* model of retinal degeneration which is simple to create and includes the pathological features of the most common ocular disorders. Therefore, the animal model of retinal degeneration obtained with intravitreal injection of ferrous sulfate will be characterized and the pathological mechanisms caused by iron accumulation in the retina and RPE will be investigated, including morphological alterations, iron overload, oxidative stress, neuroinflammation and amyloid accumulation at different epochs from iron insult.

Ophthalmic drug delivery is one of the most important challenges in the modern medicine due to the high spread of ocular pathologies in a world that is getting older. The topical treatment of posterior ocular diseases via eye drop instillation has always received wide acceptance in the management of chronic therapies with minimal risks, but the principal difficulty is the low ocular bioavailability of topically applied drugs caused by anatomical barriers of the eye. Thus, the next objective of this study is the *in vivo* analysis of topical treatment as eye drop based on the choline-calix[4]arene nanocarrier, an innovative platform for the ocular delivery of silibinin, a flavonoid with possible neuroprotective activity. To test the effectiveness of this nanostructured therapeutic approach, it will be used the iron-induced animal model of retinal degeneration, characterized in the first part of this study.

RESULTS AND DISCUSSION

1. Characterization of animal model of iron-induced retinal degeneration

1.1 Intravitreal injection of iron sulphate causes morphological change and iron accumulation in the retina and RPE of rats

Iron ocular injection or mutations of genes implicated in iron homeostasis causes retinal degeneration with features of AMD (Song and Dunaief, 2013, Dunaief, 2006). Here, we investigated the *in vivo* progressive effects of iron intravitreal injection on retina and, in particular, on RPE/choroid structure, analyzing diverse cellular mechanisms underlying retinal degeneration, including morphological alterations, oxidative stress, inflammation and amyloid accumulation.

In particular, 8-week-old male Wistar rats were subjected to intravitreal injections of iron sulphate or normal saline (Ctr) and eyes were explanted at 1, 10 and 15 days after iron insult. The concentration of 0.5mM iron sulphate intravitreal injection was chosen on the basis of previous studies in which it proved to be able of causing retinal oxidative stress and photoreceptor loss (Rogers et al., 2007). The ocular samples were fixed in paraformaldehyde and embedded in paraffin. Retina and RPE/choroid sections were stained with Haematoxylin and Eosin (HE) and Perls' Prussian blue staining in order to evaluate retinal morphology and iron accumulation, respectively.

No evident morphological changes were revealed by histopathological analysis in the retina as well as in the RPE/choroid structures in 1 day post-injection group (Fe 1D) if compared to control group (Ctr) (Fig. 1A and B). In the iron-injected retinas at 10 days (Fe 10D), we detected swelling of ganglion cell layer (GCL), atypical cell infiltration between GCL and nerve fibre layer (NFL) and in the IPL (Fig. 1 A, B and C). Focal and abnormal retinal blood vessels (arrows) and neo-vascular tufts extending into the vitreous (arrowheads) were also visible at the inner part of this retina group, shown in the Fig. 1C. Hyperplasia and severe morphological alteration of the RPE (Fig. 1C) were also observed and, in some specimens of this group, focal retinal folds and the presence of some inflammatory cells in the subretinal space, between RPE and outer segments of the photoreceptors (OS) (data not shown, see following staining). On 15 day after iron-injection (Fe 15D, Fig. 1A-B), severe morphological alterations were observed, including thinning of all retinal layers, complete loss of the RPE and segments of photoreceptors (OS, IS) leading to the formation of retinal folds, typical rosette-like structures and extracellular deposits in the subretinal space similar to drusen. Moreover, in this group, Fe 15D also showed vacuolization of INL,

reduction of outer plexiform layer (OPL) and spongy appearance in the inner plexiform layer (IPL).

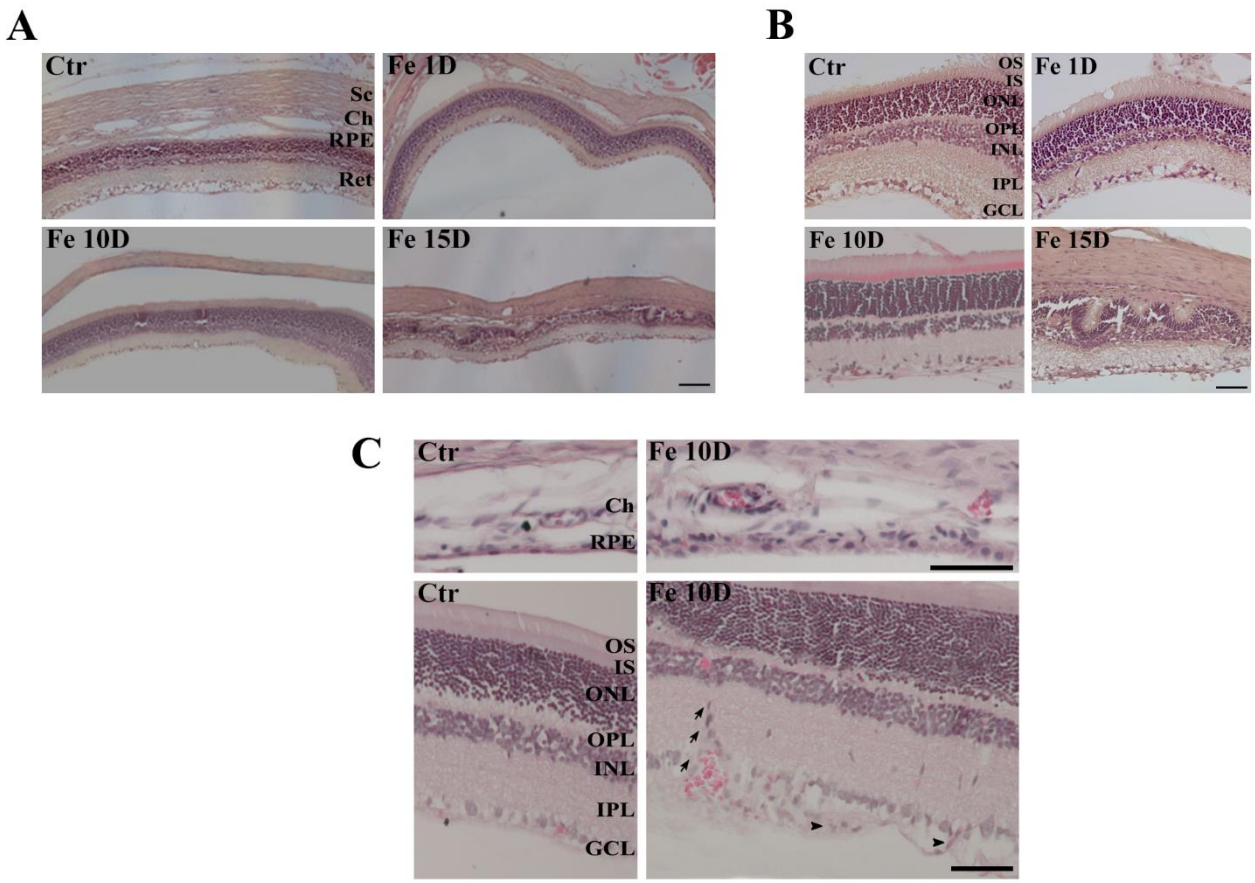

Figure 1. Intravitreous injection of $FeSO_4$ results in retinal and RPE morphological changes. Representative images at different magnifications of retinal sections stained with H&E from normal saline-injected (Ctr) group and iron-injected rats at one day (Fe1D), ten (Fe10D) and fifteen days (Fe15D) after insult. (A) General view of ocular structures including retina, RPE, choroid and sclera. Scale bar 100 μm. (B) High magnification views of retina of all experimental groups. Scale bar 50 μm. (C) High magnification views of RPE/choroid and retina of control and 10 days post-injection (Fe10D) groups. Scale bar 50 μm. Abbreviations here and in the following figures: Sc, sclera; Ch, choroid; RPE, retinal pigmental epithelium; Ret, retina; OS, outer segments; IS, inner segments; ONL, outer nuclear layer; OPL, outer plexiform layer; INL, inner nuclear layer; IPL, inner plexiform layer; GCL, ganglion cell layer.

The ocular iron overload was analyzed using Perls' staining that recognizes ferric iron. As shown in Fig 2, on 1 day after iron injection (Fe 1D), small intracellular blue granules were identified in the soma of cells located in the INL, ONL, GCL and in the RPE layer, whereas weak blue staining was also observed in the OPL and IPL. At 10 days, sporadic and dense iron deposits positive to Perl's blue stain were detected in the subretinal space, RPE and choroid. At 15 days, intense blue positive staining was evident in the drusen-like deposits and in the choroidal vessels; numerous intracellular blue granules were identified in all retinal layers.

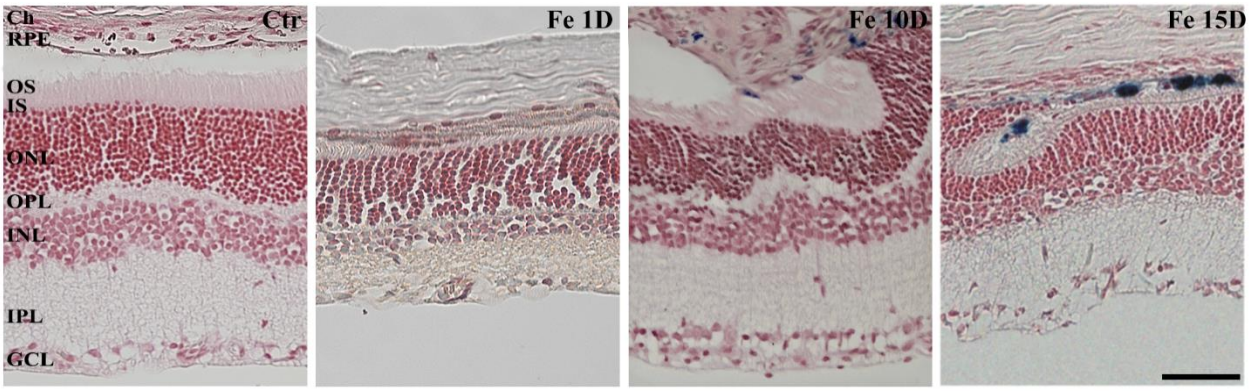

Figure 2. Intravitreal injection of iron sulphate causes progressive iron accumulation in the retina and RPE of rats. Representative images of retinal sections stained with Perls' Prussian blue from normal saline-injected (Ctr) group and iron-injected rats at one day (Fe1D) ten (Fe10D) and fifteen days (Fe15D) after insult. Scale bar, 50 μm.

Therefore, these results confirm that the intravitreal injection of iron sulphate causes primary RPE iron overload in rat and subsequent progressive retinal degeneration. In fact, the iron accumulates widely in all retinal layers already at one day after injection without causing evident signs of morphological alterations, but probably initiating cellular processes underlying ocular degeneration. After ten days, iron principally localized in the outer part of the retina and in the RPE, but consequent processes such as inflammation started in the inner portion the retina. In particular, the GCL was compromised showing numerous inflammatory cells. At 15 days after intravitreal injection, iron accumulated principally in drusen-like bodies, associated with complete alteration of retinal layers and notable loss of photoreceptors.

1.2. Oxidative stress and lipid peroxidation in the iron-induced retinal degeneration model

It has already been demonstrated that elevated levels of iron in the murine eyes lead to increase the production of superoxide radicals predominantly in photoreceptors (Rogers et al., 2007), but there are no observations concerning the retinal oxidative state over time and, in particular, about the RPE layer following to iron-intravitreal injection.

Therefore, we analyzed retinal oxidative stress for each experimental group by immunohistochemical staining using 8-OHdG antibody, marker of DNA oxidation, and by measuring the TBARS levels (determining the malondialdehyde, MDA, content), as an index of

lipid peroxidation. Oxidative stress affects a wide range of cellular targets, including membrane lipids, proteins and DNA (Sekine and Ichijo, 2015) and the 8OHdG is considered one of the main forms of free radical-induced oxidative injury of the DNA (Valavanidis et al., 2009).

No significant differences in the 8-OHdG immunoreactivity were found in the retina (Fig.3A) and in the RPE/choroid structures (Fig. 3B) of Fe 1D group if compared to Ctr group. The increase of 8-OHdG staining was observed in Fe 10D group in the ONL, INL and GCL layers. It is noteworthy that elevated 8-OHdG reactivity was detected also in the RPE layer (visible at higher magnification, Fig. 3B). On 15 day after iron-injection, large/extensive immunopositive deposits were revealed in the subretinal space (arrowheads) and a diffuse increase of 8OHdG staining was observed in all retinal layers. In line with this, retina/RPE/choroid lysates, derived from the iron-treatment at 10 days, showed higher TBARS levels compared to the control retinal levels, as shown in Fig. 3C.

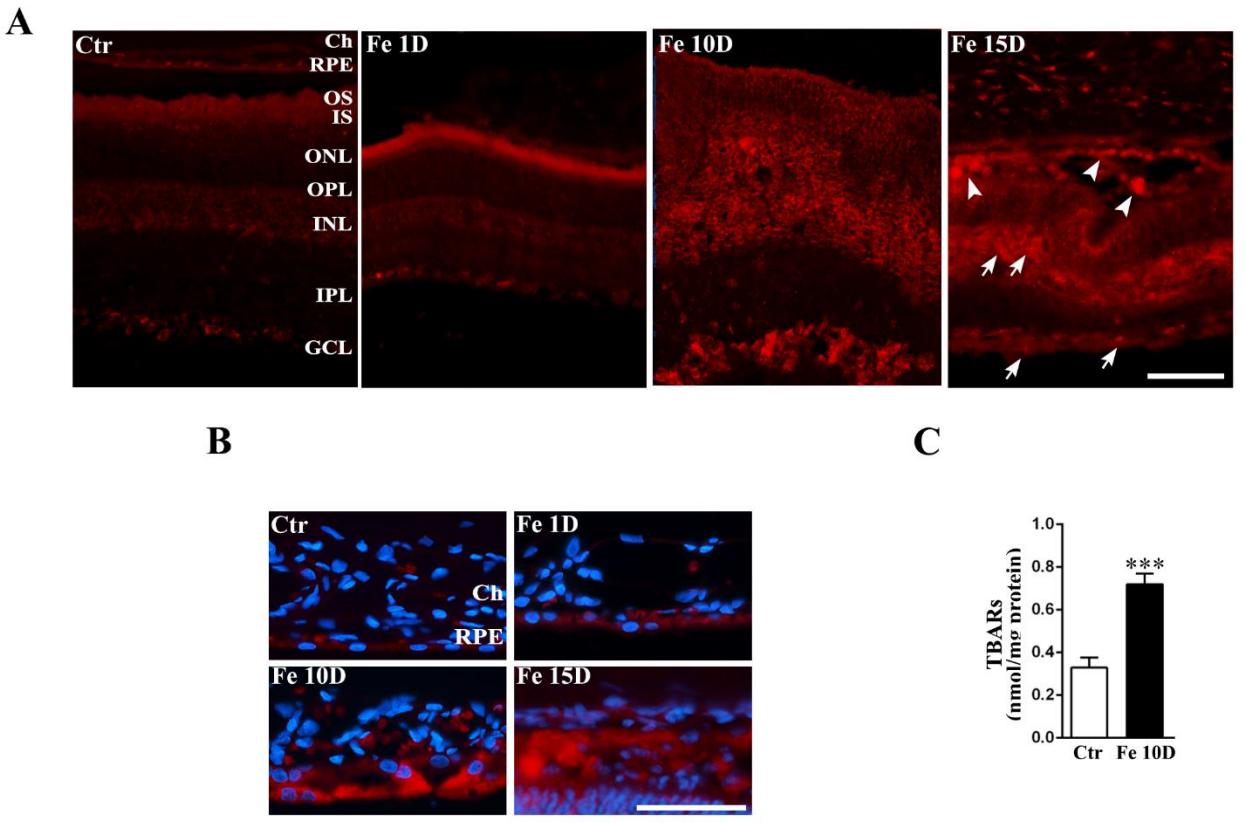

Figure 3. Intravitreal injection of iron sulphate causes progressive oxidative stress in the retina and RPE of rats. Representative images of 8-OHdG immunoreactivity of the retinal (A) and RPE/choroidal (B) sections, from normal saline-injected (Ctr) group and iron-injected rats at one day (Fe1D) ten (Fe10D) and fifteen days (Fe15D) after insult. Nuclei were stained by DAPI (blue). Scale bars 50 μm. (C) Thiobarbituric acid-reactive substances (TBARS) levels in Ctr group and 10 days iron-injected group (Fe10D). The treatment with iron increases retinal lipid peroxidation. Vertical bars represent mean ± SD. ****p<0.001 vs*. Ctr group (Student's unpaired two-tailed t test).

These results suggested that iron accumulation induced by iron intravitreal treatment causes subsequent progressive increase of oxidative state in the retina as well as in the RPE layer, which plays a critical role in triggering retinal inflammation and consequent degeneration.

1.3. Retinal inflammation in the iron-induced retinal degeneration model

The activation of glial population and the release of proinflammatory mediators has been widely described in several animal models of oxidative-stress induced retinal degeneration (Pennesi et al., 2012, Masuda et al., 2017, Vecino et al., 2016), ultimately confirming the close link between oxidative stress and inflammation underlying ocular degenerative diseases (Cuenca et al., 2014). Therefore, to determine if iron intravitreal treatment is also able to regulate retinal inflammation, we evaluated the gliosis state and microglia response by immunostaining respectively for the glial fibrillary acid protein (GFAP) and ionized calcium-binding adapter molecule 1 (Iba-1).

As shown in Fig. 4A, no GFAP immunoreactivity was detected in control and at 1 day after iron-injected groups. On the contrary, intense GFAP immunoreactivity was observed at 10 days in the iron-treated retinas, mainly in the NFL, GCL and INL retina layers and clearly labeling astrocytic and Müller cell processes throughout the retina.

The same result was found using an antibody directed against Iba-1 protein (Fig. 4B). In fact, while microglia cells were detected only in the inner part of the retina of the Ctr group, at day 10 from iron-injection an increased number of Iba-1-positive cells was observed, located in all retinal layers, including the outer part of the retina, and in the choroid. Morphology changes of retinal microglial cells were also observed: from the typical ramified and inactive observed in Ctr group, to the enlarged (soma enlarged) with short and thick processes or round and ameboid activated morphologies (insert at high magnification, Fig. 4B). In addition, we observed that the iron injection caused a substantial accumulation of Iba-1-positive cells at the NFL/GCL layers, in the swelling areas corresponding to focal increase of GFAP immunostaining and just beneath RPE layer and close to deposits in the drusen-like bodies.

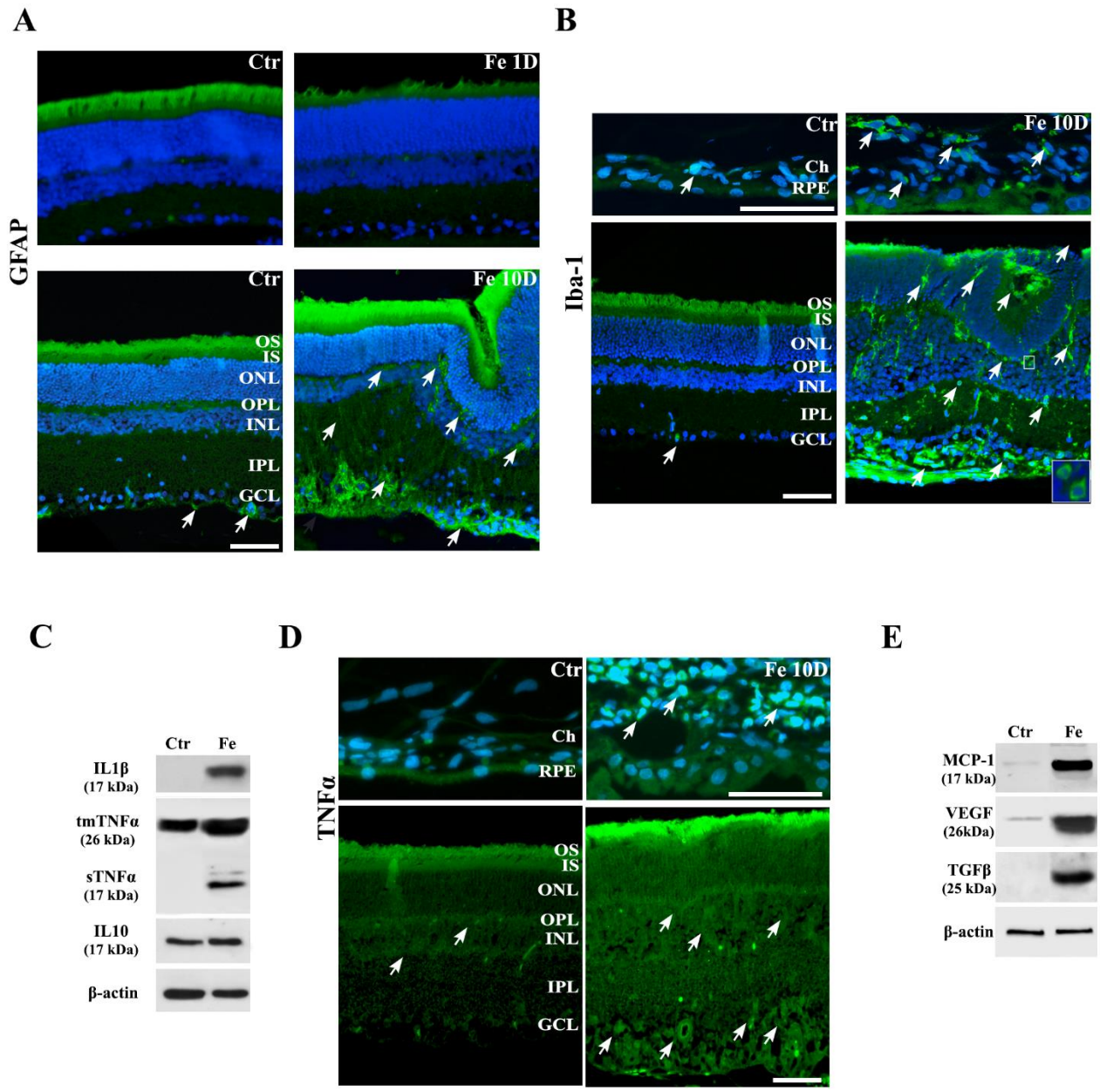

Figure 4. Intravitreous injection of $FeSO_4$ results in retinal glial activation and release of inflammatory mediators. Representative images of GFAP (A), Iba-1 (B) and TNFα (D) immunostaining in the retinal and RPE/choroid sections from normal saline-injected (Ctr) group and iron-injected rat groups at one day (Fe1D, only for GFAP staining) and 10 days (Fe10D). Nuclei were stained by DAPI (blue). Scale bars 50 μm. (D) Immunoblots of IL1β, TNFα, IL10 (C) and MCP-1, VEGF, TGFβ (E) in retina/RPE/choroid lysates from normal saline-injected (Ctr) and iron-injected rats at 10 days (Fe10D) groups. β-actin was used as a loading control.

To better characterize the effects of iron intravitreal injection on retinal inflammation at 10 days, we examined the expression of pro-inflammatory cytokines, tumor necrosis factor-alpha (TNFα) and Interleukin-1 beta (IL1β), and of the principal anti-inflammatory cytokine, Interleukin-10 (IL10), in retina/RPE/choroid lysates by Western blotting analyses. As shown in Fig. 4C, the iron injection caused a significant increase of activated form of IL1β and TNFα expression levels if compared to Ctr group, whereas no variation of expression levels for IL-10 was observed. Interestingly, we also detected the appearance of the TNFα soluble form (sTNF, 17kDa), deemed to be more toxic than transmembrane form (tmTNFα, 26 kDa), as capable of activating caspases.

In order to confirm the Western Blot results, we performed the TNFα retinal immunostaining (Fig. 4D) and we found an increase of TNFα immunoreactivity in Fe 10D group diffuse/spread across the entire retina if compared with control group, in which the immunoreactivity was confined in the INL and OPL (arrows). Numerous TNFα-positive cells were detected in the choroid layers and in the GCL and IPL retina layers of Fe 10D group (arrows).

Finally, since several inflammatory mediators, such as Monocyte Chemoattractant Protein-1 (MCP-1) and Transforming Growth Factor (TGF-β), can regulate the expression of vascular endothelial growth factor (VEGF), the principal activator of retinal angiogenesis and involved in AMD disease, we analyzed the expression of these vascular retinal mediators by Western blotting. As shown in Fig. 4E, we found that the iron injection caused the increase of chemokine MCP-1 and the vascular mediators VEGF and TGFβ at 10 days, if compared to control group.

Therefore, these data suggest that ocular iron accumulation significantly increased gliosis and microglial activation together with the expression of mediators of retinal inflammation and vascularization.

1.4. Amyloid accumulation in the iron-induced retinal degeneration model

It has been shown that the drusen, pathologic hallmark of AMD, contains also iron and amyloid β (Aβ), in addition to inflammatory mediators. From the cleavage process of amyloid precursor protein (APP) derives Aβ, which undergoes an aggregation process (fibrillization) loading to the formation of protofibrils and finally mature fibrils that constitute the senile. The protein aggregation also leads to the formation of soluble intermediates, the Aβ oligomers that usually are found surrounding amyloid plaques in brains of human patients and animal models of AD and are considered more toxic than the amyloid fibrils. Two major Aβ isoforms are present in the amyloid plaques, named Aβ40 and Aβ42.

Iron can upregulate the production of amyloid precursor protein (APP) and it has been suggested that RPE iron overload could contribute to Aβ accumulation in the retina (Guo et al., 2014).

Therefore to study the possible effect of retinal/RPE iron overload in the Aβ deposition, the progressive expression of Aβ for each experimental group has been analyzed by immunofluorescence analysis, using a specific antibody against the isoform Aβ 1-42 (Fig. 5A). Compared to control group, an increase of Aβ1-42 staining was already found at 1 day after iron injection in the IPL and OPL. Intense intracellular staining was detected in the GCL cells and in the choroidal vasculatures, whereas no Aβ1-42 staining was found in the RPE structure. On day 10, the RPE and choroidal vasculature were strongly marked by Aβ antibody and numerous immune-positive cells were detected between GCL/NFL, in the INL and ONL. Diffuse Aβ 1-42 staining was also found in the OPL, IPL and OS of photoreceptors. Finally, at 15 days after the iron-injection, strong Aβ staining was observed in the ONL and in the infiltrated cells between GCL/NFL, whereas positive Aβ 1-42 staining areas were detected in the retinal plexiform layers and in the subretinal space of the RPE (drusen-like structures). To confirm these results, we have examined the expression of Aβ1-42 oligomers in the retina/RPE/choroid lysates by Western blotting analyses (Fig. 5B). At 10 days after iron-injection, the levels of Aβ oligomers at low molecular weight (under 25 kDa) were significantly higher in lysates of the iron-injected group compared to control group, in which no Aβ1-42 oligomers expression was observed.

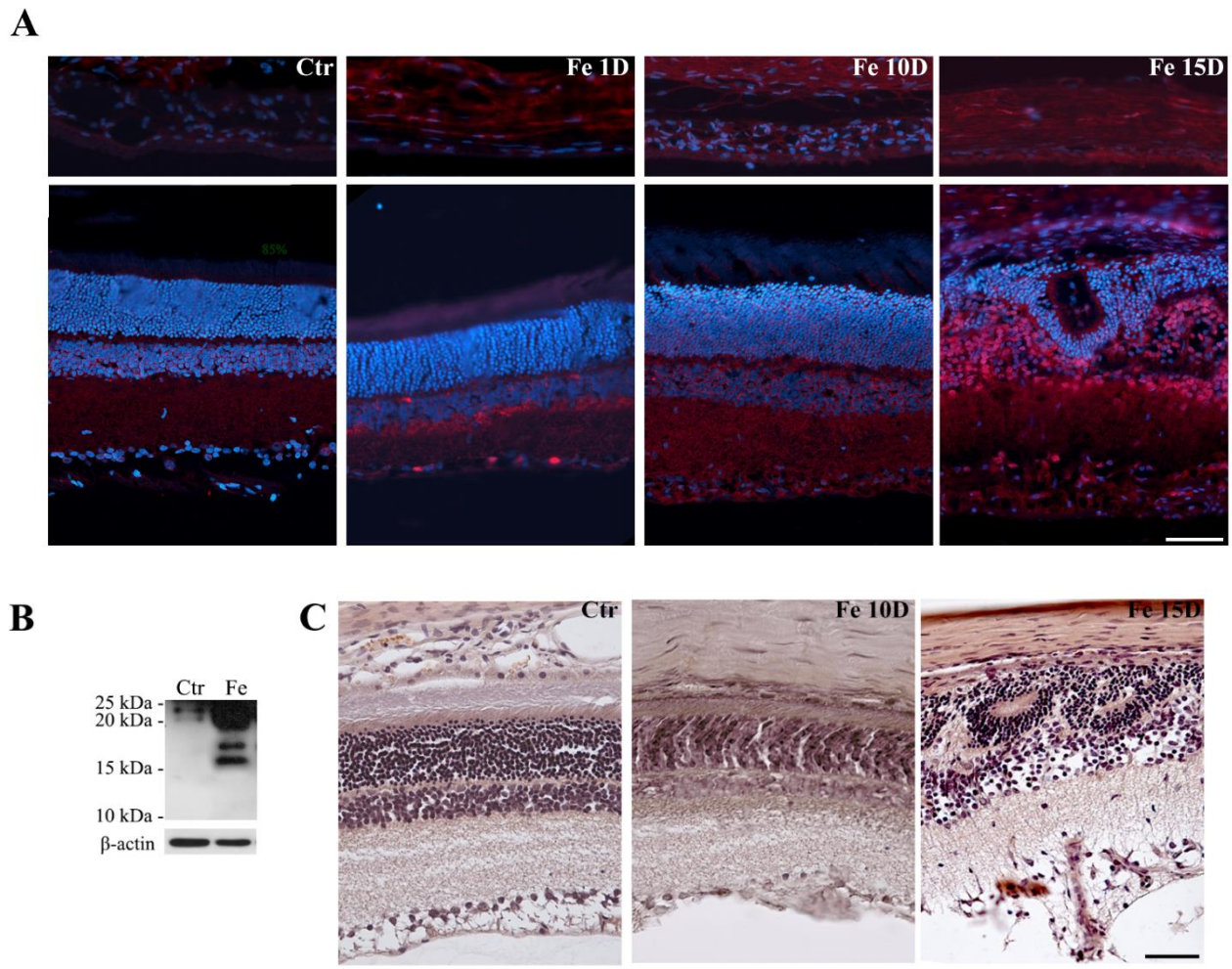

Figure 5. Intravitreous injection of $FeSO_4$ results in ocular amyloid accumulation. (A) Representative images of Aβ 1-42 immunostaining in the retinal and RPE/choroid sections from different experimental groups. Nuclei were stained by DAPI (blue). (B) Immunoblots of Aβ1-42 oligomers in retina/RPE/choroid lysates from normal saline-injected (Ctr) and iron-injected rats at 10 days (Fe) groups. β-actin was used as a loading control. (C) Representative images of retinal and RPE/choroid sections from normal saline-injected (Ctr) group and iron-injected rat groups at 10 days (Fe10D) and 15 days (Fe15D) stained with Congo red. Scale bars 50 μm.

In addition to soluble oligomers, Aβ fibrils or protofibrils were detected using the amyloidogenic Congo red dye. No positive staining was detected in the Fe 1D retina group (data not shown). Compared to control group, progressive increase of congophilic staining was revealed in the other retinal specimens (Fig. 5C); in particular, diffuse staining across the entire retina was revealed at 10 days after iron-injection, whereas intense positivity was observed in the drusen-like structures, in the RPE and in the choroid vasculatures at 15 days. In these specimens, intracellular staining was noticed in cells of the GCL together with positive congophilic staining areas that appeared most likely as extracellular Aβ plaques deposits.

Taken together, these results suggested a progressive increase of the Aβ oligomers and fibrils expression in the retina, in correlation to ocular iron overload.

1.5. Apoptotic cell death in the iron-injected retinas

Since it has been suggested that iron sulphate injection may lead to apoptosis of photoreceptors (Rogers et al., 2007) and we have observed the progressive activation of retinal oxidative stress and inflammation in our iron-treated retina groups, we examined the apoptotic cascade by Western blot analysis and TUNEL staining. As shown in Fig. 6A, activated forms of caspase-9 and caspase-3 were found in lysates of iron-treated groups at 1 day and 10 day from iron intravitreal injection. The increase in caspases expression seems to increase over time when compared to the corresponding controls. At 15 days from iron-insult, we observed no expression of cleaved caspase-9 and a decrease of cleaved caspase 3 expression. This result is probably due to the onset of caspase-independent necrotic cell death at this time.

Consistent with these results, no TUNEL-positive cells were observed in control retina group and at 1 day after iron-injection. In iron-treated eyes at 10 days, numerous TUNEL-positive cells were detected in the ONL, the GCL, the RPE and choroidal vessels (Fig. 6B), demonstrating that cell death caused by the iron intravitreal injection not only affects the photoreceptors, as already demonstrated (Rogers et al., 2007), but also the underlying RPE/choroidal cells.

On 15 day after iron-injection, TUNEL staining was detected in the cells of RPE and all retinal layers; large immunopositive deposits were also revealed in the subretinal space, suggesting the presence of apoptotic resides in these structures.

Therefore, these results suggested that iron intravitreal injection is able to lead progressive apoptotic cell death of photoreceptors and the RPE/choroidal structures.

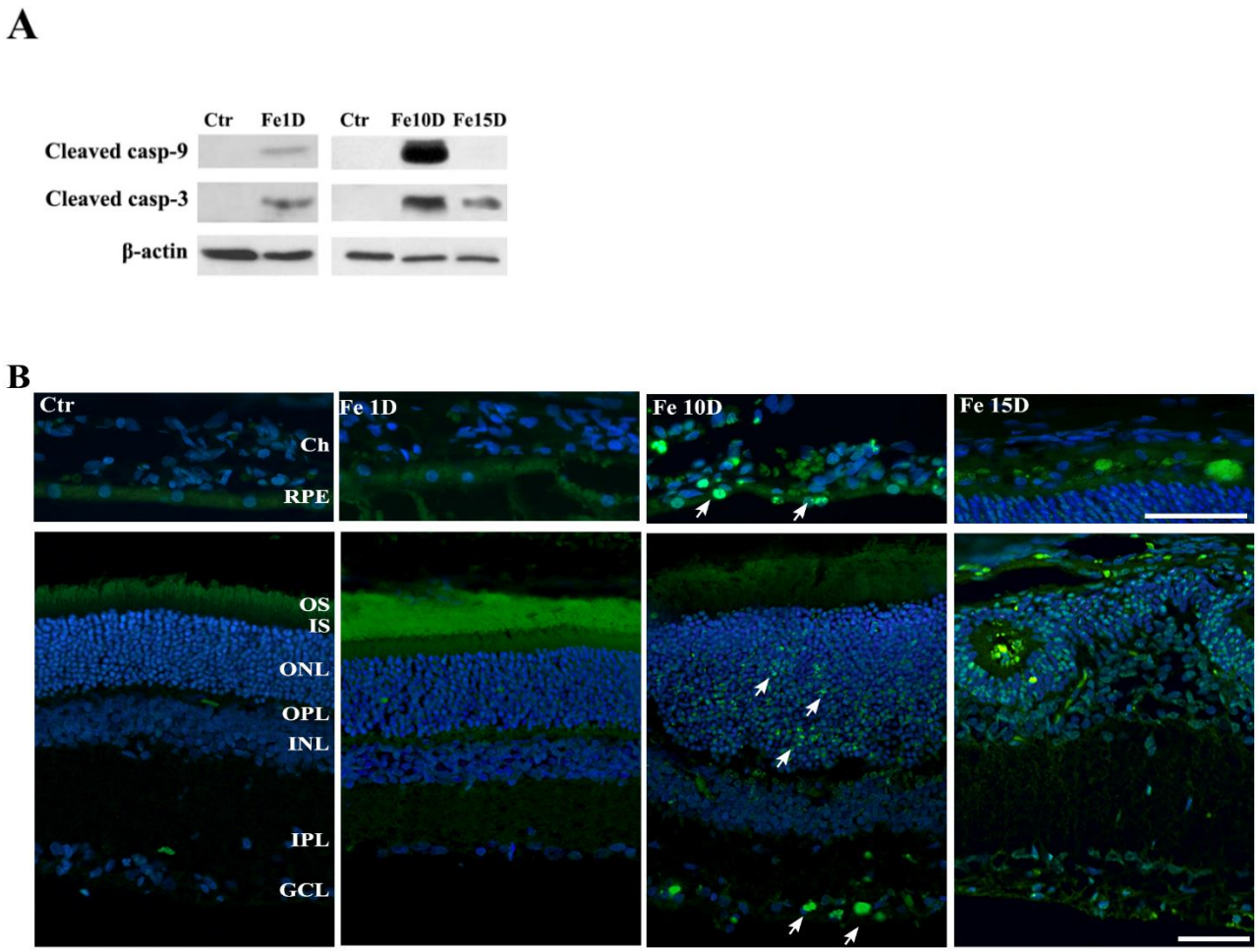

Figure 6. Intravitreous injection of $FeSO_4$ causes apoptotic cell death in the retina and RPE structures. (A) Immunoblots of cleaved and activated forms of caspase-9 and caspase-3 in retina/RPE/choroid lysates from the different experimental groups. β-actin was used as a loading control. (B) Representative images of TUNEL staining in the retinal and RPE sections from different experimental groups. Nuclei were stained by DAPI (blue). Scale bars 50 μm.

2. Study of a therapeutic approach based to nanoparticles against iron-induced retinal degeneration model

2.1 Preparation and characterization of CxSlb eye drop formulation

All procedures to prepare and characterize the Calix[4]arene-choline nanocarrier conjugated to silibinin (Cx-Slb) were conducted by the Institute of Biomolecular Chemistry (ICB)-CNR and SIFI S.p.a., similarly to those described for calix[4]arene-choline conjugated to curcumin (Granata et al., 2017). In brief, to entrap the hydrophobic Slb in the calix[4]arene nanoassembly, a phase solubility method was used by adding an excess of solid Slb to a colloidal solution of 1 mg/mL Cx in 10 mM PBS medium. To remove the unentrapped Slb, the sample was centrifuged and then filtered (0.2 μm filter), and the amount of Slb entrapped in the calixarene nanoassembly was calculated by HPLC chromatography (120 μg/mL), with a value corresponding to a drug loading capacity percentage of 10.7%. Cx-Slb formulation was prepared at the concentration of 10 mg/mL calixarene and 1.2 mg/mL Slb, about a 10-fold more concentrated formulation if compared to *in vitro* studies (Blanco, 2016). The obtained CxSlb colloidal solution and all formulations (Slb and Cx) appeared clear, transparent, and so suitable to be administrated as an eye drop. Diverse experimental analyses were conducted to establish the stability at room temperature and after the lyophilisation process. The release of Slb from the nanocarrier in PBS medium was calculated to be 9 % Slb in 30 hrs by dialysis method (data not shown).

2.2 Topical eye treatment with CxSlb reduces oxidative stress and histopathological changes in retina and RPE/choroid of iron-injected rats

To investigate the *in vivo* protective effects of the CxSlb formulation in ocular diseases, topical treatment was conducted on an animal model of iron-induced retinal degeneration. In the preliminary results, we have demonstrated the ability of pre-treatment with CxSlb nanoassembly to prevent iron-induced oxidative damage in ARPE cells, thus we decided to initiate eye drop treatments two days before iron injection (one drop daily). In particular, Wistar rats were daily topically pre-treated with diverse eye-drop formulations: free silibinin (Slb; 1.1mg/ml in vehicle; 6.3% DMSO), empty nanocarrierr choline-calix[4]arene (Cx; 10 mg/ml calixarene) and the choline-calix[4]arene-conjugated with silibinin (CxSlb;10 mg/ml Cx and 1.1 mg/mL Slb). After three days, the rats were subjected to a single intravitreal injection of iron sulphate ($FeSO_4$, 50 µM) and topical treatment was continued for ten consecutive days (Fig. 7A). Two different control rat groups were included in this study: a sham group (Ctr; not injected and treated) and a saline-injected and vehicle-treated group (SF-VH; injected intravitreally with normal saline and treated with vehicle contained 6.3% final DMSO concentration used to solubilize the free Slb).

We analyzed the RPE/choroid and retinal oxidative state by 8-hydroxy-2′-deoxyguanosine (8-OHdG) immunostaining. As shown in Fig. 7B, no positive immunoreactivity was observed in ocular structures of control groups (Ctr and SF-VH). Retina and RPE/choroid sections from Fe-injected rats exhibited a heavy positive staining for 8OH-dG (Fe). Intense staining was detected in the ONL and INL and in the GCL. The once-daily topical treatment with Cx-Slb eye drops in iron-injected rats (FeCxSlb) induced a significant decrease of the 8-OHdG staining in the RPE and in the retinal layers if compared with iron-injected rats, whereas it was significantly less reduced in Slb-treated sections (FeSb). No significant changes of 8OHdG immunoreactivity were observed in Fe group treated with Cx eye drops (FeCx), as confirmed by quantification analysis of the RPE and retina 8OHdG staining (Fig. 7C). Therefore, these results suggested that the CxSlb treatment reduced the oxidative stress in both ocular structures, RPE and retina, more effectively than free silibinin treatment.

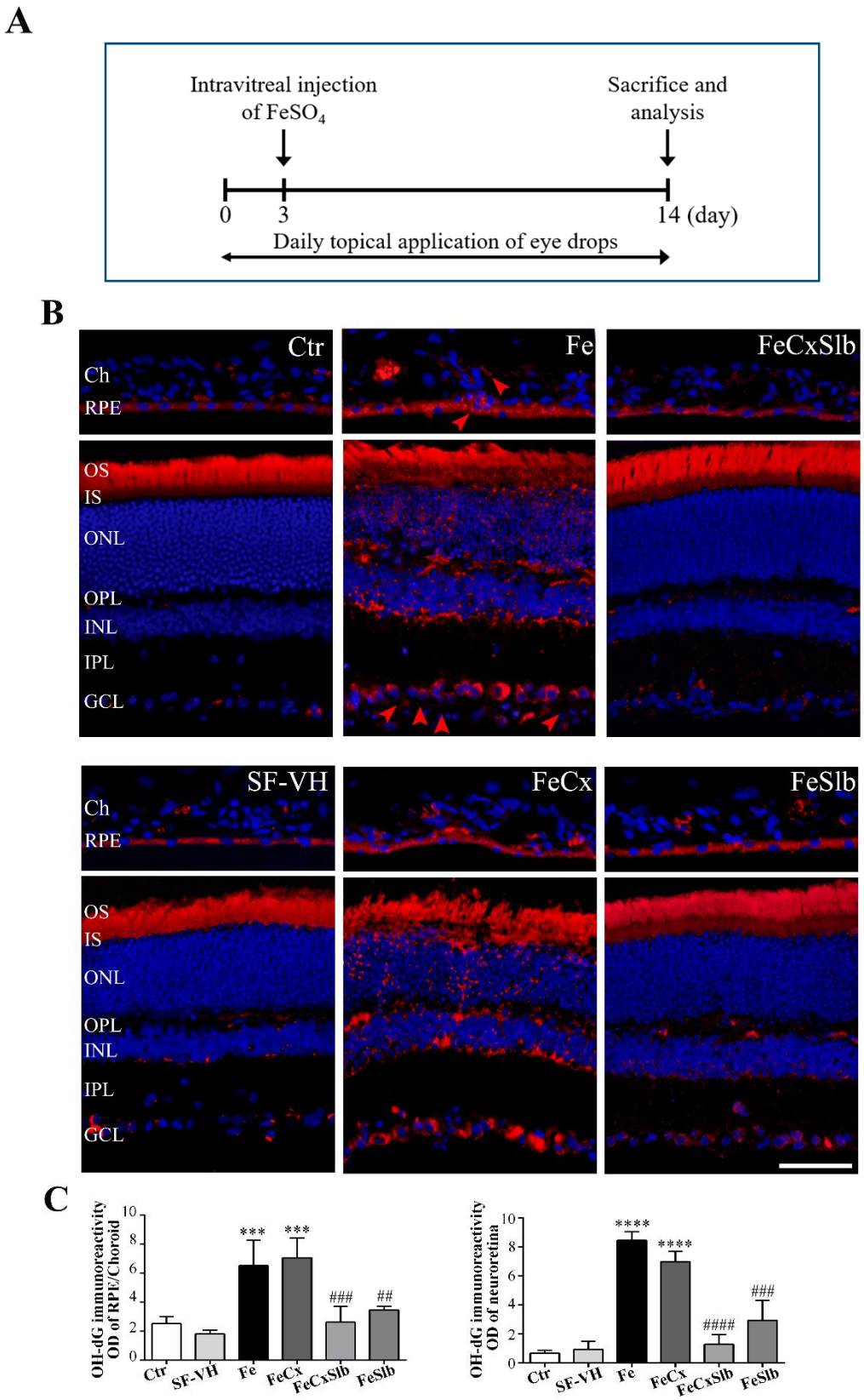

Figure 7. CxSlb treatment reduces oxidative stress in iron-insulted eyes. (A) Experimental treatment scheme. (B) Representative images of 8-OHdG immunostaining, marker of DNA oxidation, in the RPE/choroid and retinal sections from control rats no treated (Ctr), NS-injected rats no treated (SF), iron-injected rats no treated (Fe), and topically treated with CxSlb (FeCxS), free Slb (FeS) and Cx (FeCx) eye drops for 10 days. Nuclei were stained by DAPI (blue). (C) Quantification of immunofluorescence staining of 8-OHdG in the RPE and in the retina using Image J software. Vertical bars represent mean ± SD. ***$p<0.001$, ****$p<0.0001$ *vs*. Ctr group; ##$p< 0.01$, ###$p< 0.001$, ####$p<0.0001$ *vs.* Fe group (One-way ANOVA followed by Bonferroni multiple comparison test). Scale bar 50 μm.

To confirm the above results, Hematoxylin and Eosin (H&E) staining was performed to evaluate the morphological profiles of the retina and RPE/choroid cross sections treated with the different formulations (Fig.8).

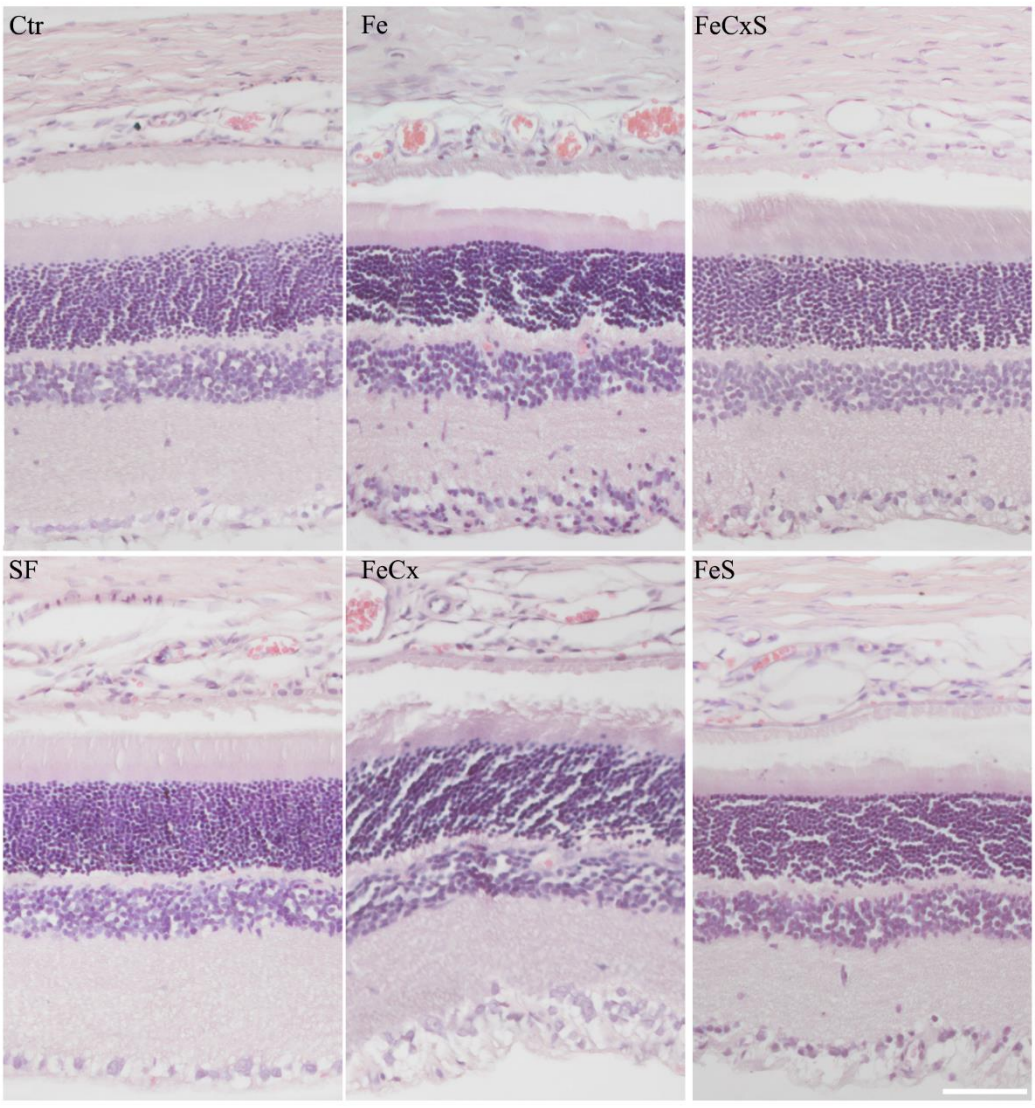

Figure 8. Treatment with CxSlb eye drops preserves retina morphology in iron-insulted eyes. (A) Representative images of RPE/choroid and retinal sections stained with H&E from different groups. Scale bar, 50 µm.

As previously shown (Fig. 1), Fe-treated group exhibited retinal damage, morphological change in RPE/choroid structures, atypical cell infiltration and vascular stasis in the choroidal layers. Furthermore, vacuoles and pyknotic cells were detected in all retinal layers, accompanied by abnormal enlargement of the GCL/ILM (inner limiting membrane) and inflammatory cell infiltration and abnormal vessels in the inner part of the retina. No morphological differences were found in FeCx sections compared to Fe-treated group. A reduced number of degenerative signs were detected in FeSlb group, whereas a complete protection was noted in FeCxSlb sections that exhibited normal structure of the retina and RPE/choroid, similar to those of control groups (Ctr and SF-VH).

2.3 CxSlb topical eye treatment suppresses inflammation in retina and RPE/choroid of the iron-injected rats

To evaluate the ocular effects of CxSlb nanoparticles on retinal gliosis, we conducted the immunostaining for Iba-1 and GFAP, specific marker for microglial cells and astrocytes respectively, for each experimental group (Fig. 9). As in previous results (Fig. 4B), we observed that iron intravitreal injection caused a marked accumulation of the Iba-1-positive cells, which were predominantly identified in the RPE/choroid and in the retina, particularly in GCL/ILM swelling areas (Fig. 9A, Fe) and in the outer portion of the OPL. No changes in the Iba-1 immunoreactivity were detected in FeCx group if compared to iron-treated group (data not shown), whereas a similar reduction in the total number of Iba-1–positive cells was observed in the retina of FeCxSlb and FeSlb groups (Figure 9B, $p<0.0001$ FeCxSlb and FeSlb *vs* Fe group). Few Iba-1-stained cells were detected at the RPE/choroid layers in the FeCxSlb group when compared to FeSlb, in which the treatment with Slb eye-drops has not been able to extensively reduce microglial cell number (Figure 9A, $p<0.0001$ FeCxS *vs* Fe group). These differences were confirmed through quantitative analyses of different sections from each group, counting both inactive and active Iba-1–positive cells since both cell types were reduced by the two treatments. No Iba-1-positive cells were visualized in control groups (see Fig. 4B).

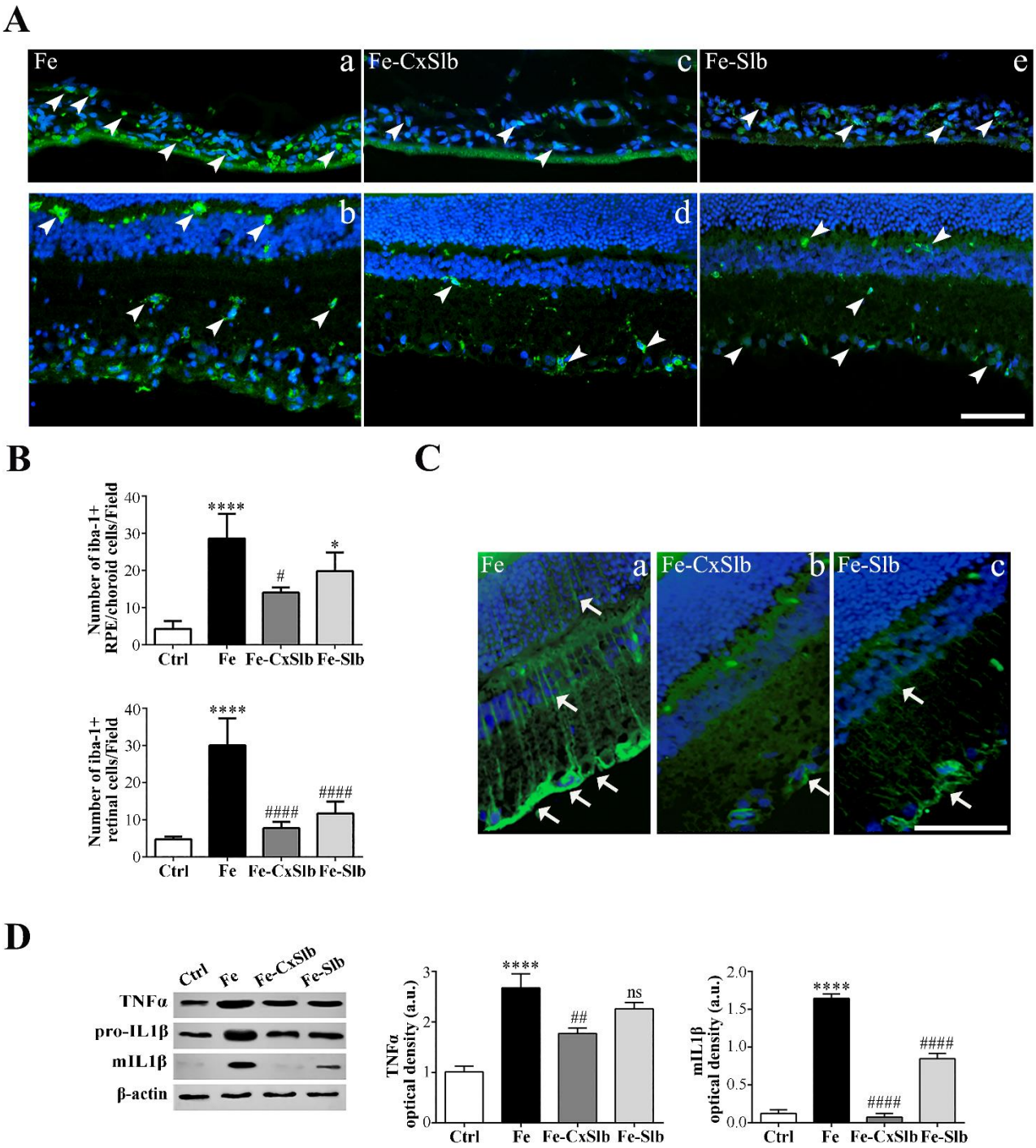

Figure 9. CxSlb treatment suppresses glial activation and decreases inflammatory mediators in iron-insulted eyes. Representative images of Iba-1 (A) and GFAP (C) immunostaining in the RPE/choroid and retinal sections from different groups. (B) Quantification of Iba-1 positive cells in the RPE and retina of different experimental groups. Data are reported as mean number of Iba-1+ microglia in the different retinal layers ±SD. (D) Immunoblots and densitometric analyses of TNFα and IL1β in retina/RPE/choroid lysates from different groups. Molecular weight of around 31 kDa for IL-1β precursor and 17 kDa for mature form. β-actin was used as a loading control. Vertical bars represent mean ± SD. *****p<0.0001, *p < 0.05 vs.* Ctr group; *#p < 0.05, ## p<0.01, #### p < 0.0001 vs.* Fe group (One-way ANOVA followed by Bonferroni multiple comparison test). Nuclei were stained by DAPI (blue). Scale bars 50 μm.

When GFAP immunostaining was examined, the labeling, so intense in astrocytic and Müller cell endfeets and processes extending throughout the retina (from the ILM to the outer retinal layers) in the Fe retina group, was greatly reduced and restricted to the GCL/ILM in the FeCxSlb group, whereas it was still significantly present in the FeSlb neuroretina (Fig. 9C). In control retinas, the GFAP expression is restricted to astrocytes at the ILM (data not shown, see Fig. 4A). As GFAP upregulation reflects reactive gliosis due to neuroretinal damage (Pekny et al., 2014), these results, together with the inhibition of microglial/macrophagic activation, suggest that CxSlb treatment conferred an improved anti-inflammatory profile with respect to the treatment with the free Slb.

Finally, to confirm the greater anti-inflammatory effect of CxSlb treatment in the iron-injected eyecups, we examined the expression of Tumor Necrosis Factor-alpha (TNFα) and Interleukin-1 beta (IL1β), principal pro-inflammatory cytokines, in the retina/RPE/choroid lysates by Western blotting analyses. As shown in Figure 9D, we found a higher efficacy of the topical CxSlb treatment in lowering and completely inhibit the increases in TNFα and IL1β induced by iron-injection, as compared to Slb-treatment. The expression level of both pro-inflammatory cytokines remained unchanged following the Cx treatment (FeCx) (data not shown).

Therefore, these results strongly suggest that the topical eye treatment with CxSlb formulation in iron-treated rats suppressed reactive gliosis and microglial activation, thus reducing the expression of the inflammatory cytokines with greater efficiency if compared to free Slb treatment.

2.4 CxSlb topical eye treatment restores VEGF levels in the retina and RPE/choroid of iron-insulted rats

An important aspect in retinal diseases is the regulation of the vascular endothelial growth factor (VEGF) expression functioning as a pro-survival and pro-angiogenic factor.

Therefore, we conducted immunofluorescence labelling using VEGF-A antibody in the retinal and RPE sections for each experimental group. As shown in Fig. 10A, intense VEGF immunostaining was observed in Fe-treated group especially in the RPE and choriocapillares, in the GCL, INL and OPL. The CxSlb treatment drastically prevented the intense VEGF immunoreactivity with an effect that was more evident at retinal level (Fig. 10C) than RPE layer (Fig. 10B), as shown in the densitometric quantification of VEGF immunohistochemistry. A reduced VEGF staining was also observed when Fe-treated rats were treated with Slb formulation (FeSlb).

Western blotting analysis of eyecup lysates confirmed increases in the expression of VEGF and its principal receptor, VEGFR2, in Fe-treated group, which were significantly lowered in lysates of Fe-CxSlb and Fe-Sb treated groups (Fig. 10D).

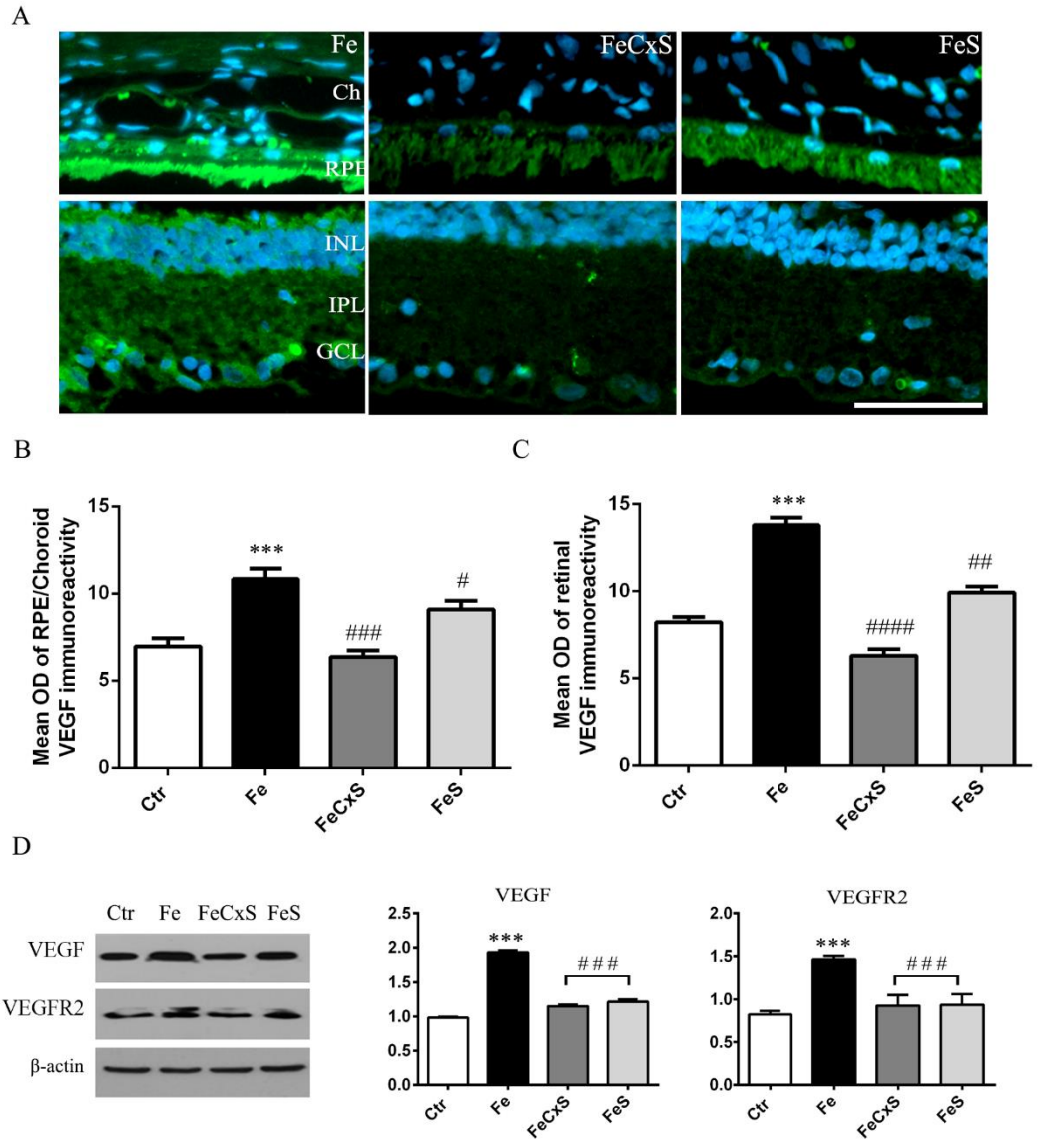

Figure 10. Treatment with CxSlb eye drops restores the expression of VEGF and VEGFR2 in iron-insulted eyes. Representative images of VEGF immunostaining in RPE/choroid and retinal sections from iron-insulted no treated (Fe) or treated with CxSlb (FeCxS) or free Slb (FeS) eye drops. The nuclei were stained using DAPI staining (blue). Scale bar, 50 µm. (B and C) Quantification of immunofluorescence staining of VEGF in the RPE and in the retina. (D) Immunoblots and densitometric analyses of VEGF and VEGFR2 in retina/RPE/choroid lysates from different groups. β-actin was used as a loading control. Vertical bars represent mean ± SD. *** *p<0.001 vs.* Ctr group; *# p < 0.05, ## p<0.01,### p<0.001, #### p<0.0001 vs.* Fe group (One-way ANOVA followed by Bonferroni multiple comparison test).

While quantitative analysis of VEGF immunoreactivity pointed out significant differences between the effects of FeCxSlb and FeSb treatments, such differences were not seen by Western blot analysis. It is possible that a higher amount of VEGF released into the vitreous was present in the eyecup lysates of FeSb treated rats, thus probably accounting for a lower effect of Slb treatment.

These data indicate that topical treatment with Cx-Slb eye drop significantly ameliorates the retinal vascular alterations and inhibits the VEGF and VEGFR2 expression in a more effective manner than free Slb administration, therefore suggesting a possible capability of the nanoparticles to improve the retinal antiangiogenic property of the silibinin.

2.5 CxSlb topical eye treatment reduces apoptotic cell death in the retina and RPE/choroid of iron-insulted rats.

Finally, to confirm the protective effects of CxSlb treatment, the apoptotic cell death that occurs after iron injection (Fig. 6) was analysed by TUNEL staining. As shown in Fig.11A, no TUNEL-positive cells were observed in control group. The total number of TUNEL-positive cells detected in the ONL, RPE and choroidal vessels of iron-treated group was significantly reduced in FeCxSlb group ($p < 0.0001$; Fig. 11B), like in control sections. A lower reduction in the number of apoptotic cells was observed in FeSlb sections with respect to Fe group, in the retina as well as in the RPE ($p<0.01$ in retina and $p<0.001$ in RPE; Fig. 11B). Quantitative analysis of TUNEL staining profiled the same results by evaluating at least three sections of eight eyes analysed for each group.

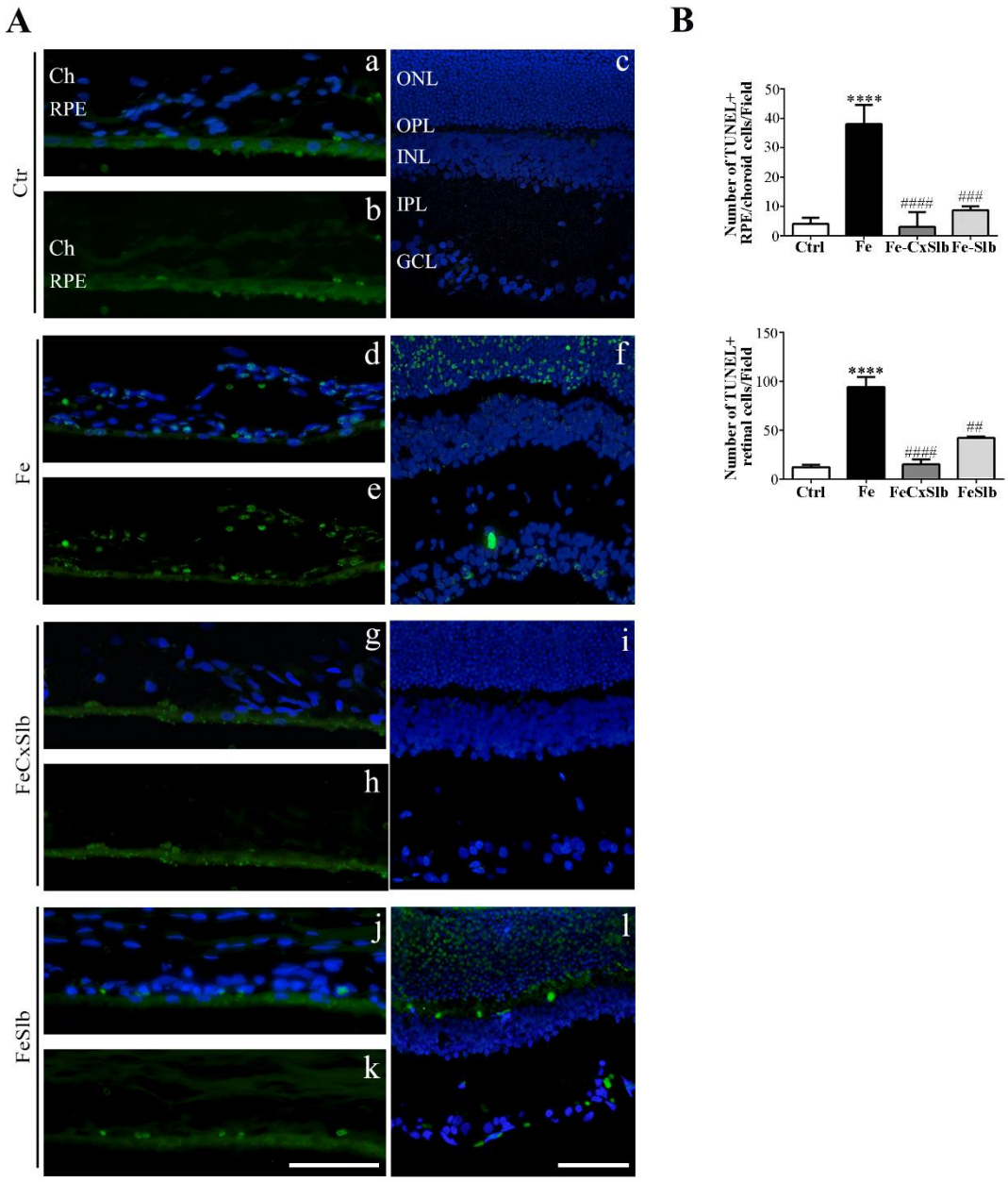

Figure 11. CxSlb topical eye treatment decreases apoptotic cell death in the iron-insulted eyes. (A) Representative images of TUNEL staining of the RPE/choroid (a-b, d-e, g-h, j-k) and retina (c,f,i,l) sections from different groups: control rats (Ctr, a-c), iron-injected rats no treated (Fe, d-f) and topically treated with CxSlb (FeCxSlb, g-i), Slb (FeSlb, j-l) eye drops. RPE/choroidal sections are visualized with (a, d, g, j) and without (b, e, h, k) nuclear dye DAPI (blue). Scale bars, 50 µm. (B) Quantitative analysis of TUNEL-positive cells in RPE/choroid and retina of the different experimental groups. Vertical bars represent mean ± SD. ****$p<0.0001$ *vs.* Ctr; ## $p<0.01$, ### $p<0.001$, #### $p<0.0001$ *vs.* Fe (One-way ANOVA, followed by Bonferroni multiple comparison test).

CONCLUSIONS

In summary, this study supports the hypothesis that iron have a crucial role in the retina and its overload contributes to the pathogenesis of retinal neurodegeneration. Beyond oxidative stress that affected neuroretina and RPE layer, the intravitreal injection of iron sulphate led to progressive retinal neuroinflammation, characterized by progressive macro- and micro-gliosis and by release of pro-inflammatory and angiogenic mediators. For the first time, it has been shown a direct association between ocular iron overload and Ab 1-42 amyloid accumulation. In brief, the iron intravitreal injection provides most of the essential features of human AMD, including the iron accumulation, inflammation, angiogenesis, apoptosis cell death and consequently degeneration of retinal and RPE structures. This simple *in vivo* model of oxidative stress-induced retinal degeneration could be an ideal platform to better understand the mechanisms underlying iron-induced degeneration, also at the basis of CNS diseases, as well as to assess safety and efficacy of ocular drugs with putative neuroprotective properties.

The property of the choline-calix[4]arene nanocarrier, i.e. its spontaneous self-assembly in well-defined micellar nanostructures, was used to entrap and deliver Slb to the posterior segment of the eye. The calixarene-silibinin (CxSlb) nanoassembly was prepared through a simple protocol, with an appreciable drug loading efficiency and a clear colloidal preparation, suitable to allow easy and safe administration as eye drop. In *in vitro* as well as *in vivo* studies, the CxSlb nanoassembly showed no toxic effects, but rather proved to be an optimal platform to improve Slb delivery and efficiency, enhancing its protective activity against oxidative stress induced by iron insult. In particular, CxSlb nanomicelles exhibited higher antioxidant efficacy and protection in the ARPE cells than the free Slb. In addition, the eye drop treatment with a CxSlb formulation presented herein, at doses and with the time schedule developed, revealed an optimal prevention of the RPE/choroidal and neuroretinal alterations induced by iron intravitreal injection. The ocular treatment with CxSlb reduced several iron-mediated pathogenic conditions: oxidative stress, macro- and microglia activation, release of pro-inflammatory mediators including VEGF, vascular alterations and RPE, photoreceptor and neuronal degeneration. The neuroprotective effects of CxSlb topical eye administration appeared to be greater than administration of free Slb.

This study also provides an additional evidence supporting that the topical eye treatment with free Slb has protective effects in the oxidative-induced animal model, albeit low and partial compared to the CxSlb formulation. This could be explained by our accurate choice of the solvent, i.e. the highly hydrophobic DMSO, considered an absorption promoter with the ability to increase drug therapeutic action in the ophthalmic formulations (Marren, 2011). Unlike the toxicity given by its intravitreal administration, no evidence of ocular toxicity has been

observed following DMSO topical application even at high doses (Brobyn, 1975, Shirley et al., 1989, Galvao et al., 2014). To confirm this data, topical administration of Slb in DMSO in corneal organ cultures have shown strong multifunctional protective effects against vesicant-induced ocular injury (Tewari-Singh et al., 2012). To date, no data is available about *in vivo* topical eye treatment with Slb formulation solubilized in DMSO.

The CxSlb micelles showed a great potential to be topically biocompatible and competent for treating posterior segment damages, probably by improving the retention time and sustaining the time-controlled release of the Slb. In addition to the advantages of low dosage and high solubility and absorption, calixarene nanoparticles may also reduce Slb metabolism and modifications, including its shift to a pro-oxidation form, that limits the Slb systemic administration not only for ophthalmic diseases. Further studies of our formulations are needed to understand the effective drug concentration reaching the posterior segment of the eye and the mechanisms of transport and intracellular uptake of the choline-calix[4]arene nanocarrier for topical treatment of posterior eye diseases. It would certainly be extremely interesting to investigate whether the same protective effects are obtained with CxSlb formulation ocular treatment following the iron intravitreal injection.

To date these results are a proof of the potential of calixarene macrocycle as a new platform for topical ocular drug delivery systems.

MATERIALS AND METHODS

Preparation and characterization of choline-calix[4]arene-silibinin nanocarrier

All procedures of preparation and characterization of the nanocarrier have been conducted by Institute of Biomolecular Chemistry (ICB), CNR, Catania. Silibinin (Slb) (MW 482.44 g/mol) and dimethyl sulfoxide (DMSO) were obtained from Sigma-Aldrich, Milan, Italy. The procedure of synthesizing calix[4]arene has been described in more detail in (Granata et al., 2017). For *in vitro* studies, 21 mg of calix[4]arene derivate **1** (0.013 mmol) was dissolved in 20 mL of 10 mM PBS (pH 7.4) and Slb was added (0.064 mmol, 1:5 molar ratio). The mixture was sonicated for 15 min and shaken at 300 rpm, 25 °C for 3 days. Sonication was performed on Ultrasonic cleaner 600^{TH}, frequency 45 kHz and power 1200 W, after 15 min the initial temperature of the sonicating bath increased from 20 to 27 °C. After centrifugation at 2,933 × g for 30 min, the supernatant was recovered and filtered through a 0.2 μm GHP filter (Acrodisc) to give a clear colloidal solution. For *in vivo* studies, 250 mg of calix[4]arene **1** (0.15 mmol) was dissolved in 25 mL of 10 mM PBS (pH 7.4)/H_2O (1:1.8, *v*/*v*) and 220 mg of Slb was added. A clear, colorless colloidal solution was obtained by following the above reported procedure. For *in vitro* and *in vivo* studies, a stock solution of Slb was prepared in DMSO.

Cell culture and Cytotoxicity of CxSlb in vitro

The human retinal pigment epithelial cell line (ARPE-19, ATCC® CRL-2302™) was cultured in Dulbecco's Modified Eagles Medium/Ham's F-12 (DMEM/F12; Gibco) (1:1), supplemented with 10% fetal bovine serum (FBS), 2mM L-glutamine and 1% penicillin/streptomycin solution (Gibco) under 37°C with 5% CO_2 humidified atmosphere. ARPE-19 cells (1×10^4) were seeded into 96-well plates and allowed to grow for 48 hours, when cells reached 80-90% confluence before the treatments. Considering a % of Loading Capacity (LC) (Entrapped Drug/*nanoparticles*) of 10.7%, the final concentrations of CxSlb were set to parallel those of free Slb, ranging from 0.01 to 1μM. The effect of nanoparticles on cell membrane integrity was measured by the lactate dehydrogenase enzyme release (LDH) assays. In brief, cells were pre-treated with different concentrations of CxSlb, Cx or Slb for 20h and after PBS washing, cells were exposed to $FeSO_4$ (50 μM , Sigma-Aldrich) dissolved in serum-free culture medium for 3h. After incubation, the medium was carefully removed from the plate and assayed in accordance with manufacturer's instruction (LDH Cytotoxicity Detection Kit) and the absorbance was measured at 490 nm (630 nm reference wavelength). The absorbance value of

a culture medium control was used to normalize the values obtained from other samples. The analysis for all assays were conducted using a microplate reader (Synergy™ HT, BioTek®). All experiments were performed in quadruplicate and repeated three times.

Animals

All experimental procedures were in accordance with local and Institutional Animal Survey Board on behalf of the Italian Ministry of Health and conducted according to Italian law (Legislative Decree 26/2014) and European Communities Council Directive (2010/63/EU) on the protection of animals used for scientific purposes. All efforts were made to minimize animal number, and to refine the behavioral procedures. Seventy male Wistar rats (Charles River Laboratories, Calco, Italy), 8 week-old (200-250g body weight), were maintained in environmentally controlled room (22 ± 2 °C, relative humidity 50 ± 10%) with 12 h light-dark cycle and free access to food and water. Before any use, after animal transport and arrival in our animal facility a period of acclimatization of 1 week was performed.

Treatment of animals

Intravitreal injection was performed as previously described (D'Anna et al., 2011). Briefly, each rat was anesthetized by intramuscular injections of a mixture of ketamine (85 mg/kg) and xylazine (14 mg/kg) for the duration of all surgical procedures. The rats received an intravitreal injection of five µl/eye of normal saline (NS, 0,9% NaCl) (SF, physiological solution) or $FeSO_4$ diluted in NS (50 µM, Sigma-Aldrich, St. Louis, MO), using a 10 µl Hamilton syringe adapted with a 25-gauge glass microneedle. The needle tip was inserted into the superior hemisphere of the eye at 45° angle through the sclera into vitreous body. Following intravitreal injections, the needle was held in place for one min and withdrawn slowly. Each animal was monitored during the procedure by possible damage of lens and loss of fluid from the eye, isolated placing in recovery box until to regain consciousness and those with retinal bleeding or lens injury from the injection procedure were excluded from the study. For the first part of the study, twenty Wistar rats were divided in four groups (n= 5 per group): (i) normal saline-injected (Ctr) group and iron-injected rats at one day (ii), ten (iii) and fifteen days (iv) after insult. For the study of therapeutic approach based on choline-calix[4]arene-silibinin, the animals were divided into six groups (n= 8 per group): (i) control group with no injection and no treatment (**sham**

injection/sham treatment; Ctr); (ii) saline solution intravitreal injected group (saline **injection/sham (vehicle) treatment**; **SF-VH)**; (iii) iron sulphate intravitreal injected group with no treatment (Fe-**injection/sham (vehicle) treatment; Fe**); (iv) iron injected group treated with 10 mg/ml calixarene in vehicle (**FeCx**); (v) iron-injected group treated with colloidal solutions 10 mg/ml calixarene and 1.1 mg/mL silibinin in vehicle (**FeCxSlb**); (vi) iron-injected group treated with silibinin formulation (1.1mg/ml) in vehicle (6.35% DMSO) (**FeSlb)**. For eyes drops administration, 15µL eye drops were instilled topically in both eyes, repeated once per day for a total of thirteen days without anaesthesia. On thirteenth day, rats were anesthetized with a ketamine/xylazine mix, sacrificed and the enucleated eyes were fixed in 4% paraformaldehyde and embedded in paraffin for immunohistochemical and histological analyses. For biochemical analyses, eyes were quickly frozen in liquid nitrogen.

Thiobarbituric Acid Reactive Substances (TBARS) Measurement

Lipid peroxidation was evaluated by measuring TBARS, including malondialdehyde, according to the method of Cascio et al. (Cascio et al., 2000). The amount of TBARS was expressed as nanomoles of TBARS per milligram of protein. All data are the mean ± SD of three independent experiments.

Histology and immunohistochemistry staining

Five-µm-thick sections of each eye were deparaffinized, rehydrated and stained with hematoxylin and eosin (H&E) or Congo red (Bioptica) used according to manufacturer's instruction. For immunofluorescence assays or TUNEL staining, sections were microwaved in citrate buffer for antigen retrieval and then blocked with 5 or 10% normal serum in PBS plus 0,1-0,3% Triton X-100 (PBS-T) for 1 hours at room temperature (RT). Primary antibodies used in this study are listed in Table 1. After incubation with primary antibodies overnight at 4°C, the slides were washed in PBS and incubated with the fluorescent-labelled secondary and appropriate antibodies for 2 hours at room temperature. The following secondary antibodies were used: Alexa Fluor 555-conjugated or Alexa Fluor 488-conjugated goat-anti-mouse IgG or Alexa Fluor 488 goat anti-rabbit IgG (Invitrogen). Finally, all sections were coverslipped using Vectashield mounting medium with 4,6-diamidino-2-phenylindole (DAPI) (Vector Laboratories, Inc. Burlingame). Negative controls were performed for every set of experiments by omitting the primary antibodies and no staining was detected in these sections. The

fluorescence images were processed by Axioskop-2 Zeiss or Leica DM4000 microscopes/software. All photomicrographs were collected using the same magnification (20x or 40x objectives), exposure time (350 ms), other parameters, and the representative images from four/five sections for each eye specimen (eyes/group) were edited with Adobe Photoshop software. For quantitative analysis, the images were imported into the ImageJ software program (NIH, Bethesda, MD), converted to gray scale, and the total area of immunoreactivity was quantified by measuring the mean intensity of all stained areas of each micrograph and the data were expressed as mean density. Total retinal area was used to normalize the data by computing the percent retinal area occupied by Ab-immunoreactivity.

Perls' stain and TUNEL assay

Perl's staining (Bioptica) specific for iron levels was carried out according the manufacturer's instruction. In situ detection of DNA fragmentation was performed using the terminal deoxyribonucleotidyl transferase (TDT)-mediated dUTP-digoxigenin nick end labelling (TUNEL) assay (Promega, Madison, WI, USA), following the manufacturer's instructions. Retina sections were counterstained with DAPI to reveal cell nuclei. The positive control tissue sections were pre-incubated for 10 min with DNase I (lg/ml) at RT, while the negative control sections were processed omitting TdT enzyme. TUNEL-positive cells were quantified in six sections for each specimen and results were expressed as mean ± SD.

Protein Isolation and Western blot Analysis

To prepare protein lysates, eyes were dissected to remove the anterior segment including the cornea, iris, and the lens, under a surgical microscope. For Western blotting analyses, protein extracts were prepared from a pool of four posterior eyecups by homogenization in ice-cold RIPA buffer (Cell Signaling), supplemented with protease and phosphatase inhibitors (Roche Applied Sciences), and centrifuged at 14,000g for 10 min at 4°C. Protein extracts of supernatants were determined by Bradford-assay (Bio-Rad) and forty micrograms of proteins were separated by SDS-PAGE and transferred onto PVDF or LiCor membranes. PVDF membranes were blocked with 5% non-fat milk in TBS buffer-T (0.1%) for 1 h at RT and immunoblotted with different primary antibodies (see Table 1) overnight at 4°C. Immunocomplexes were detected with HRP-Linked anti-rabbit IgG (Amersham Pharmacia Biotech.) or anti-mouse IgG (GE Healthcare) using enhanced chemiluminescence reagent

(Super Signal West Pico, Pierce). Monoclonal anti-β-actin antibody (Sigma) was used to confirm equal protein loading and transfer of samples. For LiCor membrane, after the blocking with LiCor blocking buffer (LCB, Lincoln, NE) for 1 h, the membrane was immunoblotted with primary antibodies overnight at 4°C (see Table 1) and, after washes, it was probed with appropriate secondary antisera in LCB buffer for 1 hour at room temperature. The following secondary antibodies were used: goat anti-mouse IR-Dye800cw, rabbit anti-goat IR-Dy680cw (Odyssey LiCor) or goat anti-rabbit Alexa Fluor 680 (Invitrogen). Immunocomplexes were detected using an Odyssey scanner and analyzed using the Odyssey Application Software to obtain the integrated intensities. Densitometry was performed using Chemi-Doc, Quantity-One analysis (Bio-Rad).

Statistical Analysis

All data were expressed as mean ± standard error (SD). Statistical analyses were performed using GraphPad Prism 6.0 software (GraphPad Software Inc., San Diego, CA, USA), using Student's unpaired two-tailed t test or One-way ANOVA with Bonferroni's multiple comparisons tests. P-values < 0.05 were considered statistically significant.

Antibody	Host	Source and diluition	Application
8OH-dG	Mouse	Santa Cruz	IF
GFAP	Mouse	Santa Cruz	IF
Iba-1	Rabbit	Wako Chemicals	IF
TNFα	Mouse	Peprotech	IF/WB
IL10	Goat	Santa Cruz	WB
IL1β	Rabbit	Santa Cruz	WB
Aβ 1-42	Mouse	Synaptic System	IF
Aβ 1-42	Rabbit	Millipore	WB
Cas9	Mouse	Santa Cruz	WB
Cas3	Goat	Santa Cruz	WB
MCP-1	Goat	Santa Cruz	WB
VEGF	Rabbit	Santa Cruz	IF/WB
TGFβ	Goat	Santa Cruz	WB
VEGFR2	Mouse	Cell Signaling	WB

Table. 1. Primary antibodies used in this study

REFERENCES

2001. A randomized, placebo-controlled, clinical trial of high-dose supplementation with vitamins C and E, beta carotene, and zinc for age-related macular degeneration and vision loss: AREDS report no. 8. *Arch Ophthalmol,* 119**,** 1417-36.

ABU EL-ASRAR, A. M., NAWAZ, M. I., KANGAVE, D., MAIRAJ SIDDIQUEI, M. & GEBOES, K. 2013. Angiogenic and vasculogenic factors in the vitreous from patients with proliferative diabetic retinopathy. *Journal of diabetes research,* 2013**,** 539658.

ACTIS, A. G., VERSINO, E., BROGLIATTI, B. & ROLLE, T. 2016. Risk Factors for Primary Open Angle Glaucoma (POAG) Progression: A Study Ruled in Torino. *Open Ophthalmol J,* 10**,** 129-39.

AGOSTA, F., WEILER, M. & FILIPPI, M. 2015. Propagation of pathology through brain networks in neurodegenerative diseases: from molecules to clinical phenotypes. *CNS Neurosci Ther,* 21**,** 754-67.

AL-GAYYAR, M. M. & ELSHERBINY, N. M. 2013. Contribution of TNF-alpha to the development of retinal neurodegenerative disorders. *Eur Cytokine Netw,* 24**,** 27-36.

ALEXANDROV, P. N., POGUE, A., BHATTACHARJEE, S. & LUKIW, W. J. 2011. Retinal amyloid peptides and complement factor H in transgenic models of Alzheimer's disease. *Neuroreport,* 22**,** 623-7.

ANDERSEN, H. H., JOHNSEN, K. B. & MOOS, T. 2014. Iron deposits in the chronically inflamed central nervous system and contributes to neurodegeneration. *Cell Mol Life Sci,* 71**,** 1607-22.

ARCHIBALD, N. K., CLARKE, M. P., MOSIMANN, U. P. & BURN, D. J. 2009. The retina in Parkinson's disease. *Brain,* 132**,** 1128-45.

AYDIN, T. S., UMIT, D., NUR, O. M., FATIH, U., ASENA, K., NEFISE, O. Y. & SERPIL, Y. 2018. Optical coherence tomography findings in Parkinson's disease. *Kaohsiung J Med Sci,* 34**,** 166-171.

AYTON, S., LEI, P. & BUSH, A. I. 2013. Metallostasis in Alzheimer's disease. *Free Radic Biol Med,* 62**,** 76-89.

BARAR, J., JAVADZADEH, A. R. & OMIDI, Y. 2008. Ocular novel drug delivery: impacts of membranes and barriers. *Expert Opin Drug Deliv,* 5**,** 567-81.

BAYER, A. U., KELLER, O. N., FERRARI, F. & MAAG, K.-P. 2002. Association of glaucoma with neurodegenerative diseases with apoptotic cell death: Alzheimer’s disease and Parkinson’s disease. *American Journal of Ophthalmology,* 133**,** 135-137.

BEATTY, S., KOH, H., PHIL, M., HENSON, D. & BOULTON, M. 2000. The role of oxidative stress in the pathogenesis of age-related macular degeneration. *Surv Ophthalmol,* 45**,** 115-34.

BELOQUI, A., SOLINIS, M. A., RODRIGUEZ-GASCON, A., ALMEIDA, A. J. & PREAT, V. 2016. Nanostructured lipid carriers: Promising drug delivery systems for future clinics. *Nanomedicine,* 12**,** 143-61.

BISCETTI, L., LUCHETTI, E., VERGARO, A., MENDUNO, P., CAGINI, C. & PARNETTI, L. 2017. Associations of Alzheimer's disease with macular degeneration. *Front Biosci (Elite Ed),* 9**,** 174-191.

BISHOP, G., DANG, T., DRINGEN, R. & ROBINSON, S. 2011. Accumulation of Non-Transferrin-Bound Iron by Neurons, Astrocytes, and Microglia. *Neurotoxicity research,* 19**,** 443-51.

BISHT, R., MANDAL, A., JAISWAL, J. K. & RUPENTHAL, I. D. 2018. Nanocarrier mediated retinal drug delivery: overcoming ocular barriers to treat posterior eye diseases. 10.

BISWAS, S. K. 2016. Does the Interdependence between Oxidative Stress and Inflammation Explain the Antioxidant Paradox? *Oxid Med Cell Longev,* 2016**,** 5698931.

BLANCO, R. B., M. L.; CAVALLARO, G.; CONSOLI, G. M. L.; CRAPARO, E. F. GIAMMMONA, G.; LICCIARDI, M.; PITARRESI, G.; GRANATA, G.; SALADINO, P.; LA MARCA, C.; DEIDDA, I.; PAPASERGI, S.; GUARNERI, P.; CUZZOCREA, S.; ESPOSITO, E.; VIOLA, S. 2016. Nanostructured formulations for the delivery of silibinin and other active ingredients for treating ocular diseases. *Patent WO/2016/055976*

BLANKS, J. C., HINTON, D. R., SADUN, A. A. & MILLER, C. A. 1989. Retinal ganglion cell degeneration in Alzheimer's disease. *Brain Res,* 501**,** 364-72.

BLASIAK, J., PETROVSKI, G., VEREB, Z., FACSKO, A. & KAARNIRANTA, K. 2014. Oxidative stress, hypoxia, and autophagy in the neovascular processes of age-related macular degeneration. *Biomed Res Int,* 2014**,** 768026.

BLASIAK, J., SZAFLIK, J. & SZAFLIK, J. P. 2011. Implications of altered iron homeostasis for age-related macular degeneration. *Front Biosci (Landmark Ed),* 16**,** 1551-9.

BODIS-WOLLNER, I. 1990. Visual deficits related to dopamine deficiency in experimental animals and Parkinson's disease patients. *Trends Neurosci,* 13**,** 296-302.

BODIS-WOLLNER, I. 2009. Retinopathy in Parkinson Disease. *J Neural Transm (Vienna),* 116**,** 1493-501.

BROBYN, R. D. 1975. The human toxicology of dimethyl sulfoxide. *Ann N Y Acad Sci,* 243**,** 497-506.
BRUIJN, L. I., MILLER, T. M. & CLEVELAND, D. W. 2004. Unraveling the mechanisms involved in motor neuron degeneration in ALS. *Annu Rev Neurosci,* 27**,** 723-49.
BURGER, P. C. & KLINTWORTH, G. K. 1974. Experimental retinal degeneration in the rabbit produced by intraocular iron. *Lab Invest,* 30**,** 9-19.
BUSH, A. I. 2002. Metal complexing agents as therapies for Alzheimer's disease. *Neurobiol Aging,* 23**,** 1031-8.
CAHILL, C. M., LAHIRI, D. K., HUANG, X. & ROGERS, J. T. 2009. Amyloid precursor protein and alpha synuclein translation, implications for iron and inflammation in neurodegenerative diseases. *Biochim Biophys Acta,* 1790**,** 615-28.
CAI, J., NELSON, K. C., WU, M., STERNBERG, P., JR. & JONES, D. P. 2000. Oxidative damage and protection of the RPE. *Prog Retin Eye Res,* 19**,** 205-21.
CAI, X. & MCGINNIS, J. F. 2012. Oxidative stress: the achilles' heel of neurodegenerative diseases of the retina. *Front Biosci (Landmark Ed),* 17**,** 1976-95.
CASCIO, C., DEIDDA, I., RUSSO, D. & GUARNERI, P. 2015. The estrogenic retina: The potential contribution to healthy aging and age-related neurodegenerative diseases of the retina. *Steroids,* 103**,** 31-41.
CASCIO, C., GUARNERI, R., RUSSO, D., DE LEO, G., GUARNERI, M., PICCOLI, F. & GUARNERI, P. 2000. Pregnenolone sulfate, a naturally occurring excitotoxin involved in delayed retinal cell death. *J Neurochem,* 74**,** 2380-91.
CHALAM, K. V., KHETPAL, V., RUSOVICI, R. & BALAIYA, S. 2011. A review: role of ultraviolet radiation in age-related macular degeneration. *Eye Contact Lens,* 37**,** 225-32.
CHAMBERLAIN, R., WENGENACK, T. M., PODUSLO, J. F., GARWOOD, M. & JACK, C. R., JR. 2011. Magnetic resonance imaging of amyloid plaques in transgenic mouse models of Alzheimer's disease. *Current medical imaging reviews,* 7**,** 3-7.
CHEN, C. L., CHEN, J. T., LIANG, C. M., TAI, M. C., LU, D. W. & CHEN, Y. H. 2017. Silibinin treatment prevents endotoxin-induced uveitis in rats in vivo and in vitro. *PLoS One,* 12**,** e0174971.
CHEN, H., LIU, B., LUKAS, T. J. & NEUFELD, A. H. 2008. The aged retinal pigment epithelium/choroid: a potential substratum for the pathogenesis of age-related macular degeneration. *PLoS One,* 3**,** e2339.
CHEN, H., LUKAS, T. J., DU, N., SUYEOKA, G. & NEUFELD, A. H. 2009. Dysfunction of the retinal pigment epithelium with age: increased iron decreases phagocytosis and lysosomal activity. *Invest Ophthalmol Vis Sci,* 50**,** 1895-902.
CHEN, H., WANG, X., WANG, M., YANG, L., YAN, Z., ZHANG, Y. & LIU, Z. 2015. Behavioral and Neurochemical Deficits in Aging Rats with Increased Neonatal Iron Intake: Silibinin's Neuroprotection by Maintaining Redox Balance. *Front Aging Neurosci,* 7**,** 206.
CHEN, X., GUO, C. & KONG, J. 2012. Oxidative stress in neurodegenerative diseases. *Neural Regeneration Research,* 7**,** 376-385.
CHEN, Y. H., CHEN, C. L., LIANG, C. M., LIANG, J. B., TAI, M. C., CHANG, Y. H., LU, D. W. & CHEN, J. T. 2014. Silibinin inhibits ICAM-1 expression via regulation of N-linked and O-linked glycosylation in ARPE-19 cells. *Biomed Res Int,* 2014**,** 701395.
CHEUNG, C. Y., ONG, Y. T., IKRAM, M. K., CHEN, C. & WONG, T. Y. 2014. Retinal microvasculature in Alzheimer's disease. *J Alzheimers Dis,* 42 Suppl 4**,** S339-52.
CHIASSEU, M., ALARCON-MARTINEZ, L., BELFORTE, N., QUINTERO, H., DOTIGNY, F., DESTROISMAISONS, L., VANDE VELDE, C., PANAYI, F., LOUIS, C. & DI POLO, A. 2017. Tau accumulation in the retina promotes early neuronal dysfunction and precedes brain pathology in a mouse model of Alzheimer's disease. 12**,** 58.
CHIU, K., CHAN, T. F., WU, A., LEUNG, I. Y., SO, K. F. & CHANG, R. C. 2012. Neurodegeneration of the retina in mouse models of Alzheimer's disease: what can we learn from the retina? *Age (Dordr),* 34**,** 633-49.
CHOLKAR, K., PATEL, A., VADLAPUDI, A. D. & MITRA, A. K. 2012. Novel Nanomicellar Formulation Approaches for Anterior and Posterior Segment Ocular Drug Delivery. *Recent Pat Nanomed,* 2**,** 82-95.
CHONG, N. V. & ADEWOYIN, T. 2007. Intravitreal injection: balancing the risks. *Eye,* 21**,** 313-316.
CHOWERS, I., WONG, R., DENTCHEV, T., FARKAS, R. H., IACOVELLI, J., GUNATILAKA, T. L., MEDEIROS, N. E., PRESLEY, J. B., CAMPOCHIARO, P. A., CURCIO, C. A., DUNAIEF, J. L. & ZACK, D. J. 2006. The iron carrier

transferrin is upregulated in retinas from patients with age-related macular degeneration. *Invest Ophthalmol Vis Sci,* 47**,** 2135-40.

CHU, K.-O. & PANG, C.-P. 2014. Herbal molecules in eye diseases. *Taiwan Journal of Ophthalmology,* 4**,** 103-109.

COLLINGWOOD, J. F., CHONG, R. K., KASAMA, T., CERVERA-GONTARD, L., DUNIN-BORKOWSKI, R. E., PERRY, G., PÓSFAI, M., SIEDLAK, S. L., SIMPSON, E. T., SMITH, M. A. & DOBSON, J. 2008. Three-dimensional tomographic imaging and characterization of iron compounds within Alzheimer's plaque core material. *J Alzheimers Dis,* 14**,** 235-45.

CONGDON, N., O'COLMAIN, B., KLAVER, C. C., KLEIN, R., MUÑOZ, B., FRIEDMAN, D. S., KEMPEN, J., TAYLOR, H. R. & MITCHELL, P. 2004. Causes and prevalence of visual impairment among adults in the United States. *Arch Ophthalmol,* 122**,** 477-85.

CONNOR, J. R., SNYDER, B. S., BEARD, J. L., FINE, R. E. & MUFSON, E. J. 1992. Regional distribution of iron and iron-regulatory proteins in the brain in aging and Alzheimer's disease. *J Neurosci Res,* 31**,** 327-35.

CONSOLI, G. M. L., GRANATA, G. & GERACI, C. 2018. Chapter 3 - Calixarene-based micelles: Properties and applications A2 - Grumezescu, Alexandru Mihai. *Design and Development of New Nanocarriers.* William Andrew Publishing.

CORNEL, S., ADRIANA, I. D., MIHAELA, T. C., SPERANTA, S., ALGERINO, D. S., MEHDI, B. & JALALADIN, H.-R. 2015. Anti-vascular endothelial growth factor indications in ocular disease. *Romanian journal of ophthalmology,* 59**,** 235-242.

CRABB, J. W., MIYAGI, M., GU, X., SHADRACH, K., WEST, K. A., SAKAGUCHI, H., KAMEI, M., HASAN, A., YAN, L., RAYBORN, M. E., SALOMON, R. G. & HOLLYFIELD, J. G. 2002. Drusen proteome analysis: an approach to the etiology of age-related macular degeneration. *Proc Natl Acad Sci U S A,* 99**,** 14682-7.

CRICHTON, R. 2016. *Iron metabolism: from molecular mechanisms to clinical consequences*, John Wiley & Sons.

CRICHTON, R. & WARD, R. 2013. *Metal-based neurodegeneration: from molecular mechanisms to therapeutic strategies*, John Wiley & Sons.

CRISTOVAO, J. S. & SANTOS, R. 2016. Metals and Neuronal Metal Binding Proteins Implicated in Alzheimer's Disease. 2016**,** 9812178.

CUENCA, N., FERNANDEZ-SANCHEZ, L., CAMPELLO, L., MANEU, V., DE LA VILLA, P., LAX, P. & PINILLA, I. 2014. Cellular responses following retinal injuries and therapeutic approaches for neurodegenerative diseases. *Prog Retin Eye Res,* 43**,** 17-75.

D'ANNA, C., CASCIO, C., CIGNA, D., GALIZZI, G., DEIDDA, I., BIANCHI, L., RUSSO, D., PASSANTINO, R., BINI, L. & GUARNERI, P. 2011. A retinal proteomics-based study identifies alphaA-crystallin as a sex steroid-regulated protein. *Proteomics,* 11**,** 986-90.

DA SILVA, S. B., FERREIRA, D., PINTADO, M. & SARMENTO, B. 2016. Chitosan-based nanoparticles for rosmarinic acid ocular delivery--In vitro tests. *Int J Biol Macromol,* 84**,** 112-20.

DAS, S. K. & MUKHERJEE, S. 2012. Biochemical and immunological basis of silymarin effect, a milk thistle (Silybum marianum) against ethanol-induced oxidative damage. *Toxicol Mech Methods,* 22**,** 409-13.

DEEP, G., GANGAR, S. C., RAJAMANICKAM, S., RAINA, K., GU, M., AGARWAL, C., OBERLIES, N. H. & AGARWAL, R. 2012. Angiopreventive efficacy of pure flavonolignans from milk thistle extract against prostate cancer: targeting VEGF-VEGFR signaling. *PLoS One,* 7**,** e34630.

DEEP, G., KUMAR, R., NAMBIAR, D. K., JAIN, A. K., RAMTEKE, A. M., SERKOVA, N. J., AGARWAL, C. & AGARWAL, R. 2017. Silibinin inhibits hypoxia-induced HIF-1alpha-mediated signaling, angiogenesis and lipogenesis in prostate cancer cells: In vitro evidence and in vivo functional imaging and metabolomics. *Mol Carcinog,* 56**,** 833-848.

DEHABADI, M. H., DAVIS, B. M., WONG, T. K. & CORDEIRO, M. F. 2014. Retinal manifestations of Alzheimer's disease. *Neurodegener Dis Manag,* 4**,** 241-52.

DEISINGER, P. J. 1996. HUMAN EXPOSURE TO NATURALLY OCCURRING HYDROQUINONE. *Journal of Toxicology and Environmental Health,* 47**,** 31-46.

DELPLACE, V., PAYNE, S. & SHOICHET, M. 2015. Delivery strategies for treatment of age-related ocular diseases: From a biological understanding to biomaterial solutions. *J Control Release,* 219**,** 652-68.

DENTCHEV, T., HAHN, P. & DUNAIEF, J. L. 2005. Strong labeling for iron and the iron-handling proteins ferritin and ferroportin in the photoreceptor layer in age-related macular degeneration. *Arch Ophthalmol,* 123**,** 1745-6.

DEV, S. & BABITT, J. L. 2017. Overview of iron metabolism in health and disease. *Hemodialysis international. International Symposium on Home Hemodialysis,* 21 Suppl 1**,** S6-S20.

DEVI, S., MAHALAXMI, I., ASWATHY, N., DHIVYA, V. & BALACHANDAR, V. 2020. Does retina play a role in Parkinson's Disease? *Acta Neurologica Belgica,* 120.

DI BARI, I., FRAIX, A., PICCIOTTO, R., BLANCO, A. R., PETRALIA, S., CONOCI, S., GRANATA, G., CONSOLI, G. M. L. & SORTINO, S. 2016a. Supramolecular activation of the photodynamic properties of porphyrinoid photosensitizers by calix[4]arene nanoassemblies. *RSC Advances,* 6**,** 105573-105577.

DI BARI, I., PICCIOTTO, R., GRANATA, G., BLANCO, A. R., CONSOLI, G. M. & SORTINO, S. 2016b. A bactericidal calix[4]arene-based nanoconstruct with amplified NO photorelease. *Org Biomol Chem,* 14**,** 8047-52.

DIEBOLD, Y. & CALONGE, M. 2010. Applications of nanoparticles in ophthalmology. *Prog Retin Eye Res,* 29**,** 596-609.

DJAMGOZ, M. B., HANKINS, M. W., HIRANO, J. & ARCHER, S. N. 1997. Neurobiology of retinal dopamine in relation to degenerative states of the tissue. *Vision Res,* 37**,** 3509-29.

DRINGEN, R., BISHOP, G. M., KOEPPE, M., DANG, T. N. & ROBINSON, S. R. 2007. The pivotal role of astrocytes in the metabolism of iron in the brain. *Neurochem Res,* 32**,** 1884-90.

DUAN, S., GUAN, X., LIN, R., LIU, X., YAN, Y., LIN, R., ZHANG, T., CHEN, X., HUANG, J., SUN, X., LI, Q., FANG, S., XU, J., YAO, Z. & GU, H. 2015. Silibinin inhibits acetylcholinesterase activity and amyloid beta peptide aggregation: a dual-target drug for the treatment of Alzheimer's disease. *Neurobiol Aging,* 36**,** 1792-807.

DUNAIEF, J. L. 2006. Iron induced oxidative damage as a potential factor in age-related macular degeneration: the Cogan Lecture. *Invest Ophthalmol Vis Sci,* 47**,** 4660-4.

DUNAIEF, J. L., RICHA, C., FRANKS, E. P., SCHULTZE, R. L., ALEMAN, T. S., SCHENCK, J. F., ZIMMERMAN, E. A. & BROOKS, D. G. 2005. Macular degeneration in a patient with aceruloplasminemia, a disease associated with retinal iron overload. *Ophthalmology,* 112**,** 1062-5.

DUTESCU, R. M., LI, Q. X., CROWSTON, J., MASTERS, C. L., BAIRD, P. N. & CULVENOR, J. G. 2009. Amyloid precursor protein processing and retinal pathology in mouse models of Alzheimer's disease. *Graefes Arch Clin Exp Ophthalmol,* 247**,** 1213-21.

EDWARDS, M. M., RODRIGUEZ, J. J., GUTIERREZ-LANZA, R., YATES, J., VERKHRATSKY, A. & LUTTY, G. A. 2014. Retinal macroglia changes in a triple transgenic mouse model of Alzheimer's disease. *Exp Eye Res,* 127**,** 252-60.

ESMAEIL, N., ANARAKI, S. B., GHARAGOZLOO, M. & MOAYEDI, B. 2017. Silymarin impacts on immune system as an immunomodulator: One key for many locks. *Int Immunopharmacol,* 50**,** 194-201.

FARBOUD, B., AOTAKI-KEEN, A., MIYATA, T., HJELMELAND, L. M. & HANDA, J. T. 1999. Development of a polyclonal antibody with broad epitope specificity for advanced glycation endproducts and localization of these epitopes in Bruch's membrane of the aging eye. *Mol Vis,* 5**,** 11.

FARNOODIAN, M., WANG, S., DIETZ, J., NICKELLS, R. W., SORENSON, C. M. & SHEIBANI, N. 2017. Negative regulators of angiogenesis: important targets for treatment of exudative AMD. *Clin Sci (Lond),* 131**,** 1763-1780.

FISCHER, M. & VOGTLE, F. 1999. Dendrimers: From Design to Application-A Progress Report. *Angew Chem Int Ed Engl,* 38**,** 884-905.

FUNKE, C., SCHNEIDER, S. A., BERG, D. & KELL, D. B. 2013. Genetics and iron in the systems biology of Parkinson's disease and some related disorders. *Neurochem Int,* 62**,** 637-52.

GALVAO, J., DAVIS, B., TILLEY, M., NORMANDO, E., DUCHEN, M. R. & CORDEIRO, M. F. 2014. Unexpected low-dose toxicity of the universal solvent DMSO. *Faseb j,* 28**,** 1317-30.

GASPARINI, L., CROWTHER, R. A., MARTIN, K. R., BERG, N., COLEMAN, M., GOEDERT, M. & SPILLANTINI, M. G. 2011. Tau inclusions in retinal ganglion cells of human P301S tau transgenic mice: effects on axonal viability. *Neurobiol Aging,* 32**,** 419-33.

GAUDANA, R., ANANTHULA, H. K., PARENKY, A. & MITRA, A. K. 2010. Ocular drug delivery. *Aaps j,* 12**,** 348-60.

GAZAK, R., WALTEROVA, D. & KREN, V. 2007. Silybin and silymarin--new and emerging applications in medicine. *Curr Med Chem,* 14**,** 315-38.

GEED, M., GARABADU, D., AHMAD, A. & KRISHNAMURTHY, S. 2014. Silibinin pretreatment attenuates biochemical and behavioral changes induced by intrastriatal MPP+ injection in rats. *Pharmacol Biochem Behav,* 117**,** 92-103.

GEROSKI, D. H. & EDELHAUSER, H. F. 2001. Transscleral drug delivery for posterior segment disease. *Adv Drug Deliv Rev,* 52**,** 37-48.

GHATE, D. & EDELHAUSER, H. 2006. Ocular drug delivery. *Expert opinion on drug delivery,* 3**,** 275-87.

GHRIBI, O., GOLOVKO, M. Y., LARSEN, B., SCHRAG, M. & MURPHY, E. J. 2006. Deposition of iron and beta-amyloid plaques is associated with cortical cellular damage in rabbits fed with long-term cholesterol-enriched diets. *J Neurochem,* 99**,** 438-49.

GIPSON, I. K. & ARGUESO, P. 2003. Role of mucins in the function of the corneal and conjunctival epithelia. *Int Rev Cytol,* 231**,** 1-49.

GNANA-PRAKASAM, J. P., MARTIN, P. M., MYSONA, B. A., ROON, P., SMITH, S. B. & GANAPATHY, V. 2008. Hepcidin expression in mouse retina and its regulation via lipopolysaccharide/Toll-like receptor-4 pathway independent of Hfe. *Biochem J,* 411**,** 79-88.

GNANA-PRAKASAM, J. P., MARTIN, P. M., SMITH, S. B. & GANAPATHY, V. 2010. Expression and function of iron-regulatory proteins in retina. *IUBMB life,* 62**,** 363-370.

GRAHAM, S. L. & KLISTORNER, A. 2017. Afferent visual pathways in multiple sclerosis: a review. *Clin Exp Ophthalmol,* 45**,** 62-72.

GRANATA, G., PATERNITI, I., GERACI, C., CUNSOLO, F., ESPOSITO, E., CORDARO, M., BLANCO, A. R., CUZZOCREA, S. & CONSOLI, G. M. L. 2017. Potential Eye Drop Based on a Calix[4]arene Nanoassembly for Curcumin Delivery: Enhanced Drug Solubility, Stability, and Anti-Inflammatory Effect. *Mol Pharm,* 14**,** 1610-1622.

GRIMALDI, A., BRIGHI, C. & PERUZZI, G. 2018. Inflammation, neurodegeneration and protein aggregation in the retina as ocular biomarkers for Alzheimer's disease in the 3xTg-AD mouse model. 9**,** 685.

GRIMM, C. & REMÉ, C. E. 2013. Light damage as a model of retinal degeneration. *Methods Mol Biol,* 935**,** 87-97.

GUAN, X., XUAN, M., GU, Q., HUANG, P., LIU, C., WANG, N., XU, X., LUO, W. & ZHANG, M. 2017. Regionally progressive accumulation of iron in Parkinson's disease as measured by quantitative susceptibility mapping. *NMR Biomed,* 30.

GUO, L., DUGGAN, J. & CORDEIRO, M. F. 2010. Alzheimer's disease and retinal neurodegeneration. *Curr Alzheimer Res,* 7**,** 3-14.

GUO, L. Y., ALEKSEEV, O., LI, Y., SONG, Y. & DUNAIEF, J. L. 2014. Iron increases APP translation and amyloid-beta production in the retina. *Exp Eye Res,* 129**,** 31-7.

HADZIAHMETOVIC, M., DENTCHEV, T., SONG, Y., HADDAD, N., HE, X., HAHN, P., PRATICO, D., WEN, R., HARRIS, Z. L., LAMBRIS, J. D., BEARD, J. & DUNAIEF, J. L. 2008. Ceruloplasmin/hephaestin knockout mice model morphologic and molecular features of AMD. *Invest Ophthalmol Vis Sci,* 49**,** 2728-36.

HAHN, P., DENTCHEV, T., QIAN, Y., ROUAULT, T., HARRIS, Z. L. & DUNAIEF, J. L. 2004a. Immunolocalization and regulation of iron handling proteins ferritin and ferroportin in the retina. *Mol Vis,* 10**,** 598-607.

HAHN, P., MILAM, A. H. & DUNAIEF, J. L. 2003. Maculas affected by age-related macular degeneration contain increased chelatable iron in the retinal pigment epithelium and Bruch's membrane. *Arch Ophthalmol,* 121**,** 1099-105.

HAHN, P., QIAN, Y., DENTCHEV, T., CHEN, L., BEARD, J., HARRIS, Z. L. & DUNAIEF, J. L. 2004b. Disruption of ceruloplasmin and hephaestin in mice causes retinal iron overload and retinal degeneration with features of age-related macular degeneration. *Proc Natl Acad Sci U S A,* 101**,** 13850-5.

HAHN, P., YING, G. S., BEARD, J. & DUNAIEF, J. L. 2006. Iron levels in human retina: sex difference and increase with age. *Neuroreport,* 17**,** 1803-6.

HALLIWELL, B. & GUTTERIDGE, J. M. 1984. Oxygen toxicity, oxygen radicals, transition metals and disease. *Biochem J,* 219**,** 1-14.

HANUS, J., ANDERSON, C. & WANG, S. 2015. RPE necroptosis in response to oxidative stress and in AMD. *Ageing Res Rev*.

HE, X., HAHN, P., IACOVELLI, J., WONG, R., KING, C., BHISITKUL, R., MASSARO-GIORDANO, M. & DUNAIEF, J. L. 2007. Iron homeostasis and toxicity in retinal degeneration. *Prog Retin Eye Res,* 26**,** 649-73.

HINTON, D. R., SADUN, A. A., BLANKS, J. C. & MILLER, C. A. 1986. Optic-nerve degeneration in Alzheimer's disease. *N Engl J Med,* 315**,** 485-7.

HOU, Y. C., LIOU, K. T., CHERN, C. M., WANG, Y. H., LIAO, J. F., CHANG, S., CHOU, Y. H. & SHEN, Y. C. 2010. Preventive effect of silymarin in cerebral ischemia-reperfusion-induced brain injury in rats possibly through impairing NF-kappaB and STAT-1 activation. *Phytomedicine,* 17**,** 963-73.

HUNTER, J. J., MORGAN, J. I. W., MERIGAN, W. H., SLINEY, D. H., SPARROW, J. R. & WILLIAMS, D. R. 2012. The susceptibility of the retina to photochemical damage from visible light. *Progress in Retinal and Eye Research,* 31**,** 28-42.

HUSSAIN, M. A., ASHRAF, M. U., MUHAMMAD, G., TAHIR, M. N. & BUKHARI, S. N. A. 2017. Calixarene: A Versatile Material for Drug Design and Applications. *Curr Pharm Des,* 23**,** 2377-2388.

HUYNH, T.-P., MANN, S. N. & MANDAL, N. A. 2013. Botanical compounds: effects on major eye diseases. *Evidence-based complementary and alternative medicine : eCAM,* 2013**,** 549174-549174.

ISERI, P. K., ALTINAS, O., TOKAY, T. & YUKSEL, N. 2006. Relationship between cognitive impairment and retinal morphological and visual functional abnormalities in Alzheimer disease. *J Neuroophthalmol,* 26**,** 18-24.

JAMES, E., EGGERS, P. K., HARVEY, A. R., DUNLOP, S. A., FITZGERALD, M., STUBBS, K. A. & RASTON, C. L. 2013. Antioxidant phospholipid calix[4]arene mimics as micellular delivery systems. *Org Biomol Chem,* 11**,** 6108-12.

JANGRA, A., KASBE, P., PANDEY, S. N., DWIVEDI, S., GURJAR, S. S., KWATRA, M., MISHRA, M., VENU, A. K., SULAKHIYA, K., GOGOI, R., SARMA, N., BEZBARUAH, B. K. & LAHKAR, M. 2015. Hesperidin and Silibinin Ameliorate Aluminum-Induced Neurotoxicity: Modulation of Antioxidants and Inflammatory Cytokines Level in Mice Hippocampus. *Biol Trace Elem Res,* 168**,** 462-71.

JIANG, H., WANG, J., ROGERS, J. & XIE, J. 2017. Brain Iron Metabolism Dysfunction in Parkinson's Disease. *Mol Neurobiol,* 54**,** 3078-3101.

JOSHI, R., GARABADU, D., TEJA, G. R. & KRISHNAMURTHY, S. 2014. Silibinin ameliorates LPS-induced memory deficits in experimental animals. *Neurobiol Learn Mem,* 116**,** 117-31.

JUNG, U. J., JEON, M. T., CHOI, M. S. & KIM, S. R. 2014. Silibinin attenuates MPP(+)-induced neurotoxicity in the substantia nigra in vivo. *J Med Food,* 17**,** 599-605.

KAARNIRANTA, K., SALMINEN, A., HAAPASALO, A., SOININEN, H. & HILTUNEN, M. 2011. Age-related macular degeneration (AMD): Alzheimer's disease in the eye? *J Alzheimers Dis,* 24**,** 615-31.

KALE, N. 2016. Optic neuritis as an early sign of multiple sclerosis. *Eye and brain,* 8**,** 195-202.

KARAKOCAK, B. B., RALIYA, R., DAVIS, J. T., CHAVALMANE, S., WANG, W. N., RAVI, N. & BISWAS, P. 2016. Biocompatibility of gold nanoparticles in retinal pigment epithelial cell line. *Toxicol In Vitro,* 37**,** 61-69.

KARIMI, G., VAHABZADEH, M., LARI, P., RASHEDINIA, M. & MOSHIRI, M. 2011. "Silymarin", a promising pharmacological agent for treatment of diseases. *Iran J Basic Med Sci,* 14**,** 308-17.

KARLSTETTER, M., SCHOLZ, R., RUTAR, M., WONG, W. T., PROVIS, J. M. & LANGMANN, T. 2015. Retinal microglia: just bystander or target for therapy? *Prog Retin Eye Res,* 45**,** 30-57.

KAUPPINEN, A., PATERNO, J. J., BLASIAK, J., SALMINEN, A. & KAARNIRANTA, K. 2016. Inflammation and its role in age-related macular degeneration. *Cellular and molecular life sciences : CMLS,* 73**,** 1765-1786.

KHAN, J. C., THURLBY, D. A., SHAHID, H., CLAYTON, D. G., YATES, J. R., BRADLEY, M., MOORE, A. T. & BIRD, A. C. 2006. Smoking and age related macular degeneration: the number of pack years of cigarette smoking is a major determinant of risk for both geographic atrophy and choroidal neovascularisation. *Br J Ophthalmol,* 90**,** 75-80.

KIERNAN, M. C., VUCIC, S., CHEAH, B. C., TURNER, M. R., EISEN, A., HARDIMAN, O., BURRELL, J. R. & ZOING, M. C. 2011. Amyotrophic lateral sclerosis. *Lancet,* 377**,** 942-55.

KIM, S. H., LUTZ, R. J., WANG, N. S. & ROBINSON, M. R. 2007. Transport barriers in transscleral drug delivery for retinal diseases. *Ophthalmic Res,* 39**,** 244-54.

KLIFFEN, M., SHARMA, H. S., MOOY, C. M., KERKVLIET, S. & DE JONG, P. T. 1997. Increased expression of angiogenic growth factors in age-related maculopathy. *Br J Ophthalmol,* 81**,** 154-62.

KONO, S. 2012. Aceruloplasminemia. *Curr Drug Targets,* 13**,** 1190-9.

KORONYO-HAMAOUI, M., KORONYO, Y., LJUBIMOV, A. V., MILLER, C. A., KO, M. K., BLACK, K. L., SCHWARTZ, M. & FARKAS, D. L. 2011. Identification of amyloid plaques in retinas from Alzheimer's patients and noninvasive in vivo optical imaging of retinal plaques in a mouse model. *Neuroimage,* 54 Suppl 1**,** S204-17.

KREN, V., MARHOL, P., PURCHARTOVA, K., GABRIELOVA, E. & MODRIANSKY, M. 2013. Biotransformation of silybin and its congeners. *Curr Drug Metab,* 14**,** 1009-21.

LALLEMAND, F., DAULL, P., BENITA, S., BUGGAGE, R. & GARRIGUE, J. S. 2012. Successfully improving ocular drug delivery using the cationic nanoemulsion, novasorb. *J Drug Deliv,* 2012**,** 604204.

LANGMANN, T. 2007. Microglia activation in retinal degeneration. *J Leukoc Biol,* 81**,** 1345-51.

LEE, S. J., HE, W., ROBINSON, S. B., ROBINSON, M. R., CSAKY, K. G. & KIM, H. 2010. Evaluation of clearance mechanisms with transscleral drug delivery. *Invest Ophthalmol Vis Sci,* 51**,** 5205-12.

LEE, Y., PARK, H. R., CHUN, H. J. & LEE, J. 2015. Silibinin prevents dopaminergic neuronal loss in a mouse model of Parkinson's disease via mitochondrial stabilization. *J Neurosci Res,* 93**,** 755-65.

LEVIN, M. H., BENNETT, J. L. & VERKMAN, A. S. 2013. Optic neuritis in neuromyelitis optica. *Progress in retinal and eye research,* 36**,** 159-171.

LEVINE, S. M. & MACKLIN, W. B. 1990. Iron-enriched oligodendrocytes: a reexamination of their spatial distribution. *J Neurosci Res,* 26**,** 508-12.

LI, J., LI, Z., LIANG, Z., HAN, L., FENG, H., HE, S. & ZHANG, J. 2018. Fabrication of a drug delivery system that enhances antifungal drug corneal penetration. *Drug Deliv,* 25**,** 938-949.

LI, J., O, W., LI, W., JIANG, Z. G. & GHANBARI, H. A. 2013. Oxidative stress and neurodegenerative disorders. *Int J Mol Sci,* 14**,** 24438-75.

LILL, R., HOFFMANN, B., MOLIK, S., PIERIK, A. J., RIETZSCHEL, N., STEHLING, O., UZARSKA, M. A., WEBERT, H., WILBRECHT, C. & MÜHLENHOFF, U. 2012. The role of mitochondria in cellular iron-sulfur protein biogenesis and iron metabolism. *Biochim Biophys Acta,* 1823**,** 1491-508.

LIN, C. H., LI, C. H., LIAO, P. L., TSE, L. S., HUANG, W. K., CHENG, H. W. & CHENG, Y. W. 2013. Silibinin inhibits VEGF secretion and age-related macular degeneration in a hypoxia-dependent manner through the PI-3 kinase/Akt/mTOR pathway. *Br J Pharmacol,* 168**,** 920-31.

LIU, B., RASOOL, S., YANG, Z., GLABE, C. G., SCHREIBER, S. S., GE, J. & TAN, Z. 2009. Amyloid-peptide vaccinations reduce {beta}-amyloid plaques but exacerbate vascular deposition and inflammation in the retina of Alzheimer's transgenic mice. *Am J Pathol,* 175**,** 2099-110.

LIU, B. N., HAN, B. X. & LIU, F. 2014. Neuroprotective effect of pAkt and HIF-1 alpha on ischemia rats. *Asian Pac J Trop Med,* 7**,** 221-5.

LIU, J.-L., FAN, Y.-G., YANG, Z.-S., WANG, Z.-Y. & GUO, C. 2018. Iron and Alzheimer's Disease: From Pathogenesis to Therapeutic Implications. *Frontiers in neuroscience,* 12**,** 632-632.

LIU, R. T., GAO, J., CAO, S., SANDHU, N., CUI, J. Z., CHOU, C. L., FANG, E. & MATSUBARA, J. A. 2013. Inflammatory mediators induced by amyloid-beta in the retina and RPE in vivo: implications for inflammasome activation in age-related macular degeneration. *Invest Ophthalmol Vis Sci,* 54**,** 2225-37.

LONDON, A., BENHAR, I. & SCHWARTZ, M. 2013. The retina as a window to the brain-from eye research to CNS disorders. *Nat Rev Neurol,* 9**,** 44-53.

LORENZ, D., LUCKER, P. W., MENNICKE, W. H. & WETZELSBERGER, N. 1984. Pharmacokinetic studies with silymarin in human serum and bile. *Methods Find Exp Clin Pharmacol,* 6**,** 655-61.

LU, P., MAMIYA, T., LU, L. L., MOURI, A., NIWA, M., HIRAMATSU, M., ZOU, L. B., NAGAI, T., IKEJIMA, T. & NABESHIMA, T. 2009. Silibinin attenuates amyloid beta(25-35) peptide-induced memory impairments: implication of inducible nitric-oxide synthase and tumor necrosis factor-alpha in mice. *J Pharmacol Exp Ther,* 331**,** 319-26.

MACCORMICK, I. J., CZANNER, G. & FARAGHER, B. 2015. Developing retinal biomarkers of neurological disease: an analytical perspective. *Biomark Med,* 9**,** 691-701.

MACHA, S., HUGHES, P. & MITRA, A. 2003. Overview of Ocular Drug Delivery.

MADEIRA, M. H., BOIA, R., SANTOS, P. F., AMBROSIO, A. F. & SANTIAGO, A. R. 2015. Contribution of microglia-mediated neuroinflammation to retinal degenerative diseases. *Mediators Inflamm,* 2015**,** 673090.

MAJUMDAR, S. & SRIRANGAM, R. 2010. Potential of the bioflavonoids in the prevention/treatment of ocular disorders. *J Pharm Pharmacol,* 62**,** 951-65.

MANNERMAA, E., VELLONEN, K. S. & URTTI, A. 2006. Drug transport in corneal epithelium and blood-retina barrier: emerging role of transporters in ocular pharmacokinetics. *Adv Drug Deliv Rev,* 58**,** 1136-63.

MARALDI, T., PRATA, C., CALICETI, C., VIECELI DALLA SEGA, F., ZAMBONIN, L., FIORENTINI, D. & HAKIM, G. 2010. VEGF-induced ROS generation from NAD(P)H oxidases protects human leukemic cells from apoptosis. *Int J Oncol,* 36**,** 1581-9.

MARC, R. E., JONES, B. W., WATT, C. B., VAZQUEZ-CHONA, F., VAUGHAN, D. K. & ORGANISCIAK, D. T. 2008. Extreme retinal remodeling triggered by light damage: implications for age related macular degeneration. *Molecular vision,* 14**,** 782-806.

MARRAZZO, G., BOSCO, P., LA DELIA, F., SCAPAGNINI, G., DI GIACOMO, C., MALAGUARNERA, M., GALVANO, F., NICOLOSI, A. & LI VOLTI, G. 2011. Neuroprotective effect of silibinin in diabetic mice. *Neurosci Lett,* 504**,** 252-6.

MARREN, K. 2011. Dimethyl sulfoxide: an effective penetration enhancer for topical administration of NSAIDs. *Phys Sportsmed,* 39**,** 75-82.

MARTIN, W. R., WIELER, M. & GEE, M. 2008. Midbrain iron content in early Parkinson disease: a potential biomarker of disease status. *Neurology,* 70**,** 1411-7.

MASUDA, T., SHIMAZAWA, M. & HARA, H. 2017. Retinal Diseases Associated with Oxidative Stress and the Effects of a Free Radical Scavenger (Edaravone). *Oxid Med Cell Longev,* 2017**,** 9208489.

MASUDA, T., SHIMAZAWA, M., TAKATA, S., NAKAMURA, S., TSURUMA, K. & HARA, H. 2016. Edaravone is a free radical scavenger that protects against laser-induced choroidal neovascularization in mice and common marmosets. *Exp Eye Res,* 146**,** 196-205.

MATLACH, J., WAGNER, M., MALZAHN, U., SCHMIDTMANN, I., STEIGERWALD, F., MUSACCHIO, T., VOLKMANN, J., GREHN, F., GOBEL, W. & KLEBE, S. 2018. Retinal changes in Parkinson's disease and glaucoma. *Parkinsonism Relat Disord,* 56**,** 41-46.

MATSUMOTO, H., SHIBASAKI, K., UCHIGASHIMA, M., KOIZUMI, A., KURACHI, M., MORIWAKI, Y., MISAWA, H., KAWASHIMA, K., WATANABE, M., KISHI, S. & ISHIZAKI, Y. 2012. Localization of acetylcholine-related molecules in the retina: implication of the communication from photoreceptor to retinal pigment epithelium. *PLoS One,* 7**,** e42841.

MCCARTHY, R. C. & KOSMAN, D. J. 2013. Ferroportin and exocytoplasmic ferroxidase activity are required for brain microvascular endothelial cell iron efflux. *J Biol Chem,* 288**,** 17932-40.

MEADOWCROFT, M. D., CONNOR, J. R., SMITH, M. B. & YANG, Q. X. 2009. MRI and histological analysis of beta-amyloid plaques in both human Alzheimer's disease and APP/PS1 transgenic mice. *J Magn Reson Imaging,* 29**,** 997-1007.

MITRA, A. K., ANAND, B. S. & DUVVURI, S. 2006. Drug Delivery to the Eye. *Advances In Organ Biology,* 10**,** 307-351.

MOGI, M., HARADA, M., KONDO, T., RIEDERER, P., INAGAKI, H., MINAMI, M. & NAGATSU, T. 1994. Interleukin-1 beta, interleukin-6, epidermal growth factor and transforming growth factor-alpha are elevated in the brain from parkinsonian patients. *Neurosci Lett,* 180**,** 147-50.

MOISEYEV, G., CHEN, Y., TAKAHASHI, Y., WU, B. X. & MA, J.-X. 2005. RPE65 is the isomerohydrolase in the retinoid visual cycle. *Proceedings of the National Academy of Sciences of the United States of America,* 102**,** 12413-12418.

MOKHTARI, B. & POURABDOLLAH, K. 2013. Applications of nano-baskets in drug development: high solubility and low toxicity. *Drug Chem Toxicol,* 36**,** 119-32.

MOON, J. Y., KIM, H. J., PARK, Y. H., PARK, T. K., PARK, E.-C., KIM, C. Y. & LEE, S. H. 2018. Association between Open-Angle Glaucoma and the Risks of Alzheimer's and Parkinson's Diseases in South Korea: A 10-year Nationwide Cohort Study. *Scientific reports,* 8**,** 11161-11161.

MOOS, T., NIELSEN, T. R., SKJØRRINGE, T. & MORGAN, E. H. 2007. Iron trafficking inside the brain. *Journal of Neurochemistry,* 103**,** 1730-1740.

MORGAN, J. I. W., HUNTER, J. J., MERIGAN, W. H. & WILLIAMS, D. R. 2009. The Reduction of Retinal Autofluorescence Caused by Light Exposure. *Investigative Ophthalmology & Visual Science,* 50**,** 6015-6022.

MORRIS, C. M., CANDY, J. M., OAKLEY, A. E., BLOXHAM, C. A. & EDWARDSON, J. A. 1992. Histochemical distribution of non-haem iron in the human brain. *Acta Anat (Basel),* 144**,** 235-57.

MOSS, H. E., MCCLUSKEY, L., ELMAN, L., HOSKINS, K., TALMAN, L., GROSSMAN, M., BALCER, L. J., GALETTA, S. L. & LIU, G. T. 2012. Cross-sectional evaluation of clinical neuro-ophthalmic abnormalities in an amyotrophic lateral sclerosis population. *Journal of the neurological sciences,* 314**,** 97-101.

NAMBIAR, D., PRAJAPATI, V., AGARWAL, R. & SINGH, R. P. 2013. In vitro and in vivo anticancer efficacy of silibinin against human pancreatic cancer BxPC-3 and PANC-1 cells. *Cancer Lett,* 334**,** 109-17.

NASEER, M. M., AHMED, M. & HAMEED, S. 2017. Functionalized calix[4]arenes as potential therapeutic agents. *Chemical Biology & Drug Design,* 89**,** 243-256.

NERI, P. S., J. L.; WANG, M.-X. 2016. Calixarenes and Beyond. *Springer: Berlin-Heidelberg*.

NIEDZIELSKA, E., SMAGA, I., GAWLIK, M., MONICZEWSKI, A., STANKOWICZ, P., PERA, J. & FILIP, M. 2016. Oxidative Stress in Neurodegenerative Diseases. *Molecular Neurobiology,* 53**,** 4094–4125.

NIMSE, S. B. & KIM, T. 2013. Biological applications of functionalized calixarenes. *Chem Soc Rev,* 42**,** 366-86.

NING, A., CUI, J., TO, E., ASHE, K. H. & MATSUBARA, J. 2008. Amyloid-beta deposits lead to retinal degeneration in a mouse model of Alzheimer disease. *Invest Ophthalmol Vis Sci,* 49**,** 5136-43.

NISHIYAMA, N. & KATAOKA, K. 2006. Current state, achievements, and future prospects of polymeric micelles as nanocarriers for drug and gene delivery. *Pharmacol Ther,* 112**,** 630-48.

NNAH, I. C. & WESSLING-RESNICK, M. 2018. Brain Iron Homeostasis: A Focus on Microglial Iron. *Pharmaceuticals (Basel, Switzerland),* 11**,** 129.

OHNO-MATSUI, K. 2011. Parallel findings in age-related macular degeneration and Alzheimer's disease. *Prog Retin Eye Res,* 30**,** 217-38.

PASCOLINI, D. & MARIOTTI, S. P. 2012. Global estimates of visual impairment: 2010. *Br J Ophthalmol,* 96**,** 614-8.

PATEL, A., CHOLKAR, K., AGRAHARI, V. & MITRA, A. K. 2013. Ocular drug delivery systems: An overview. *World J Pharmacol,* 2**,** 47-64.

PEKNY, M., WILHELMSSON, U. & PEKNA, M. 2014. The dual role of astrocyte activation and reactive gliosis. *Neurosci Lett,* 565**,** 30-8.

PENNESI, M. E., NEURINGER, M. & COURTNEY, R. J. 2012. Animal models of age related macular degeneration. *Mol Aspects Med,* 33**,** 487-509.

PEREZ, S. E., LUMAYAG, S., KOVACS, B., MUFSON, E. J. & XU, S. 2009. Beta-amyloid deposition and functional impairment in the retina of the APPswe/PS1DeltaE9 transgenic mouse model of Alzheimer's disease. *Invest Ophthalmol Vis Sci,* 50**,** 793-800.

PERRI, P., ZAULI, G., GONELLI, A., MILANI, D., CELEGHINI, C., LAMBERTI, G. & SECCHIERO, P. 2015. TNF-related apoptosis inducing ligand in ocular cancers and ocular diabetic complications. *Biomed Res Int,* 2015**,** 424019.

PETERS, D. G., CONNOR, J. R. & MEADOWCROFT, M. D. 2015. The relationship between iron dyshomeostasis and amyloidogenesis in Alzheimer's disease: Two sides of the same coin. *Neurobiol Dis,* 81**,** 49-65.

PEYMAN, G. A., LAD, E. M. & MOSHFEGHI, D. M. 2009. Intravitreal injection of therapeutic agents. *Retina,* 29**,** 875-912.

PIGNATELLO, R. & PUGLISI, G. 2011. Nanotechnology in Ophthalmic Drug Delivery: A Survey of Recent Developments and Patenting Activity. *Recent Patents on Nanomedicine (Discontinued),* 1**,** 42-54.

PIRCHER, M. & ZAWADZKI, R. J. 2017. Review of adaptive optics OCT (AO-OCT): principles and applications for retinal imaging [Invited]. *Biomedical optics express,* 8**,** 2536-2562.

PONS, M. & MARIN-CASTAÑO, M. E. 2011. Nicotine Increases the VEGF/PEDF Ratio in Retinal Pigment Epithelium: A Possible Mechanism for CNV in Passive Smokers with AMD. *Investigative Ophthalmology & Visual Science,* 52**,** 3842-3853.

POSS, K. D. & TONEGAWA, S. 1997. Heme oxygenase 1 is required for mammalian iron reutilization. *Proc Natl Acad Sci U S A,* 94**,** 10919-24.

PUTTING, B. J., ZWEYPFENNING, R. C., VRENSEN, G. F., OOSTERHUIS, J. A. & VAN BEST, J. A. 1992. Blood-retinal barrier dysfunction at the pigment epithelium induced by blue light. *Investigative Ophthalmology & Visual Science,* 33**,** 3385-3393.

RAMASAMY, K., DWYER-NIELD, L. D., SERKOVA, N. J., HASEBROOCK, K. M., TYAGI, A., RAINA, K., SINGH, R. P., MALKINSON, A. M. & AGARWAL, R. 2011. Silibinin prevents lung tumorigenesis in wild-type but not in iNOS-/- mice: potential of real-time micro-CT in lung cancer chemoprevention studies. *Clin Cancer Res,* 17**,** 753-61.

RANSOHOFF, R. M. 2016. How neuroinflammation contributes to neurodegeneration. *Science,* 353**,** 777-83.
RODIK, R. V., ANTHONY, A.-S., KALCHENKO, V. I., MELY, Y. & KLYMCHENKO, A. S. 2015. Cationic amphiphilic calixarenes to compact DNA into small nanoparticles for gene delivery. *New Journal of Chemistry,* 39**,** 1654-1664.
RODRIGUEZ DIEZ, G., SANCHEZ CAMPOS, S., GIUSTO, N. M. & SALVADOR, G. A. 2013. Specific roles for Group V secretory PLA(2) in retinal iron-induced oxidative stress. Implications for age-related macular degeneration. *Exp Eye Res,* 113**,** 172-81.
RODRIGUEZ DIEZ, G., URANGA, R. M., MATEOS, M. V., GIUSTO, N. M. & SALVADOR, G. A. 2012. Differential participation of phospholipase A2 isoforms during iron-induced retinal toxicity. Implications for age-related macular degeneration. *Neurochem Int,* 61**,** 749-58.
ROGERS, B. S., SYMONS, R. C., KOMEIMA, K., SHEN, J., XIAO, W., SWAIM, M. E., GONG, Y. Y., KACHI, S. & CAMPOCHIARO, P. A. 2007. Differential sensitivity of cones to iron-mediated oxidative damage. *Invest Ophthalmol Vis Sci,* 48**,** 438-45.
ROTTKAMP, C. A., RAINA, A. K., ZHU, X., GAIER, E., BUSH, A. I., ATWOOD, C. S., CHEVION, M., PERRY, G. & SMITH, M. A. 2001. Redox-active iron mediates amyloid-beta toxicity. *Free Radic Biol Med,* 30**,** 447-50.
ROUAULT, T. A. 2013. Iron metabolism in the CNS: implications for neurodegenerative diseases. *Nat Rev Neurosci,* 14**,** 551-64.
ROUAULT, T. A., ZHANG, D.-L. & JEONG, S. Y. 2009. Brain iron homeostasis, the choroid plexus, and localization of iron transport proteins. *Metabolic brain disease,* 24**,** 673.
RUBSAM, A., PARIKH, S. & FORT, P. E. 2018. Role of Inflammation in Diabetic Retinopathy. *Int J Mol Sci,* 19.
SACHDEVA, M. M., CANO, M. & HANDA, J. T. 2014. Nrf2 signaling is impaired in the aging RPE given an oxidative insult. *Experimental Eye Research,* 119**,** 111-114.
SADUN, A. A. & BASSI, C. J. 1990. Optic nerve damage in Alzheimer's disease. *Ophthalmology,* 97**,** 9-17.
SAHA, P., KIM, K. J. & LEE, V. H. 1996. A primary culture model of rabbit conjunctival epithelial cells exhibiting tight barrier properties. *Curr Eye Res,* 15**,** 1163-9.
SAHIBZADA, M. U. K., SADIQ, A., KHAN, S., FAIDAH, H. S., NASEEMULLAH, KHURRAM, M., AMIN, M. U. & HASEEB, A. 2017. Fabrication, characterization and in vitro evaluation of silibinin nanoparticles: an attempt to enhance its oral bioavailability. *Drug design, development and therapy,* 11**,** 1453-1464.
SAMUEL, W., JAWORSKI, C., POSTNIKOVA, O. A., KUTTY, R. K., DUNCAN, T., TAN, L. X., POLIAKOV, E., LAKKARAJU, A. & REDMOND, T. M. 2017. Appropriately differentiated ARPE-19 cells regain phenotype and gene expression profiles similar to those of native RPE cells. *Mol Vis,* 23**,** 60-89.
SEKINE, S. & ICHIJO, H. 2015. Mitochondrial proteolysis: its emerging roles in stress responses. *Biochim Biophys Acta,* 1850**,** 274-80.
SHARMA, R., HICKS, S., BERNA, C. M., KENNARD, C., TALBOT, K. & TURNER, M. R. 2011. Oculomotor Dysfunction in Amyotrophic Lateral Sclerosis: A Comprehensive Review. *Archives of Neurology,* 68**,** 857-861.
SHICHI, H. 1969. Microsomal electron transfer system of bovine retinal pigment epithelium. *Exp Eye Res,* 8**,** 60-8.
SHIRLEY, H. H., LUNDERGAN, M. K., WILLIAMS, H. J. & SPRUANCE, S. L. 1989. Lack of ocular changes with dimethyl sulfoxide therapy of scleroderma. *Pharmacotherapy,* 9**,** 165-8.
SMITH, M. A., PERRY, G., RICHEY, P. L., SAYRE, L. M., ANDERSON, V. E., BEAL, M. F. & KOWALL, N. 1996. Oxidative damage in Alzheimer's. *Nature,* 382**,** 120-1.
SOELBERG, K., SPECOVIUS, S., ZIMMERMANN, H. G., GRAUSLUND, J., MEHLSEN, J. J., OLESEN, C., NEVE, A. S. B., PAUL, F., BRANDT, A. U. & ASGARI, N. 2018. Optical coherence tomography in acute optic neuritis: A population-based study. 138**,** 566-573.
SONG, D. & DUNAIEF, J. L. 2013. Retinal iron homeostasis in health and disease. *Front Aging Neurosci,* 5**,** 24.
SONG, N., WANG, J., JIANG, H. & XIE, J. 2010. Ferroportin 1 but not hephaestin contributes to iron accumulation in a cell model of Parkinson's disease. *Free radical biology & medicine,* 48**,** 332-341.
SONG, X., ZHOU, B., CUI, L., LEI, D., ZHANG, P., YAO, G., XIA, M., HAYASHI, T., HATTORI, S., USHIKI-KAKU, Y., TASHIRO, S. I., ONODERA, S. & IKEJIMA, T. 2017. Silibinin ameliorates Abeta25-35-induced memory deficits in rats by modulating autophagy and attenuating neuroinflammation as well as oxidative stress. *Neurochem Res,* 42**,** 1073-1083.

SONG, X., ZHOU, B., ZHANG, P., LEI, D., WANG, Y., YAO, G., HAYASHI, T., XIA, M., TASHIRO, S., ONODERA, S. & IKEJIMA, T. 2016. Protective Effect of Silibinin on Learning and Memory Impairment in LPS-Treated Rats via ROS-BDNF-TrkB Pathway. *Neurochem Res,* 41**,** 1662-72.

SPATARO, G., MALECAZE, F., TURRIN, C. O., SOLER, V., DUHAYON, C., ELENA, P. P., MAJORAL, J. P. & CAMINADE, A. M. 2010. Designing dendrimers for ocular drug delivery. *Eur J Med Chem,* 45**,** 326-34.

STEWART, M. W. 2014. Anti-VEGF therapy for diabetic macular edema. *Curr Diab Rep,* 14**,** 510.

STRUBLE, R. G., ALA, T., PATRYLO, P. R., BREWER, G. J. & YAN, X. X. 2010. Is brain amyloid production a cause or a result of dementia of the Alzheimer's type? *J Alzheimers Dis,* 22**,** 393-9.

SUNKARA, G. & KOMPELLA, U. 2003. Membrane Transport Processes in the Eye.

SURAI, P. F. 2015. Silymarin as a Natural Antioxidant: An Overview of the Current Evidence and Perspectives. *Antioxidants (Basel),* 4**,** 204-47.

TAYARA, N., DELATOUR, B., CUDENNEC, C., GUÉGAN, M., VOLK, A. & DHENAIN, M. 2006. Age-related evolution of amyloid burden, iron load, and MR relaxation times in a transgenic mouse model of Alzheimer's disease. *Neurobiology of disease,* 22**,** 199-208.

TEWARI-SINGH, N., JAIN, A. K., INTURI, S., AMMAR, D. A., AGARWAL, C., TYAGI, P., KOMPELLA, U. B., ENZENAUER, R. W., PETRASH, J. M. & AGARWAL, R. 2012. Silibinin, dexamethasone, and doxycycline as potential therapeutic agents for treating vesicant-inflicted ocular injuries. *Toxicol Appl Pharmacol,* 264**,** 23-31.

THOMSEN, M. S., ANDERSEN, M. V., CHRISTOFFERSEN, P. R., JENSEN, M. D., LICHOTA, J. & MOOS, T. 2015. Neurodegeneration with inflammation is accompanied by accumulation of iron and ferritin in microglia and neurons. *Neurobiol Dis,* 81**,** 108-18.

TOMANY, S. C., WANG, J. J., VAN LEEUWEN, R., KLEIN, R., MITCHELL, P., VINGERLING, J. R., KLEIN, B. E. K., SMITH, W. & DE JONG, P. T. V. M. 2004. Risk factors for incident age-related macular degeneration: Pooled findings from 3 continents. *Ophthalmology,* 111**,** 1280-1287.

TOMI, M., ARAI, K., TACHIKAWA, M. & HOSOYA, K. 2007. Na(+)-independent choline transport in rat retinal capillary endothelial cells. *Neurochem Res,* 32**,** 1833-42.

TOTA, S., KAMAT, P. K., SHUKLA, R. & NATH, C. 2011. Improvement of brain energy metabolism and cholinergic functions contributes to the beneficial effects of silibinin against streptozotocin induced memory impairment. *Behav Brain Res,* 221**,** 207-15.

TSAI, M. J., LIAO, J. F., LIN, D. Y., HUANG, M. C., LIOU, D. Y., YANG, H. C., LEE, H. J., CHEN, Y. T., CHI, C. W., HUANG, W. C. & CHENG, H. 2010. Silymarin protects spinal cord and cortical cells against oxidative stress and lipopolysaccharide stimulation. *Neurochem Int,* 57**,** 867-75.

TSAI, Y., LU, B., LJUBIMOV, A. V., GIRMAN, S., ROSS-CISNEROS, F. N., SADUN, A. A., SVENDSEN, C. N., COHEN, R. M. & WANG, S. 2014. Ocular changes in TgF344-AD rat model of Alzheimer's disease. *Invest Ophthalmol Vis Sci,* 55**,** 523-34.

TSUBOTA, K. 2007. [Oxidative stress and inflammation: hypothesis for the mechanism of aging]. *Nippon Ganka Gakkai Zasshi,* 111**,** 193-205; discussion 206.

TZEKOV, R. & MULLAN, M. 2014. Vision function abnormalities in Alzheimer disease. *Surv Ophthalmol,* 59**,** 414-33.

UGARTE, M., OSBORNE, N. N., BROWN, L. A. & BISHOP, P. N. 2013. Iron, zinc, and copper in retinal physiology and disease. *Surv Ophthalmol,* 58**,** 585-609.

URRUTIA, P., AGUIRRE, P., ESPARZA, A., TAPIA, V., MENA, N. P., ARREDONDO, M., GONZÁLEZ-BILLAULT, C. & NÚÑEZ, M. T. 2013. Inflammation alters the expression of DMT1, FPN1 and hepcidin, and it causes iron accumulation in central nervous system cells. *J Neurochem,* 126**,** 541-9.

URTTI, A. 2006. Challenges and obstacles of ocular pharmacokinetics and drug delivery. *Adv Drug Deliv Rev,* 58**,** 1131-5.

VADLAPUDI, A. D. & MITRA, A. K. 2013. Nanomicelles: an emerging platform for drug delivery to the eye. *Therapeutic delivery,* 4**,** 1-3.

VALAVANIDIS, A., VLACHOGIANNI, T. & FIOTAKIS, C. 2009. 8-hydroxy-2' -deoxyguanosine (8-OHdG): A critical biomarker of oxidative stress and carcinogenesis. *J Environ Sci Health C Environ Carcinog Ecotoxicol Rev,* 27**,** 120-39.

VANDAMME, T. F. 2002. Microemulsions as ocular drug delivery systems: recent developments and future challenges. *Prog Retin Eye Res,* 21**,** 15-34.

VECINO, E., RODRIGUEZ, F. D., RUZAFA, N., PEREIRO, X. & SHARMA, S. C. 2016. Glia-neuron interactions in the mammalian retina. *Prog Retin Eye Res,* 51**,** 1-40.

VOHRA, R., TSAI, J. C. & KOLKO, M. 2013. The role of inflammation in the pathogenesis of glaucoma. *Surv Ophthalmol,* 58**,** 311-20.

WADHWA, S., PALIWAL, R., PALIWAL, S. R. & VYAS, S. P. 2009. Nanocarriers in ocular drug delivery: an update review. *Curr Pharm Des,* 15**,** 2724-50.

WANG, C., WANG, Z., ZHANG, X., ZHANG, X., DONG, L., XING, Y., LI, Y., LIU, Z., CHEN, L., QIAO, H., WANG, L. & ZHU, C. 2012. Protection by silibinin against experimental ischemic stroke: up-regulated pAkt, pmTOR, HIF-1alpha and Bcl-2, down-regulated Bax, NF-kappaB expression. *Neurosci Lett,* 529**,** 45-50.

WANG, H., HAN, X., WITTCHEN, E. S. & HARTNETT, M. E. 2016a. TNF-α mediates choroidal neovascularization by upregulating VEGF expression in RPE through ROS-dependent β-catenin activation. *Molecular vision,* 22**,** 116-128.

WANG, J., JIANG, H. & XIE, J.-X. 2007. Ferroportin1 and hephaestin are involved in the nigral iron accumulation of 6-OHDA-lesioned rats. *The European journal of neuroscience,* 25**,** 2766-2772.

WANG, J., SONG, N., JIANG, H., WANG, J. & XIE, J. 2013. Pro-inflammatory cytokines modulate iron regulatory protein 1 expression and iron transportation through reactive oxygen/nitrogen species production in ventral mesencephalic neurons. *Biochim Biophys Acta,* 1832**,** 618-25.

WANG, M., LI, Y. J., DING, Y., ZHANG, H. N., SUN, T., ZHANG, K., YANG, L., GUO, Y. Y., LIU, S. B., ZHAO, M. G. & WU, Y. M. 2016b. Silibinin Prevents Autophagic Cell Death upon Oxidative Stress in Cortical Neurons and Cerebral Ischemia-Reperfusion Injury. *Mol Neurobiol,* 53**,** 932-43.

WANG, M. J., LIN, W. W., CHEN, H. L., CHANG, Y. H., OU, H. C., KUO, J. S., HONG, J. S. & JENG, K. C. 2002. Silymarin protects dopaminergic neurons against lipopolysaccharide-induced neurotoxicity by inhibiting microglia activation. *Eur J Neurosci,* 16**,** 2103-12.

WANG, P. & WANG, Z. Y. 2017. Metal ions influx is a double edged sword for the pathogenesis of Alzheimer's disease. *Ageing Res Rev,* 35**,** 265-290.

WANG, Y., ZHANG, L., WANG, Q. & ZHANG, D. 2014. Recent advances in the nanotechnology-based drug delivery of Silybin. *J Biomed Nanotechnol,* 10**,** 543-58.

WANG, Z. J., LAM, K. W., LAM, T. T. & TSO, M. O. 1998. Iron-induced apoptosis in the photoreceptor cells of rats. *Invest Ophthalmol Vis Sci,* 39**,** 631-3.

WATANABE, H. 2002. Significance of mucin on the ocular surface. *Cornea,* 21**,** S17-22.

WESSLING-RESNICK, M. 2010. Iron homeostasis and the inflammatory response. *Annu Rev Nutr,* 30**,** 105-22.

WIGGLESWORTH, J. & BAUM, H. 1988. Topics in neurochemistry and neuropharmacology.

WILLIAMS, M. A., MCGOWAN, A. J., CARDWELL, C. R., CHEUNG, C. Y., CRAIG, D., PASSMORE, P., SILVESTRI, G., MAXWELL, A. P. & MCKAY, G. J. 2015. Retinal microvascular network attenuation in Alzheimer's disease. *Alzheimer's & Dementia: Diagnosis, Assessment & Disease Monitoring,* 1**,** 229-235.

WILLIAMS, M. A., SILVESTRI, V., CRAIG, D., PASSMORE, A. P. & SILVESTRI, G. 2014. The prevalence of age-related macular degeneration in Alzheimer's disease. *J Alzheimers Dis,* 42**,** 909-14.

WINKLER, B. S., BOULTON, M. E., GOTTSCH, J. D. & STERNBERG, P. 1999. Oxidative damage and age-related macular degeneration. *Molecular vision,* 5**,** 32-32.

WOLKOW, N., SONG, Y., WU, T. D., QIAN, J., GUERQUIN-KERN, J. L. & DUNAIEF, J. L. 2011. Aceruloplasminemia: retinal histopathologic manifestations and iron-mediated melanosome degradation. *Arch Ophthalmol,* 129**,** 1466-74.

WONG, R. W., RICHA, D. C., HAHN, P., GREEN, W. R. & DUNAIEF, J. L. 2007. Iron toxicity as a potential factor in AMD. *Retina,* 27**,** 997-1003.

WU, J. W., LIN, L. C., HUNG, S. C., CHI, C. W. & TSAI, T. H. 2007. Analysis of silibinin in rat plasma and bile for hepatobiliary excretion and oral bioavailability application. *J Pharm Biomed Anal,* 45**,** 635-41.

WU, L. J.-C., LEENDERS, A. G. M., COOPERMAN, S., MEYRON-HOLTZ, E., SMITH, S., LAND, W., TSAI, R. Y. L., BERGER, U. V., SHENG, Z.-H. & ROUAULT, T. A. 2004. Expression of the iron transporter ferroportin in synaptic vesicles and the blood–brain barrier. *Brain Research,* 1001**,** 108-117.

XU, H., WANG, Y., SONG, N., WANG, J., JIANG, H. & XIE, J. 2018. New Progress on the Role of Glia in Iron Metabolism and Iron-Induced Degeneration of Dopamine Neurons in Parkinson's Disease. *Frontiers in Molecular Neuroscience,* 10.

YANG, D., ELNER, S. G., BIAN, Z. M., TILL, G. O., PETTY, H. R. & ELNER, V. M. 2007. Pro-inflammatory cytokines increase reactive oxygen species through mitochondria and NADPH oxidase in cultured RPE cells. *Exp Eye Res,* 85**,** 462-72.

YAP, T. E., BALENDRA, S. I., ALMONTE, M. T. & CORDEIRO, M. F. 2019. Retinal correlates of neurological disorders. *Therapeutic advances in chronic disease,* 10**,** 2040622319882205-2040622319882205.

YAU, K. W. & BAYLOR, D. A. 1989. Cyclic GMP-activated conductance of retinal photoreceptor cells. *Annu Rev Neurosci,* 12**,** 289-327.

YEFIMOVA, M. G., JEANNY, J.-C., KELLER, N., SERGEANT, C., GUILLONNEAU, X., BEAUMONT, C. & COURTOIS, Y. 2002. Impaired retinal iron homeostasis associated with defective phagocytosis in Royal College of Surgeons rats. *Investigative ophthalmology & visual science,* 43**,** 537-545.

YOO, H. G., JUNG, S. N., HWANG, Y. S., PARK, J. S., KIM, M. H., JEONG, M., AHN, S. J., AHN, B. W., SHIN, B. A., PARK, R. K. & JUNG, Y. D. 2004. Involvement of NF-kappaB and caspases in silibinin-induced apoptosis of endothelial cells. *Int J Mol Med,* 13**,** 81-6.

YOUDIM, M. 1990. Brain, behavior, and iron in the infant diet.

YOUSAF, A., HAMID, S. A., BUNNORI, N. M. & ISHOLA, A. A. 2015. Applications of calixarenes in cancer chemotherapy: facts and perspectives. *Drug Design, Development and Therapy,* 9**,** 2831-2838.

YUXI, H., YAN, Z. & GUANFANG, S. 2015. Recent Advances in Treatment of Retinitis Pigmentosa. *Current Stem Cell Research & Therapy,* 10**,** 258-265.

ZAKIN, M. M., BARON, B. & GUILLOU, F. 2002. Regulation of the Tissue-Specific Expression of Transferrin Gene. *Developmental Neuroscience,* 24**,** 222-226.

ZHANG, H. T., SHI, K., BASKOTA, A., ZHOU, F. L., CHEN, Y. X. & TIAN, H. M. 2014a. Silybin reduces obliterated retinal capillaries in experimental diabetic retinopathy in rats. *Eur J Pharmacol,* 740**,** 233-9.

ZHANG, H. Y., SONG, N., JIANG, H., BI, M. X. & XIE, J. X. 2014b. Brain-derived neurotrophic factor and glial cell line-derived neurotrophic factor inhibit ferrous iron influx via divalent metal transporter 1 and iron regulatory protein 1 regulation in ventral mesencephalic neurons. *Biochim Biophys Acta,* 1843**,** 2967-75.

ZHOU, X., WONG, L. L., KARAKOTI, A. S., SEAL, S. & MCGINNIS, J. F. 2011. Nanoceria Inhibit the Development and Promote the Regression of Pathologic Retinal Neovascularization in the Vldlr Knockout Mouse. *PLoS ONE,* 6**,** e16733.

ZHU, H. J., BRINDA, B. J., CHAVIN, K. D., BERNSTEIN, H. J., PATRICK, K. S. & MARKOWITZ, J. S. 2013. An assessment of pharmacokinetics and antioxidant activity of free silymarin flavonolignans in healthy volunteers: a dose escalation study. *Drug Metab Dispos,* 41**,** 1679-85.

ZHUKOVSKAYA, E., KARELIN, A. & RUMYANTSEV, A. 2019. Neurocognitive Dysfunctions in Iron Deficiency Patients.

INDEX